5-2013

The Role Of Type I Insulin-Like Growth Factor Receptor Signaling In Breast Cancer Brain Metastasis

Sandra M. Saldana

THE ROLE OF TYPE I INSULIN-LIKE GROWTH FACTOR RECEPTOR SIGNALING IN BREAST CANCER BRAIN METASTASIS

by

Sandra Maria Saldaña, BA

APPROVED:

_____
Mien-Chie Hung, PhD

_____
Hesham Amin, MD

_____
Elsa Flores, PhD

_____
David McConkey, PhD

_____
Ennio Tasciotti, PhD

APPROVED:

_____
Dean, The University of Texas
Graduate School of Biomedical Sciences at Houston

THE ROLE OF TYPE I INSULIN-LIKE GROWTH FACTOR RECEPTOR SIGNALING IN BREAST CANCER BRAIN METASTASIS

A

THESIS

Presented to the Faculty of The University of Texas Health Science Center at Houston and The University of Texas MD Anderson Cancer Center Graduate School of Biomedical Sciences in Partial Fulfillment

of the Requirements

for the Degree of

DOCTOR OF PHILOSOPHY

by

Sandra Maria Saldaña, BA

Houston, Texas

May 2013

ACKNOWLEDGEMENTS

I would like to thank my mentor, Dr. Mien-Chie Hung for providing his support of my graduate education and all of the necessary resources to carry out this thesis project. I would also like to thank my committee members, Dr. Hesham Amin, Dr. Elsa Flores, Dr. Jun Kameoka, Dr. David McConkey, and Dr. Ennio Tasciotti for their suggestions in the refining of my thesis work and in helping to develop my scientific thinking skills. I also thank our collaborators Dr. Dihua Yu and Dr. Patricia Steeg for providing both resources and suggestions for this project. I'd like to thank Heng-Huan Lee and Dr. Chao-Kai Chou for providing guidance in my research project, their friendship and a pleasant work environment. I also thank Frank Lowery for lending his expertise in animal handling and performing intracarotid injections that were instrumental in the experimental brain metastasis model. Dr. Yekaterina B. Khotskaya introduced me to animal handling and lent her technical expertise with the mammary fat pad tumor study.

I would have not made it this far without my parents, Orlando and Maria Saldaña, who always motivated me to work hard for my goals and provided a strong support system for me to succeed. I thank my brother Orlando Saldaña for being the best sibling I could ask for, and for making me a proud older sister. I'm thankful to my future husband, Dr. Marcus V. Ortega Alves, for his unconditional love and support since the beginning. Finally, I would like to thank Alison Fitzgerald, Dr. Sara Gorjestani, Dr. Kristen Holmes, Dr. Brian Pickering, and Sumaiyah Rehman for their friendship throughout graduate school.

The Role of Type I Insulin-Like Growth Factor Receptor Signaling in Breast Cancer Brain Metastasis

Publication No._____

Sandra M. Saldaña, B.A.

Supervisory Professor: Mien-Chie Hung, Ph.D.

ABSTRACT

Brain metastasis is a common cause of mortality in cancer patients. Approximately 20-30% of breast cancer patients acquire brain metastasis, yet potential therapeutic targets remain largely unknown. The type I insulin-like growth factor receptor (IGF-IR) is known to play a role in the progression of breast cancer and is currently being investigated in the clinical setting for various types of cancer. The present study demonstrates that the IGF-IR signaling axis is constitutively active in brain-seeking sublines of breast cancer cells, driving an increase in *in vitro* metastatic properties. We demonstrate that IGF-IR signaling is activated in an autocrine manner as a result of IGFBP3 overexpression in brain-seeking cells. Transient and stable knockdown of IGF-IR results in a downregulation of IGF-IR downstream signaling through phospho-AKT, as well as decreased *in vitro* migration and invasion of MDA-MB-231Br brain-seeking cells. Using an *in vivo* experimental brain metastasis model, we show that IGF-IR ablation attenuates the establishment of brain metastases and prolongs survival. Finally, we demonstrate that the malignancy of brain-seeking cells is attenuated by pharmacological inhibition with

picropodophyllin, an IGF-IR-specific tyrosine kinase inhibitor. Together, our data suggest that the IGF-IR is an important mediator of brain metastasis and its ablation delays the onset of brain metastases in our model system.

TABLE OF CONTENTS **PAGE**

LIST OF ILLUSTRATIONS **PAGE**

LIST OF TABLES **PAGE**

ABBREVIATIONS

AKT	**protein kinase B (PKB), a serine/threonine protein kinase**
BBB	**blood-brain barrier**
BSA	**bovine serum albumin**
Br	**brain-seeking**
BTB	**blood-tumor barrier**
cDNA	**complementary DNA**
DMEM/F12	**Dulbecco's modified eagle medium and Ham's F12 nutrient mixture**
DMSO	**dimethyl sulfoxide**
EDTA	**ethylenediaminetetraacetic acid**
EGFR (ErbB1)	**epidermal growth factor receptor**
ERK	**mitogen activated protein kinase 1 (MAPK1), member of extracellular regulated protein kinase family**
FBS	**fetal bovine serum**
GFAP	**glial fibrillary acidic protein**
H&E	**hematoxylin and eosin stain**

Her2/neu (ErbB2)	**human epidermal growth factor receptor 2**
HPRT1	**hypoxanthine phosphoriboryltransferase 1**
IACUC	**institutional animal care and use committee**
IP	**immunoprecipitation, immunoprecipitate**
IGF-1 (IGF-I)	**Insulin-like growth factor 1**
IGF-2 (IGF-II)	**Insulin-like growth factor 2**
IGF-IR	**Type I Insulin-like growth factor receptor**
IGFBP3	**Insulin-like growth factor binding protein 3**
IHC	**immunohistochemistry**
IRS-1	**Insulin receptor substrate 1**
IRS-2	**Insulin receptor substrate 2**
IVIS	***in vivo* imaging system**
kDa	**kilodalton**
Ki-67	**nuclear protein, cellular marker for proliferation**
Luc	**luciferase**
MAPK	**mitogen activated protein kinase, serine/threonine kinase**
MBT	**Metastatic Brain Tumors**

MFI	**median fluorescence intensity**
mTOR	**mammalian target of rapamycin, serine/threonine kinase downstream of AKT**
MTT	**(3-(4,5-Dimethylthiazol-2-yl)-2,5-diphenyltetrazolium bromide**
p70S6K	**serine/threonine serine kinase downstream of mTOR signaling pathway**
PAGE	**polyacrylamide gel electrophoresis**
PCR	**polymerase chain reaction**
PBS	**phosphate buffered saline**
PI3K	**phosphatidylinositide 3 kinase, upstream member of PI3K/AKT/mTOR pathway**
PPP	**picropodophyllin**
PTEN	**phosphatase and tensin homolog protein, tumor suppressor**
qRT-PCR	**quantitative real time RT-PCR**
RIPA buffer	**radioimmunoprecipitation assay buffer**
RT-PCR	**reverse transcriptase polymerase chain reaction**

SDS	**sodium dodecyl sulfate**
SEM	**standard error of the mean**
Ser	**serine**
SF	**serum-free**
shRNA	**short hairpin RNA**
siRNA	**small interfering RNA**
SphK1	**sphingosine kinase 1**
STR	**short tandem repeats**
TKI	**tyrosine kinase inhibitor**
TNBC	**triple-negative breast cancer**
Tyr	**tyrosine**
WB	**western blot**

CHAPTER 1

INTRODUCTION

1.1 Metastatic Brain Tumors (MBTs) of Breast Cancer

Brain metastases are the most frequent type of malignant brain tumors, and they commonly originate from lung, breast, melanoma, renal, and colon cancers (Barnholtz-Sloan et al., 2004; Eichler et al., 2011; Weil, Palmieri, Bronder, Stark, & Steeg, 2005). Approximately 10-16% of breast cancer patients develop brain metastases, and this continues to be a major cause of mortality in women (Barnholtz-Sloan et al., 2004; Cheng & Hung, 2007; Saunus, Momeny, Simpson, Lakhani, & Da Silva, 2011; Weil et al., 2005). The mean survival of patients with brain metastases ranges from 3-18 months, with a one-year survival rate of 20% (Andrews et al., 2004; Cheng & Hung, 2007; Sperduto et al., 2010). One recent retrospective study found that the presence of leptomeningeal disease (LMD) or triple-negative/Her2 status correlated with an even poorer than overall median survival of 3.1 months (Quigley, Fukui, Chew, Bhatia, & Karlovits, 2012). A retrospective study found that survival time is longer in patients who had a single metastatic lesion at diagnosis that was resected by surgery or gamma knife surgery (14.9 months), followed by patients who received whole brain radiotherapy alone (5.4 months), as compared to the patients who received no treatment (2.1 months) (S. S. Lee et al., 2008). The incidence of brain metastases is thought to be on the rise as patients are living longer due to the success of current therapies at controlling systemic disease while increasing the likelihood of circulating tumor cells to infiltrate the blood brain barrier (Cheng & Hung, 2007; Steeg, Camphausen, & Smith, 2011). Brain metastases are even more common in patients with Her2-

positive breast cancer who received treatment with Trastuzumab, which is very effective at controlling Her2-positive systemic disease but has poor effectiveness in the brain due to presence of the blood-brain barrier (N. U. Lin & Winer, 2007). Unfortunately, the increase in the proportion of patients presenting with brain metastases has not been met with a corresponding increase in available treatments, and there remains an urgent need for effective therapies to prevent and treat this condition.

1.2 Organ specificity of breast cancer metastasis

Stephen Paget's 1889 "seed and soil" hypothesis predicted that cancer cells, or "seeds" crosstalk with certain organ microenvironments, or "soil", during the process of metastasis (Paget, 1989). Another theory of cancer metastasis is the anatomical or mechanical model, which posits that tumor cells metastasize to the first organ they encounter in the circulation, as in the case of colon cancer liver metastasis (Langley & Fidler, 2011). The extent to which each of the models most closely describes the process of metastasis remains unclear, but the consensus is that both anatomical and microenvironmental factors are at play. Like several other cancer types, breast cancer preferentially metastasizes to certain organs, including the bone, lungs and liver. Figure 1 shows a schematic of a metastasizing breast cancer cell and the various barriers it must overcome in order to establish successful metastases. The brain is typically the last organ to acquire metastatic lesions, due to the initial protection provided by the blood-brain-barrier.

Molecular mechanisms underlying organ-specificity are continuously being uncovered, but there is still a long way to go in our understanding. A major determinant of breast cancer cells' ability to colonize in a new niche depends on the ability of the tumor cells to arrest, adhere to and penetrate the different organ barriers, and subsequent survival and proliferation of the cells in the metastatic niche. Figure 1 depicts a metastatic breast cancer cell in the circulation, and the various layers that must be overcome in order for the cell to invade the bone, lung and brain (Nguyen, Bos, & Massague, 2009).

In bone metastasis, chemokines such as SDF-1, osteonectin and osteopontin, among others, are known to promote breast cancer cell homing to the bone (Langley & Fidler, 2011). Expression level of CXCR4, the SDF-1 receptor in breast cancer cells was found to predict bone relapse in a recent clinical trial of patients with breast cancer (Sacanna et al., 2011). Furthermore, a gene signature comprising mainly of cell surface and secreted proteins was found to determine the bone-specific metastasis of 231 breast cancer cells (Kang et al., 2003). Two of the genes, interleukin-11 and CTGF, corresponded to osteolytic factors that are further enhanced by the prometastatic cytokine TGF beta, which is commonly secreted in bone (Buijs, Stayrook, & Guise, 2011).

Brain metastasis is a relatively new field of study, and it has recently come into focus due to its increasing incidence, limited treatment options and dismal survival rates. A 2009 study by Bos. et al. identified several genes that mediate extravasation of breast cancer cells through the blood-brain-barrier.

Cyclooxygenase COX2, HB-EGF (an EGFR ligand) and ST6GALNAC5, a sialyltransferase collectively accounted for the brain-metastatic properties of breast cancer cell lines (Bos et al., 2009). Another study by Palmieri et al. found Her2 overexpression increases brain metastasis of 231 breast cancer cells in a mouse model (Palmieri et al., 2007). In a subsequent study, the same group discovered that PEDF, a secreted cytokine, is downregulated in brain metastases, and its restoration inhibits the outgrowth of large brain metastases, while simultaneously offering neuroprotection to neuronal cells (Fitzgerald et al., 2012). Furthermore, a recent study by Su et. al. found that TAp63-/- mice can develop mammary carcinomas that spontaneously metastasize to the lung, liver and brain (Su et al., 2010). Another study showed that CXCR4 and its ligand SDF-1 alpha promoted migration the transendothelial migration of breast cancer cells by increasing permeability of monolayers of brain microvascular endothelial cells (B. C. Lee, Lee, Avraham, & Avraham, 2004). Most recently, a study by Okuda et al showed microRNA-7 is downregulated in brain metastases of breast cancer, resulting in upregulation of KLF4, which endows metastatic breast cancer cells with stem-like qualities and brain-specificity (Okuda et al., 2013).

Despite these advances in the study of brain metastasis in breast cancer, there is much work to be done to complete our understanding of the disease.

Figure 1

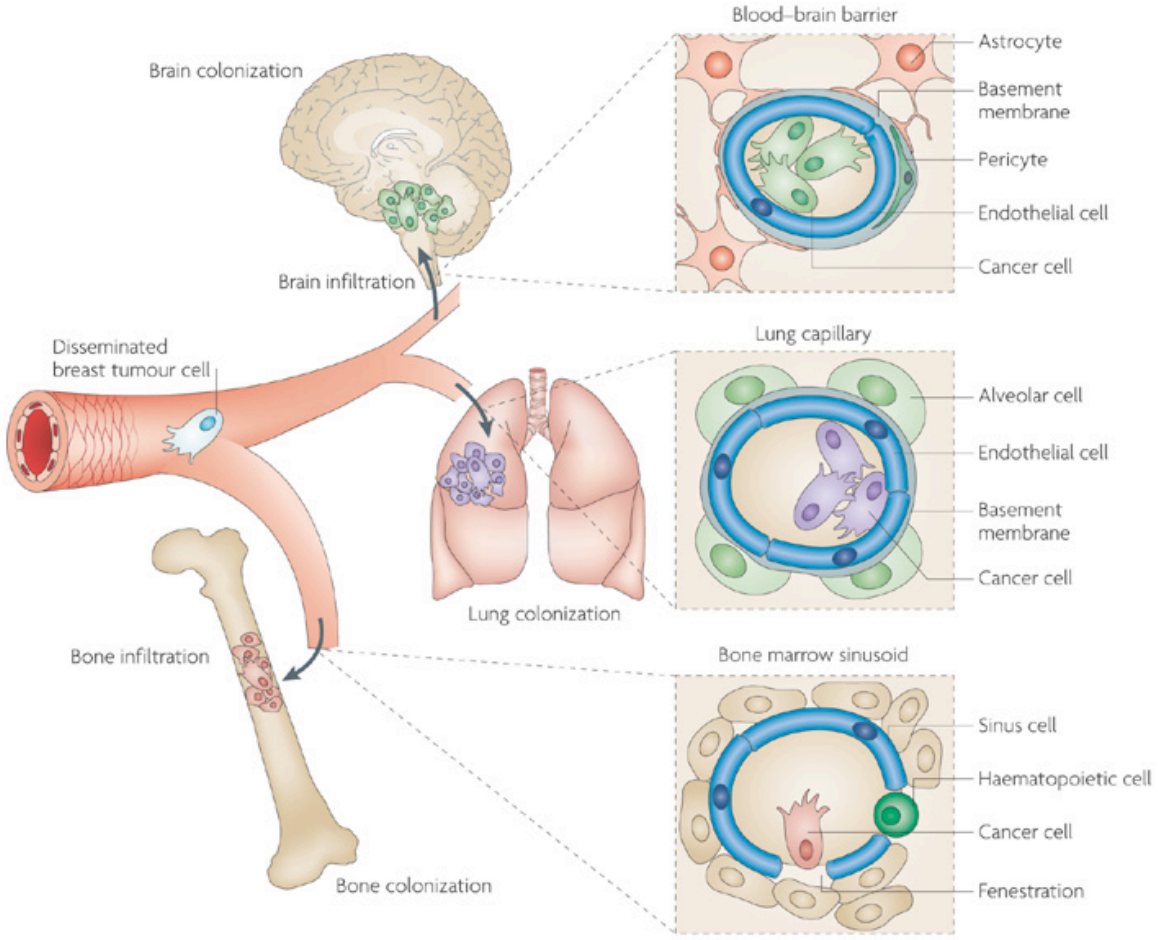
Blood–brain barrier
Astrocyte
Basement membrane
Pericyte
Endothelial cell
Cancer cell
Brain colonization
Brain infiltration
Disseminated breast tumour cell
Lung capillary
Alveolar cell
Endothelial cell
Basement membrane
Cancer cell
Lung colonization
Bone infiltration
Bone marrow sinusoid
Sinus cell
Haematopoietic cell
Cancer cell
Fenestration
Bone colonization
Nature Reviews | Cancer

Figure 1. Potential barriers to metastasis of breast cancer to different sites.

"Breast cancer cells entering the circulation can infiltrate a distant organ if they carry the necessary functions for extravasation. The fenestrated structure of bone marrow sinusoid capillaries is more permissive to cancer cell infiltration than the contiguous structure of lung capillary walls. Brain capillaries are more difficult to penetrate, owing to the unique nature of the blood-brain-barrier. Infiltration through these barriers selects for tumor cells that express the necessary extravasation functions. These functions can be provided by genes for which expression in primary tumors independently provides a selective growth advantage (such as vascular remodeling) or by genes for which expression in primary tumors provides no benefit but is a consequence of tumor microenvironment signals."

Reprinted with permission from Macmillan Publishers LTD: [Nature Reviews Cancer] (Nguyen et al., 2009), copyright 2009.

1.3 Role of the organ microenvironment in metastasis

It is well established that the tumor microenvironment actively participates in the metastatic process, through the interaction with the Extracellular Matrix (ECM) and recruitment of a variety of cells including tumor-associated fibroblasts, immune cells and bone-marrow derived cells (Joyce & Pollard, 2009). A recent study published by Luga et. al. showed that breast cancer associated fibroblasts secrete exosomes that activate the Wnt-PCP (planar cell polarity) pathway which induces cancer cell protrusions and motility, leading to metastasis (Luga et al., 2012). The tumor microenvironment, thus, is an important factor in determining whether metastatic foci will establish successfully.

1.4 EMT and tumor cell plasticity in metastasis

EMT, or epithelial-mesenchymal-transition, is the process by which cells switch their morphology and biochemical properties from epithelial to mesenchymal type (Kalluri & Weinberg, 2009). This process involves loss of expression of epithelial markers such as E-cadherin, adherens junction proteins and catenins, concomitant with a gain of expression in mesenchymal markers such as vimentin and fibronectin (Thiery, 2002). EMT allows cancer cells to dissociate from the tumor and acquire the ability for invasion and metastasis (Kalluri & Weinberg, 2009). However, the role of EMT in metastasis is considered “controversial”, due to a scarcity of *in vivo* evidence of the EMT process. The controversy is fueled by studies that found metastatic tumors tend to have epithelial-like properties, not mesenchymal properties as suggested by the EMT theory (Ledford, 2011). However, many argue that EMT must be a reversible process, termed MET, necessary for metastatic cells

to survive and proliferate in the target organ. A recent paper by Tsai and colleagues in the journal Cancer Cell showed that inducible expression of the transcription factor Twist1 is sufficient to promote the EMT transition in cancer cells, and shutting off this protein in the target organ where cells have metastasized results in a reversion of EMT, or MET, and allows cells to proliferate successfully in the metastatic site (Tsai, Donaher, Murphy, Chau, & Yang, 2012). In addition, Tsai et al. argue that a "partial EMT" may be sufficient for metastasis in some cases, a feature that facilitates the MET process in the distant organ and which has been reported in a recent study of bladder cancer metastasis (Tran et al., 2013). Furthermore, it has been shown that repression of MET-inducing factors (Ocana et al., 2012) and a reversal of EMT is a hallmark of successful metastasis (Chaffer et al., 2006). Interestingly, a partial MET phenotype was reported by Chao et al. in prostate cancer and breast cancer metastases, including brain metastases, characterized by re-expression of E-cadherins with mostly conserved expression of mesenchymal markers (Y. Chao, Wu, Acquafondata, Dhir, & Wells, 2012). The authors postulated that a partial MET not only facilitates metastasis in the first target distant site, but also facilitates the subsequent round of EMT that enables metastasis from metastasis. Taken together, these recent studies point to a metastasis model whereby tumor cells possess a degree of plasticity that is molded by the primary tumor and the metastatic site's stromal microenvironment, rather than a fixed genetic signature that dictates a sequence of metastatic steps.

However, even with mounting evidence in favor of EMT/MET theory, there is a different school of thought that advocates for genetic selection, or a kind of

Darwinian adaptation as the basis for metastasis. This theory posits that metastasis is the end result of a series of genetic mutations that occur in response to environmental pressures. Rather than one theory prevailing over the other, it is likely that both mechanisms are at play in metastasis formation. Scheel et al., for example, propose that genetic selection is likely responsible for the early stages of metastasis leading up to the pre-invasive stage, while it is unlikely that genetic evolution is responsible for all of the biochemical and morphological changes that allow cells to dissociate from the solid tumor. This is supported by observations that EMT typically takes place in the outer edges of "epithelial islands" within solid tumors (Scheel, Onder, Karnoub, & Weinberg, 2007); in other words, EMT happens primarily in those cells that are in direct contact with the host microenvironment, not in the entire tumor as would be expected in a genetic adaptation model. Still, other cases exist that support a clonal selection model in which particular genetic profiles give rise to metastasis, such as evidenced in medulloblastoma metastases that have nearly identical genetic profiles to each other, but different from their primary tumor of origin (Wu et al., 2012). Therefore, it is important to keep in mind both of these theories when evaluating the role of IGF-IR in brain metastasis of breast cancer in our model system.

1.5 Blood-Brain Barrier

The blood-brain barrier (BBB) is the layer that separates the brain microvessels' capillary lumen from the brain parenchyma, and it plays an important role in both initially blocking tumor cell invasion and protection of the tumor cells once they have begun the process of invasion (Wilhelm, Molnar, Fazakas, Hasko, & Krizbai, 2013).

The BBB is composed of endothelial cells, a basal membrane, pericytes and astrocytes(Cheng & Hung, 2007; Wilhelm et al., 2013). The BBB endothelial cells are connected by tight junctions and adherens junctions, which are composed of transmembrane proteins such as occludin, claudins, immunoglobulin-like molecules also known as junctional adhesion molecules, and others that have not been well characterized(Cheng & Hung, 2007; Wilhelm et al., 2013).

1.6 Therapies for brain metastatic breast cancer

Therapeutic approaches for the treatment of brain metastasis are limited. In cases where brain metastases are diffuse, whole-brain radiotherapy (WBRT) is a standard therapy, but mainly provides a palliative solution, since tumors inevitably become resistant to radiation and recur (Padovani, Muracciole, & Regis, 2012). One recent study identified the Hepatocyte growth factor (HGF) – c-Met pathway as overexpressed in breast cancer lines that were irradiated. By combination of radiotherapy and c-Met inhibitors, they were able to harness this resistance pathway and synergistic effects in a mouse model, which may be a future direction for this line of treatment (Yang et al., 2013).

Stereotactic radiosurgery (SRS), or gamma-knife radiosurgery, is used in cases with 3 or less metastatic lesions. Survival rates of patients treated by gamma-knife vary by subtype of the primary tumor, with HR+/Her2+ (luminal Her2) subtypes showing the longest survival and HR-/Her2- (basal type) with the lowest survival (Vern-Gross et al., 2012). However, whether survival times are dependent on gamma-knife surgery itself is unknown. A study of WBRT in combination with SRS showed

improved local control of disease, although overall survival remained the same (Tsao et al., 2012). However, another study found that omission of WBRT with SRS led to progression of brain metastases (Dyer et al., 2012). Discrepancies between the conclusions of these and many other studies highlight the complexity of the disease and the need for a better understanding of the underlying mechanisms that mediate response to the different available therapies.

Despite the dearth of therapies for brain metastasis, some new approaches are beginning to show promise in the clinic. In patients with Her2 positive metastatic breast cancer, Trastuzumab is the standard of care therapy. When administered after the diagnosis of brain-metastatic disease, Trastuzumab extends overall survival, presumably due to control of systemic disease and relatively easier access to the brain in patients with a leaky blood-brain barrier (Mehta, Brufsky, & Sampson, 2012). In patients with an intact BBB, however, the drug's molecular weight is too large to gain access into the brain parenchyma. A recent Phase II clinical trial tested the efficacy of systemic treatment with lapatinib in combination with capecitabine as a first-line therapy for Her2-positive metastatic breast cancers previously untreated for brain metastases. In this setting, the drug combination achieved 65% response consisting of at least 50% volumetric reduction of brain metastases, and all patients in the study achieved at least a partial response (Bachelot et al., 2013). Interestingly, patients treated with the combination of lapatinib plus capecitabine received a 7 month increase in survival compared to patients who were treated with trastuzumab-based therapy (Kaplan et al., 2013).

Since it is believed that the efficacy of brain metastasis therapies are mostly limited by the presence of the blood-brain-barrier, new techniques are under development that focus on overcoming this obstacle. One such new technique is called ultrasound-mediated blood-brain-barrier disruption, which permeabilizes the BBB/BTB using focused ultrasound bursts and microbubbles in the circulation. When combined with trastuzumab treatment, this technique was shown to significantly extend the survival of rat model of brain metastasis of BT474 breast cancer cells, compared to controls treated with trastuzumab alone (Park, Zhang, Vykhodtseva, & McDannold, 2012).

1.7 The type-I Insulin-like growth factor signaling axis

Figure 2 shows the key components of the IGF-I Receptor signaling axis discussed in the sections that follow.

1.7.I IGF-I Receptor

The type I insulin-like growth factor receptor (IGF-IR) is known to promote metastasis in several cancers, including those of the colon, pancreas, prostate, and breast (Chitnis, Yuen, Protheroe, Pollak, & Macaulay, 2008; Lopez & Hanahan, 2002; Sachdev, Zhang, Matise, Gaillard-Kelly, & Yee, 2010). IGF-IR is composed of an extracellular α ligand-binding subunit and an intracellular β subunit responsible for signal transduction. IGF-IR shares 84% homology with the intracellular tyrosine kinase domain of the Insulin Receptor (IR) (Fujita-Yamaguchi et al., 1986), and the homology is even higher in the ATP-binding site, at 95%. It is therefore not surprising that IGF-IR receptors have been found to heterodimerize with IR and

successfully transduce IGF-1-dependent downstream signals (Takata & Kobayashi, 1994).

IGF-IR is activated upon binding the IGF-I ligand, although IGF-II ligand, which shares 62% amino acid sequence homology with IGF-I, can also bind and activate the receptor with a two to fifteen-fold lower affinity (Fernandez & Torres-Aleman, 2012; Vashisth & Abrams, 2010; Yu & Rohan, 2000). Upon ligand binding, IGF-IR becomes autophosphorylated at Tyr 1131, 1135, and 1136 in the β subunit and subsequently recruits a host of proteins, including IRS-2, that activate signaling via PI3K/AKT and Ras/Raf/MAPK pathways to promote cell motility and pro-metastatic behavior in breast cancer cells (Chitnis et al., 2008; Jackson, Zhang, Yoneda, & Yee, 2001; Kato, Faria, Stannard, Roberts, & LeRoith, 1994). It is common for breast tumor tissues to express high amounts of IGF-IR, although amplification at the DNA level has been found in some cases as well (Adelaide et al., 2007).

1.7.II IGF-I and IGF-II ligands

In models of breast cancer bone metastasis, IGF-I ligand promotes motility of bone-metastatic cells through IGF-IR activation (Yoneda, Williams, Hiraga, Niewolna, & Nishimura, 2001), and bone-derived IGF-1 can activate the process of bone metastases in breast cancer in a paracrine manner (Hiraga et al., 2012). Inhibition of astrocyte-derived IGF-1 ligand was shown to reduce *in vitro* growth and adhesion of a brain metastatic variant of MDA-MB-435 breast cancer cells (Sierra et al., 1997).

In breast cancer patients, phosphorylated IGF-IR associates with poor survival, and a recent study further showed that phosphorylation of IGF-IR at Tyr 1135/1136 is correlated with brain metastases of breast and lung cancers (Improta et al., 2011; Law et al., 2008). However, the biological significance of IGF-IR activation in brain metastases of breast cancer has not been addressed to date.

1.7.II.A IGFBP3

The regulation of IGF-IR signaling is complex and not yet fully understood; however, it is well established that the IGF-IR signaling axis can be dysregulated by altered expression of the IGF ligands and IGF-binding proteins. The insulin-like growth factor binding protein-3 (IGFBP3) is the major binding protein and regulator of IGF-1 ligand bioavailability and has been reported to inhibit as well as potentiate the activity of IGF-IR signaling in different cancers (Firth & Baxter, 2002; Martin & Baxter, 2011; Schedlich & Graham, 2002). In the least malignant breast cancer cell lines, IGFBP3 plays an inhibitory role as a tumor suppressor, and this function is reversed in highly malignant breast cancer cells which express higher levels of IGFBP3 (Schedlich & Graham, 2002). IGFBP3 also promotes migration in breast cancer cells (O'Han, Baxter, & Schedlich, 2009). In melanoma metastasis, IGFBP3 is overexpressed in metastatic tissues and is associated with malignant progression (Xi et al., 2006). IGFBP3 was also shown to stimulate IGF-IR phosphorylation indirectly through activation of sphingosine kinase 1 (SphK1) and EGFR transactivation (Martin & Baxter, 2011). Adding yet another layer of complexity is the finding that IGFBP3 expression itself can be regulated by IGF-1 ligand through

PI3K/AKT signaling in mammary epithelial cells, suggesting that the IGF-IR axis is self-regulated in an autocrine manner (Sivaprasad et al., 2004).

1.7.III Insulin receptor substrate (IRS) proteins

Insulin Receptor substrate proteins act as signaling intermediates between cell surface receptors, such as Insulin Receptor and Insulin-like growth factor receptor, and downstream signaling molecules such as PI3K and MAPK pathways. They do not possess kinase activity, but instead act as scaffolds upon which other signaling molecules dock to form signaling complexes (Mardilovich, Pankratz, & Shaw, 2009). The IRS protein family consists of several isoforms: IRS-1 was the first described as a phosphoprotein that became phosphorylated in response to insulin stimulation, IRS-2 was the second discovered, believed to be homologous to IRS-1, and IRS-4 which is only expressed in the brain, thymus, liver and kidney (Shaw, 2011).

The two most significant IRS isoforms in normal physiology are IRS-1 and IRS-2, and they perform essential complementary roles in the regulation of glucose metabolism (Taniguchi, Ueki, & Kahn, 2005). Knockdown of IRS-1 in livers of normal mice resulted in accumulation of gluconeogenic enzymes and increased blood sugar levels, whereas IRS-2 knockdown resulted in upregulation of lipogenic enzymes and accumulation of hepatic lipid (Taniguchi et al., 2005). The general consensus about the roles of IRS proteins in cancer is that IRS-1 and IRS-4 associate with tumor growth and cell proliferation, while IRS-2 promotes invasion and motility (Mardilovich et al., 2009). In breast cancer metastasis specifically, IRS-

1 appears to be a metastasis suppressor while IRS-2 promotes the metastatic process (Gibson, Ma, & Shaw, 2007).

Figure 2

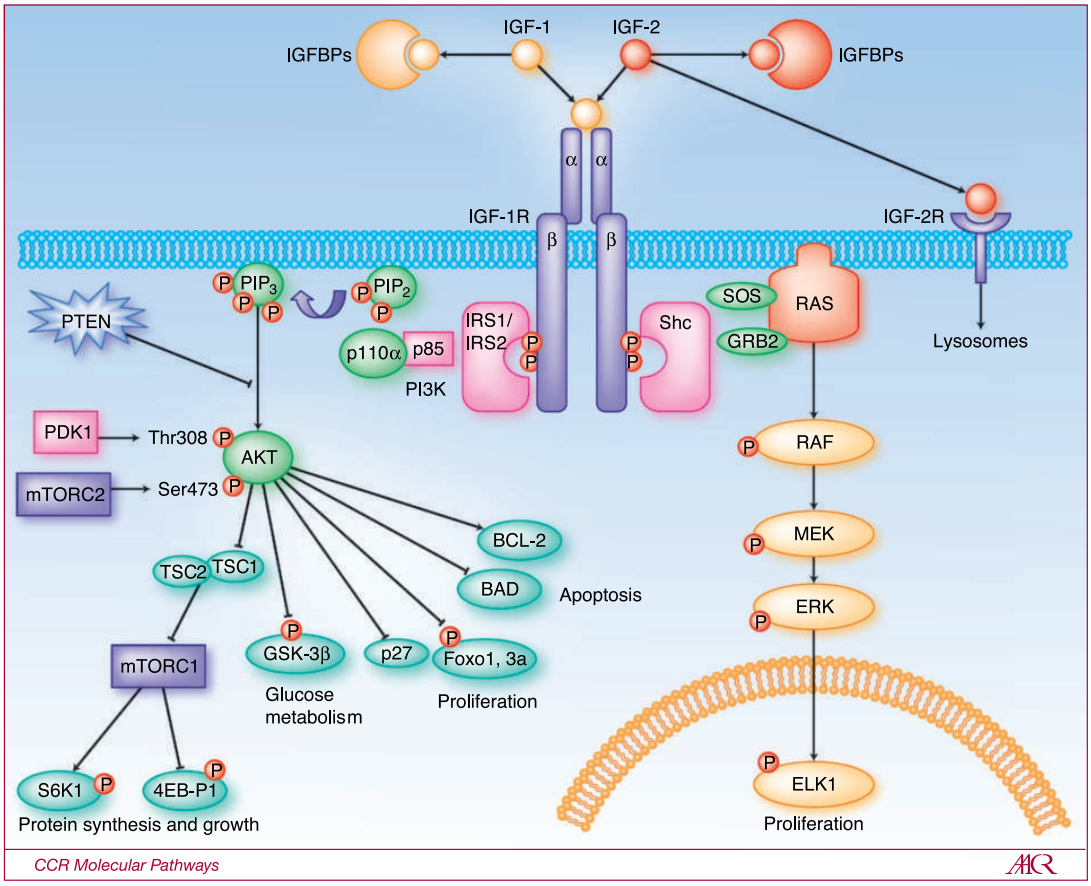
IGFBPs
IGF-1
IGF-2
IGFBPs
α
α
IGF-1R
β
β
IGF-2R
PIP3
PIP2
PTEN
p110α
p85
PI3K
IRS1/
IRS2
Shc
SOS
RAS
GRB2
Lysosomes
PDK1
Thr308
AKT
mTORC2
Ser473
RAF
MEK
ERK
BCL-2
BAD
Apoptosis
TSC2
TSC1
mTORC1
GSK-3β
p27
Foxo1, 3a
Glucose
metabolism
Proliferation
S6K1
4EB-P1
Protein synthesis and growth
ELK1
Proliferation
CCR Molecular Pathways
AACR

Figure 2. Key components of the IGF-IR pathway.

The IGF-1 and IGF-2 ligands are both capable of binding and stimulating the catalytic activity of the IGF-IR. Bioavailability of IGF-1 is modulated by a family of IGFBPs. Upon binding either IGF-1 or IGF-2, the IGF-IR undergoes receptor cross-linking and autophosphorylation, leading to the creation of multiple docking sites for the adaptor proteins IRS-1, IRS-2 and SHC. IRS-1 and IRS-2 binding results in activation of the class I PI3 Kinase, whose catalytic activity is the conversion of PIP2 to the lipid messenger PIP3. This event recruits the AKT family of kinases to the plasma membrane, where they can be phosphorylated and activated by PDK1 and the mTOR-containing complex MTORC2. Activated AKT then mediates a host of cell signaling events, including disinhibition of the mTORC1 complex and increased protein synthesis and cell growth, increased conversion of glucose to glycogen via inhibition of GSK-3B, and increased proliferation and survival by activation or inhibition of key effectors such as the FOXO transcription factors, p27, BAD, and BCL-2. In contrast, Shc binding to activated IGF-IR results in stimulation of the RAS/MAP kinase pathway, which also leads to increased cell proliferation.

1.8 IGF-IR Inhibitors

IGF-IR has become an attractive target in the clinic over the last ten years, due to its central role in cancer cell signaling. Various monoclonal antibodies and tyrosine kinase inhibitors (TKIs) against IGF-IR are under investigation for treatment of solid tumors (Chitnis et al., 2008). Most antibody-based IGF-IR inhibitors function by blocking IGF-ligand binding to the receptor, decrease expression of IGF-IR at the cell surface by mediating receptor internalization, and blocking intracellular signaling primarily through PI3K/AKT pathway (Zha & Lackner, 2010). It is believed that monoclonal antibodies are more specific, due to the amino-acid sequence similarity of tyrosine kinase domain which makes specificity of TKIs a significant issue (Rodon, DeSantos, Ferry, & Kurzrock, 2008). Initial results of IGF-IR treatment in large clinical trials have not been as successful as hoped; however, anecdotal cases of individual positive responses to IGF-IR therapies have encouraged continued study into biomarkers that will enable selection of the best target population (Gombos, Metzger-Filho, Dal Lago, & Awada-Hussein, 2012).

Picropodophyllin (PPP) is the only tyrosine kinase inhibitor currently available that can discriminate between insulin receptor and IGF-IR (Girnita et al., 2004). PPP is thought to inhibit IGF-IR by utilizing the MDM2 E3 ligase, which is known to ubiquitinate the IGF-IR and causes its downregulation (R. Vasilcanu et al., 2008).

1.9 *In vivo* models of brain metastasis

Although brain metastasis studies typically rely on a combination between *in vitro* and *in vivo* experimental approaches to formulate conclusions, some researchers

have recently argued that *in vitro* and *in vivo* studies of the early steps of brain colonization from the bloodstream should only be studied in vivo (Lorger, Lee, Forsyth, & Felding-Habermann, 2011). Behavior of breast cancer cells in *in vitro* cell adhesion and transendothelial migration analyses, for example, correlate poorly with the behavior of the same cells in *in vivo* brain metastasis models. Since cells are injected in the carotid artery, our model of brain metastasis circumvents many anatomical barriers and primarily addresses the late stages of brain metastasis.

1.10 Statement of problem, hypothesis and project goals

The functional role of IGF-IR in primary breast cancer and breast cancer metastasis has been well documented by others. Furthermore, Improta et. al. have found a correlation of phosphorylated IGF-IR in patient samples of brain metastases from breast cancer. However, whether IGF-IR directly plays a functional role in the establishment of brain metastases has not been addressed. It is possible that IGF-IR activation in brain metastases is a result of the highly malignant primary and/or metastatic breast tumors from which they arise. However, it is also possible that IGF-IR activation itself enables the establishment of breast cancer cells in the brain by means of a survival advantage. Further studies are needed in order to discern whether IGF-IR provides a survival advantage to breast cancer cells in the brain.

In the present study, we sought to address the biological relevance of IGF-IR signaling in the metastasis of breast cancer to the brain. **We hypothesized that IGF-IR activation confers a metastatic advantage and enables the outgrowth of breast cancer cells in the brain.** Figure 3 depicts a model of our hypothesis.

First, we test whether IGF-IR signaling plays a role in the metastatic potential of brain-seeking breast cancer cells *in vitro*. Using an *in vivo* experimental brain metastasis model, we found that ablation of IGF-IR expression can prevent the outgrowth of brain metastases, suggesting that this signaling pathway merits further study as a potential target for the treatment of breast cancer brain metastasis.

Figure 3

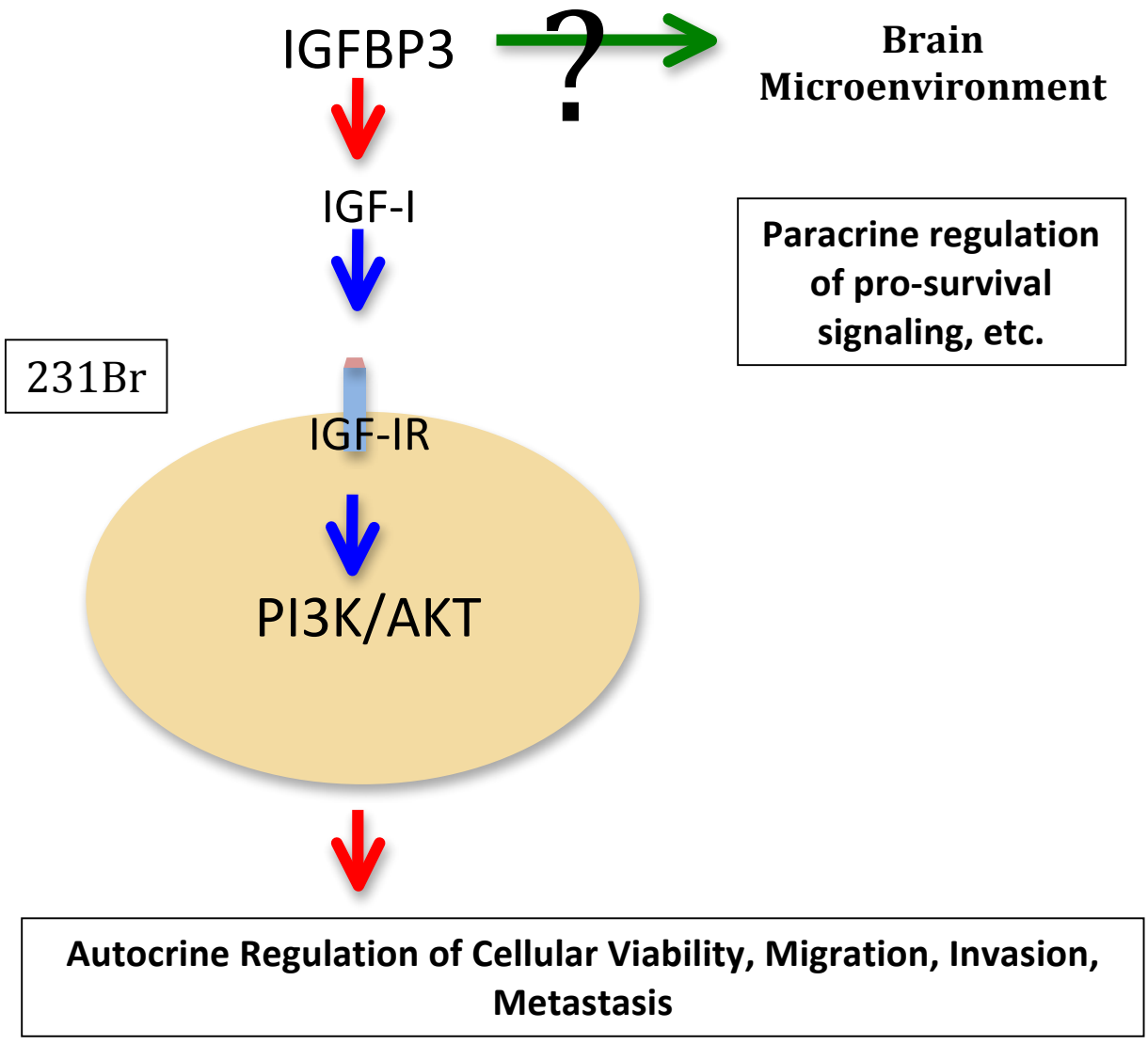
IGFBP3
?
Brain Microenvironment
IGF-I
Paracrine regulation of pro-survival signaling, etc.
231Br
IGF-IR
PI3K/AKT
Autocrine Regulation of Cellular Viability, Migration, Invasion, Metastasis

Figure 3. Model depicting project hypothesis.

Brain-seeking breast cancer cells overexpress the secreted form of IGFBP3, which may enhance the bioavailability of IGF-1 or independently activate IGF-I Receptor phosphorylation. Once activated, IGF-IR recruits docking proteins such as IRS-2, which enable the assembly of protein complexes that transduce signaling downstream through the PI3K/AKT pathway. IGFBP3 may also modulate the brain microenvironment in a paracrine manner, but future studies should explore that possibility in further detail.

CHAPTER 2

MATERIALS AND METHODS

2.1 Cell Culture

All cancer cell lines were maintained at 37°C in a 5% CO_2 incubator. Unless otherwise noted, cells were cultured in complete medium containing DMEM/F12 with 10% fetal bovine serum (FBS) and penicillin/streptomycin. The human MDA-MB-231Br (brain-seeking) cell line and its corresponding MDA-MB-231P (parental) cells were contributed by Dr. Patricia Steeg and previously described (Yoneda et al., 2001). The BT474 M1 (parental) and BT474 Br3 (brain-seeking) cell lines were established by Dr. Dihua Yu (MD Anderson, Houston, TX) and a detailed description of the BT474Br3 cell line will be published later by Dr. Yu's group. Cell lines were validated by STR DNA fingerprinting using the AmpF/STR Identifiler kit according to manufacturer instructions (Applied Biosystems). The STR profiles were compared to known ATCC fingerprints (ATCC.org), to the Cell Line Integrated Molecular Authentication database (CLIMA) version 0.1.200808 (Nucleic Acids Research 37:D925-D932 PMCID: PMC2686526) and to the MD Anderson fingerprint database. The STR profiles matched known DNA fingerprints or were unique. Cells were incubated with 50 ng/mL human recombinant IGF-1 (#I3769, Sigma) for the indicated time points in ligand-stimulation experiments.

2.2 Immunoprecipitation and Western blotting

Equal numbers of cells per sample well were seeded and cultured in complete medium and/or treated as specified. For analysis, cells were washed with PBS, trypsinized, and pelleted. Equal amounts of protein were resuspended in IP binding buffer (10x RIPA containing 0.5 M Tris-HCl (pH 7.4), 10% NP-40, 1.5 M NaCl, and

10 nM EDTA). Either Rabbit IgG (#sc-2027, Santa Cruz Biotechnology) or anti-IGF-IRβ (#sc-462, Santa Cruz Biotechnology) were added at 4°C overnight. Lysates were incubated with Protein G agarose beads for 4 hr at 4°C, pulled down by centrifugation, and then washed extensively with IP binding buffer containing protease and phosphatase inhibitors. Immunoprecipitates were denatured using sample buffer containing β-mercaptoethanol, centrifuged, and the protein-containing supernatants were then analyzed by SDS-PAGE. Membranes were incubated with anti-IGF-IRβ-pY1131/InsRβ-pY1146 (#3021, Cell Signaling Technology), anti-IGF-IRβ-pY1135 (#3918, Cell Signaling Technology), and anti-p-Tyr-100 (#9411, Cell Signaling Technology) to measure phosphorylation level of IGF-IR. For IP-Western input controls and all other samples analyzed by SDS-PAGE, wells were loaded with 70 μg of protein. Western blot membranes were probed with anti-IGFBP3 (C-19; #sc-6003, Santa Cruz Biotechnology), anti-AKT (#9272, Cell Signaling Technology), anti-pAkt (S473; #9271, Cell Signaling Technology), anti-S6K1 (#sc-230, Santa Cruz Biotechnology), anti-pS6K1 (T389; #9205, Cell Signaling Technology), and anti-tubulin (#T5168, Sigma). For IGFBP3 Western blots, 48-hr conditioned medium was collected and concentrated 40-fold using Millipore Amicon Ultra-4 centrifugal filters (Fisher). Equal protein amounts were loaded into each well of an SDS-PAGE.

2.3 Flow Cytometry

IGF-IR phosphorylation was measured by flow cytometry. Cells were prepared as previously described (Krutzik & Nolan, 2003). Briefly, cells were serum-starved for

24 hr and then fixed for 10 min at room temperature with 1.5% paraformaldehyde by adding it directly into the medium used to collect cells after trypsinization. Cells were pelleted, permeabilized by adding ice-cold methanol and vortexing vigorously, and then incubated for 10 min at 4°C. Cells were then washed twice with staining buffer (PBS containing 1% BSA) and resuspended in staining buffer at 500,000 cells per 100 µl. Finally, cells were stained with AlexaFluor 647 mouse anti-IGF-1 Receptor (pY1131; #558588, BD Biosciences) and analyzed using the BC Gallios flow cytometer. Unstained cells were used as a control. All data were analyzed using the FlowJo version X software.

2.4 Production of stable cell lines

MDA-MB-231Br cells were first transduced with the luciferase expression vector pLenti CMV V5-LUC Blast w567-1 (plasmid #21474, Addgene) and the selected using blasticidin. Stable IGF-IR knockdowns (shIGFR) were obtained by transfection of MDA-MB-231Br cells with two lentiviral pLKO.1 constructs containing shRNA against IGF-IR target sequences, GAGACAGAGTACCCTTTCTTT and GCCGAAGATTTCACAGTCAAA (TRCN0000121135 and TRCN0000039675, respectively, Open Biosystems). MDA-MB-231Br control cells (Vector) were obtained by stable transfection with a pLKO.1 puro empty vector control plasmid (Sigma). Luciferase, shRNA, or control constructs were co-transfected with lentiviral packaging plasmids into 293T cells, and viral particles were harvested at 24 and 48 hr post-transfection. MDA-MB-231Br cells were infected with virus for 48 hr in the presence of 5 µg/mL polybrene. Luciferase-expressing cells were first selected by

incubation in complete medium containing blasticidin (2 μg/ml) for 2 weeks. After stable luciferase-expressing MDA-MB-231Br cells were obtained, shRNA and control vector infections were carried out and stable clones were selected using culture medium containing puromycin (2 μg/ml) for 2 weeks. Knockdown of IGF-IR was verified by Western blot. Luciferase expression was measured using the IVIS imaging system to ensure all cell lines retained similar expression level.

2.5 Wound-healing assays

MDA-MB-231Br shIGF-IR or shControl stable cells were seeded in a Costar 12-well dish (Sigma CLS3513) and cultured until confluent. A wound was introduced using a 200-μl pipette tip, and cell migration was monitored using the Zeiss Axiovert 200M time-lapse microscope and 10x phase contrast objective. Images of specific positions were taken at 30-min intervals over 24 hr and recorded using the AxioVision 4.6 software. Relative migration was calculated by measuring wound area at different time points using ImageJ.

2.6 Intracarotid mouse model of experimental brain metastasis

Female Swiss nu/nu mice 8 weeks of age were purchased in-house from MD Anderson's Department of Veterinary Medicine and Surgery – ERO Animal Resources. Mice were anesthetized with ketamine/xylazine and inoculated with 200,000 MDA-MB-231Br-shControl, -shIGFIR (B) or -shIGFIR (F) cells in 100 μl HBSS via injection into the right common carotid artery. Cells were verified to have a minimum of 95% viability prior to inoculation in mice. Development of brain

metastasis was observed once weekly by luciferase imaging using the IVIS imaging system by Caliper Life Sciences. For imaging, mice were anesthetized by isofluorane/O_2 and injected intraperitoneally with 100 µL D-luciferin (Caliper Life sciences). Ten minutes after D-luciferin injection, images of brain metastases were captured using the Living Image 3.2 software. To obtain brain tissues, mice were euthanized according to animal facility guidelines under CO_2 asphyxiation followed by cervical dislocation. Brains were excised immediately following euthanasia and fixed in 10% neutral buffered formalin 24-48 hr at room temperature. Samples were then washed thoroughly with PBS and cut into sections across the coronal plane. Brain cross sections were paraffin embedded for analysis by immunohistochemistry (IHC). All animal procedures were performed under the guidelines approved by the Institutional Animal Care and Use Committee (IACUC) at MD Anderson Cancer Center.

2.7 Immunohistochemistry (IHC)

For IHC, a modified immunoperoxidase staining method from the avidin-biotin complex technique was used as described previously (Xia et al., 2004). Slides (4 µm thick) were first deparaffinized. Following antigen retrieval, the slides were digested with 10 mM Tween 20 citrate buffer (pH 6.0). The endogenous peroxidase activity was blocked by incubation in 0.3% hydrogen peroxide. The slides were then blocked with 10% normal goat or horse serum for 30 min and incubated overnight with primary antibodies, including anti-IGF-IR pAb (1:80 dilution; Santa Cruz Biotechnology), anti-IGF-IR pAb (1:50; Cell Signaling Technology), anti-phospho-

AKT (Ser473; 1:100; Cell Signaling Technology), anti-ki-67 pAb (ready to use; Zymed); and anti-GFAP pAb (1:50; Cell Signaling Technology). After primary antibody hybridization, slides were incubated with biotinylated secondary antibodies, followed by incubation with avidin-biotin-horseradish peroxidase complex (Vector Laboratories). Antibody detection was performed with the 0.125% aminoethylcarbazole chromogen (AEC) substrate solution (Sigma). The slides were counterstained with Mayer's hematoxylin (Sigma) and then mounted. For the negative control, all incubation steps were identical except that PBS was used instead of primary antibody. For the positive control, a previously identified strongly staining tumor tissue section was used. The prepared slides were examined by light microscopy. To ensure absolute objectivity of these IHC studies, experienced pathologists, who stained and evaluated primary tumor sections, conducted the experiments. The slides in which there was a scoring discrepancy >10% were re-evaluated and reconciled on a two-headed microscope.

2.8 Cell cycle analysis

Equal cell numbers were seeded in complete medium overnight and were either untreated or treated with picropodophyllin (Sigma) at 1 µg/mL for 48 hr. Cells were then washed with PBS, trypsinized, and fixed in 70% ethanol for 24 hr. After fixation, cells were washed twice with PBS and incubated with 40 µg/ml propidium iodide to stain DNA and 0.5 µg/ml RNAseH to degrade RNA to prevent it from being included in the cell cycle analysis. Cell cycle was then analyzed using the BC Gallios flow cytometer.

2.9 Quantitative real-time PCR of IGFBP3

RNA from MDA-MB-231P and MDA-MB-231br cells was extracted using the Qiagen RNEasy mini kit (Qiagen). cDNA was obtained by using the SuperScript First-Strand System for RT-PCR (Life Technologies). Real-time PCR reactions were prepared with 1x iQ SybrGreen Supermix (Bio-Rad) and 0.250 nM forward and reverse primers. Cycling conditions consisted of annealing, amplification and melt steps using the Applied Biosystems Veriti real-time PCR thermal cycler. Relative gene expression was calculated by dividing the IGFBP3 expression value by the HPRT1 expression value.

2.10 Transwell migration and invasion assay

Migration assays were performed using a 24-well transwell plate (Corning) and invasion assays were performed using the 24-well BD BioCoat Matrigel Invasion Chambers (BD Biosciences) according to the manufacturer's instructions. MDA-MB-231P (25,000) or MDA-MB-231Br (40,000) cells were seeded in the chamber inserts and allowed to migrate for 24 hr. Migrated cells were fixed with 4% paraformaldehyde, stained with crystal violet (0.1% in ethanol), and counted. Experiments were performed a minimum of 3 times in triplicate, and 5 fields of cells were counted at 10x magnification per chamber insert.

2.11 Proliferation assays

MTT (3-(4,5-Dimethylthiazol-2-yl)-2,5-diphenyltetrazolium bromide) assay of shIGF-IR and shControl cells was performed by seeding cells overnight at a concentration

of 10,000 cells per well in a 96-well plate. After 24, 48, and 72 hr, MTT reagent was added and cells were incubated at 37°C in 5% CO2 for 4 hr. Medium was then aspirated, and cells were lysed with DMSO and shaken gently for 1 hr at room temperature before measuring the optical density at 595 nm with a spectrophotometer. The growth of shIGF-IR stable transfectants was also measured by seeding cells at a concentration of 100,000 cells per well in a 6-well dish and counting cells using the Z1 Coulter Particle Counter (Beckman Coulter). All wells for MTT Assay and cell counting experiment were seeded in triplicate and experiments performed a minimum of 3 times.

2.12 Statistical analysis

Significance in the brain metastasis-free survival curve was calculated using the Gehan-Wilcoxon test. All other samples were analyzed using a two-tailed student's t test. Results with $p < 0.05$ were considered statistically significant.

CHAPTER 3

THE ROLE OF TYPE I INSULIN-LIKE GROWTH FACTOR RECEPTOR IN BRAIN-SEEKING BREAST CANCER CELLS

3.1 Brain-seeking breast cancer cells express higher amounts of IGF-I Receptor

In order to assess the importance of IGF-IR in our model system, we were interested characterizing the expression profile of the receptor in our sets of 231 and BT-474 parental and brain-seeking cell lines. We performed a western blot of total IGF-IR expression in 231P/Br and BT474M1/Br3 cells, and found that IGF-IR is highly expressed in parental breast cancer cells, and expression is further increased in brain-seeking sublines (Figure 4, top). Densitometric analysis was done using ImageJ software to confirm the increase in IGF-IR expression normalized to tubulin loading control (Figure 4, bottom). Increased IGF-IR expression in brain-seeking cell lines suggested that this receptor may be enriched in highly metastatic cells.

3.2 Type I IGFR is autophosphorylated in brain-seeking breast cancer cells

Previous studies suggest that IGF-1 signaling and IGF-IR activation play a role in the brain specificity of metastatic breast cancer (Improta et al., 2011; Sierra et al., 1997). To determine the relevance of IGF-IR activation in our model of brain metastasis, we characterized the activation profile of IGF-IR in parental MDA-MB-231 (231P) and parental BT474 M1 breast cancer cells for comparison to their respective brain-seeking sublines, MDA-MB-231Br (231Br) (Yoneda et al., 2001) and BT474Br3. One of the current limitations of studying the phosphorylated form of IGF-IR is the cross-reactivity of commercially available antibodies with homologous phosphorylation sites on the insulin receptor. To circumvent this issue, we first immunoprecipitated the IGF-IR β subunit with a specific antibody that does

not cross-react with the insulin receptor, followed by immunoblotting with phospho-IGF-IR antibody against Tyr 1131, the earliest autophosphorylation site that is absolutely required for IGF-I ligand-dependent IGF-IR function (Kato et al., 1994). We found that 231Br and BT474Br3 cells had higher IGF-IR autophosphorylation compared to the parental cells under normal growth conditions in complete medium (Figures 5A and 5B). After normalizing each cell line's phosphorylation signal to its own total IGF-IR protein band, autophosphorylation of IGF-IR was increased by 27.4% and 21.6% in 231Br and BT474 Br3, respectively (Figures 5C and 5D).

To confirm this observation and to obtain a more detailed picture of the IGF-IR activation profile in brain-seeking cells, we examined IGF-IRβ phosphorylation using flow cytometry with an Alexa647-conjugated phospho-Tyr1131-IGF-IRβ antibody. We found that both 231Br and BT474Br3 cell lines expressed more phosphorylated IGF-IR than parental breast cancer cells under normal growth conditions in complete medium (Figures 6A and 6B). An average of 36.4% of the 231Br cell population was positive for phospho-Tyr1131 IGF-IRβ, compared to 14.6% of 231 parental cells ($p < 0.005$, Figure 6C, bottom left panel). Likewise, 81.9% of the BT474Br3 cell population was positive for phospho-Tyr1131 IGF-IRβ, compared to an average of 51.3% of the BT474 M1 parental cells ($p < 0.05$, Figure 6D, bottom right panel). In addition to the percentage of phospho-Tyr1131 IGF-IR positive cells, we also measured the median fluorescence intensity (MFI) of these populations, which refers to the shift in overall intensity of the phospho-Tyr1131 IGF-IRβ signal. Consistent with the results shown in Figure 6C and 6D, we observed an increase in MFI of the 231Br and BT474Br3 cell populations compared to the parental cells

such that the MFI of 231Br cells was 3.24, compared to 2.1 in the 231 parental cells ($p < 0.0005$; Figure 6E) while the BT474Br3 cell lines exhibited a similar trend with an MFI of 7.29 compared to 4.38 in the parental BT474 cells ($p < 0.05$, Figure 6F). One possible explanation for the higher phospho-IGF-IR observed in brain-seeking cells in Figures 5 and 6 is the higher expression level of total IGF-IR protein detected in whole cell lysates (Figure 4). The flow cytometry data indicated that IGF-IR is autophosphorylated in a higher percentage of brain-seeking cells, and that the mean intensity of IGF-IR phosphorylation in these cells is also higher. Collectively, these findings demonstrated that the total protein level and autophosphorylation of IGF-IR is higher in brain-seeking cells than in parental breast cancer cells.

Figure 4

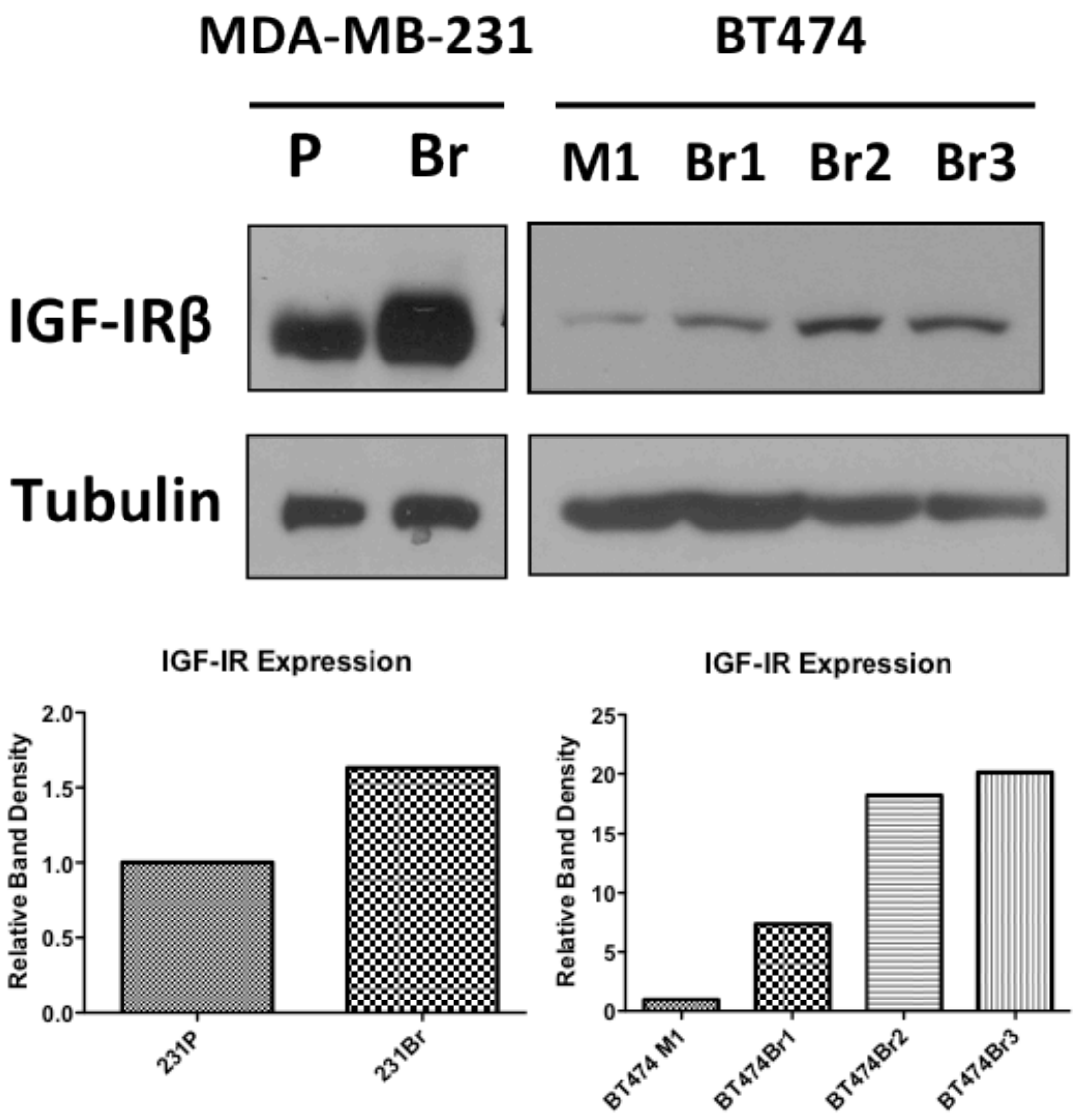
MDA-MB-231
BT474
P
Br
M1
Br1
Br2
Br3
IGF-IRβ
Tubulin
IGF-IR Expression
Relative Band Density
2.0
1.5
1.0
0.5
0.0
231P
231Br
IGF-IR Expression
Relative Band Density
25
20
15
10
5
0
BT474 M1
BT474Br1
BT474Br2
BT474Br3

Figure 4. IGF-IR expression profile of breast cancer cell lines and brain-seeking subclones.

Top, Western Blot of total IGF-IR expression in 231P/Br and BT474M1/Br3 cells.

Bottom, densitometric analysis of IGF-IR bands from top panel, normalized to Tubulin. ImageJ software was used for analysis.

Figure 5

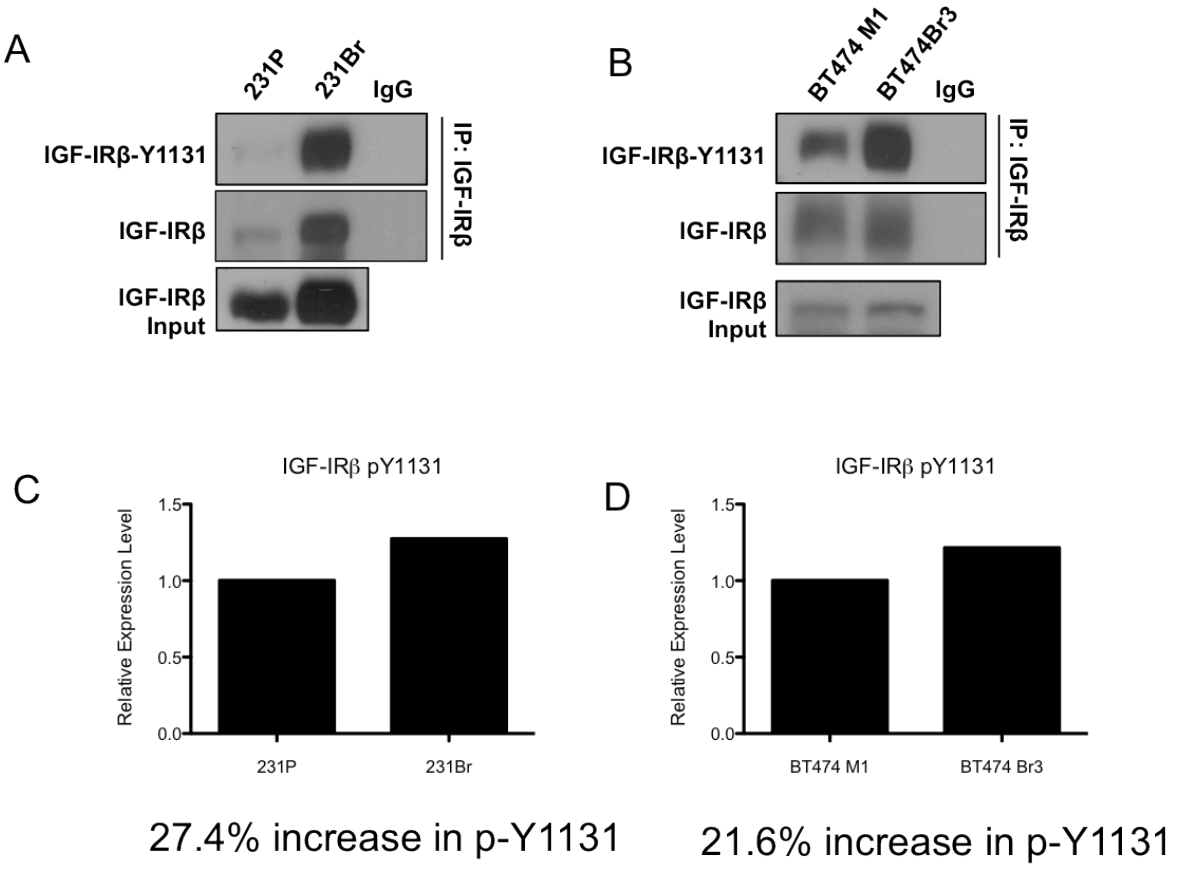
A
231P
231Br
IgG
IGF-IRβ-Y1131
IGF-IRβ
IGF-IRβ Input
IP: IGF-IRβ
B
BT474 M1
BT474Br3
IgG
IGF-IRβ-Y1131
IGF-IRβ
IGF-IRβ Input
IP: IGF-IRβ
C
IGF-IRβ pY1131
Relative Expression Level
1.5
1.0
0.5
0.0
231P
231Br
27.4% increase in p-Y1131
D
IGF-IRβ pY1131
Relative Expression Level
1.5
1.0
0.5
0.0
BT474 M1
BT474 Br3
21.6% increase in p-Y1131

Figure 5. IGF-IR is activated in brain seeking breast cancer cells.

A and B, Immunoprecipitates of IGF-IRβ from lysates of the parental MDA-MB-231 and BT474 breast cancer cells (231P, BT474 M1) and their respective brain-seeking sublines (231Br, BT474 BR3), were analyzed by SDS-PAGE and immunoblotted with antibodies against the IGF-IR Tyr1131 autophosphorylation site. Cells were serum-starved overnight prior to lysis.

C and D, Quantification of IGF-IR-pY1131 expression in 231P/Br, BT474M1/Br3 cells after normalization to total IGF-IR IP band. Phosphorylation of IGF-IR increased in both brain seeking cell lines.

Figure 6

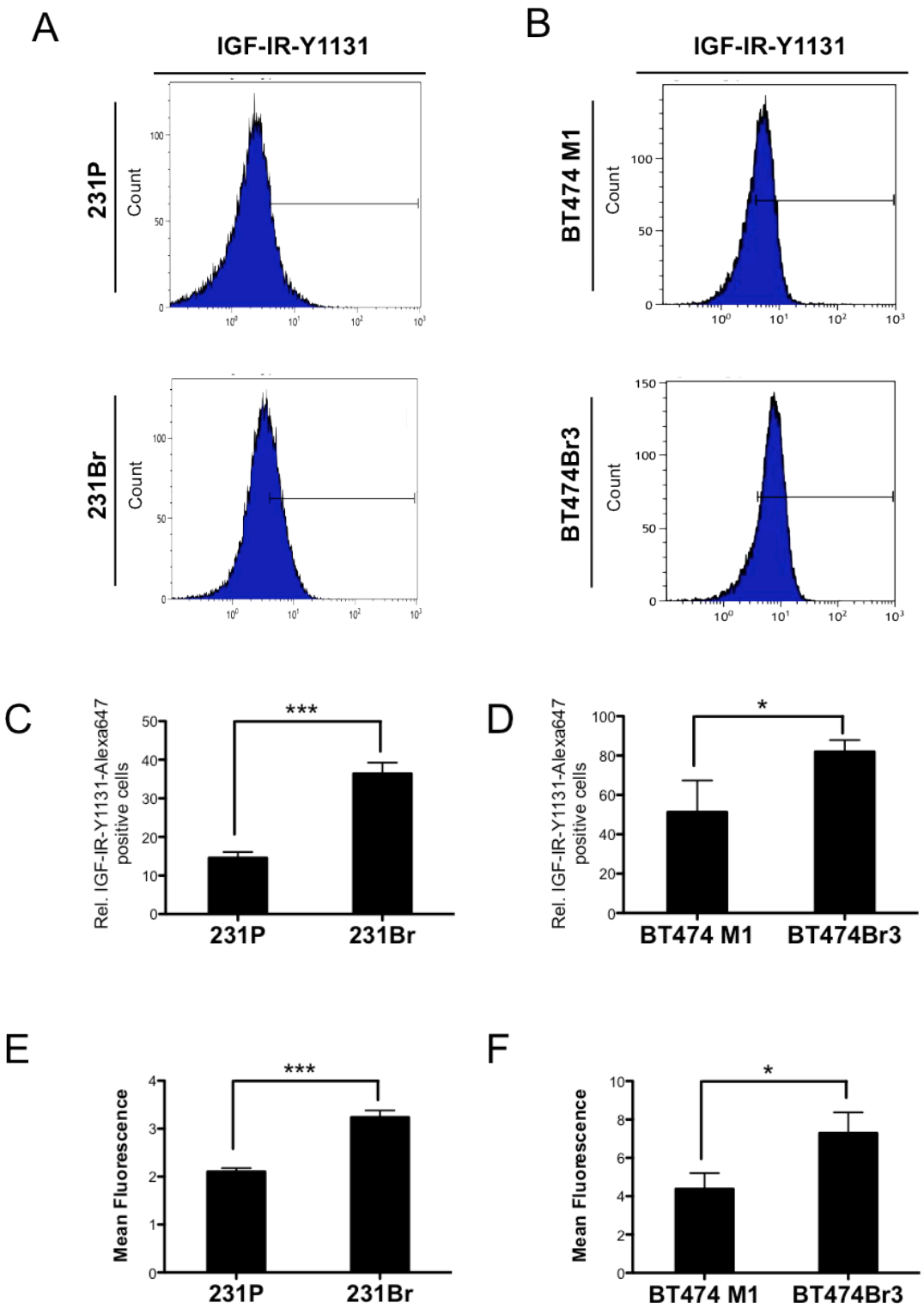
A
IGF-IR-Y1131
231P
Count
231Br
B
IGF-IR-Y1131
BT474 M1
BT474Br3
C
Rel. IGF-IR-Y1131-Alexa647 positive cells
***
231P
231Br
D
Rel. IGF-IR-Y1131-Alexa647 positive cells
*
BT474 M1
BT474Br3
E
Mean Fluorescence
***
231P
231Br
F
Mean Fluorescence
*
BT474 M1
BT474Br3

Figure 6. IGF-IR is activated in brain seeking breast cancer cells.

A and B, Flow cytometric analysis of IGF-IR activation in 231P & BT474 M1 breast cancer cells and respective brain-seeking sublines, 231Br and BT474 Br3, shown in Figure 5. Cells were serum-starved for 24h and stained with AlexaFluor 647-phospho Y1131 IGF-IR antibody.

C and D, Quantitation of flow cytometric analyses of fluorescent cells per group is shown below each panel. Values shown represent mean ± SEM from 3 replicates (*, $p < 0.05$, ***, $p < 0.0005$).

E and F, Median Fluorescence Intensity shift captured by flow cytometric measurement of parental and brain-seeking breast cancer cells stained with Tyr1131-IGFR-Ax647 antibody. Values represent mean ± SEM (*, $p < 0.05$, ***, $p < 0.0005$).

3.3 IGF-1 ligand stimulation drives migration and invasion in brain-seeking cells

In order to test whether IGF-IR autophosphorylation and downstream functions are mediated by IGF-1 ligand bioavailability in brain-seeking cells, we examined the malignancy of brain-seeking cells under IGF-1 ligand stimulation. In order to evaluate whether 231P and 231Br cells are IGF-1-responsive, we first serum-depleted cells overnight in order to minimize the IGF-IR autophosphorylation observed in Figure 5A. We then stimulated serum-depleted 231P and 231Br cells with IGF-1 and immuniprecipitated of the IGF-I Receptor. In the IGF-IR immunoprecipitates, we observed phosphorylation at Tyr1135 in the 231Br but not 231P cells, suggesting that brain-seeking cells are driven by ligand stimulation (Figure 7A). We also examined the phosphorylation status of the insulin-receptor substrate (IRS)-1 and -2, which are immediately activated upon IGF-IR activation. IRS-2 is known to mediate motility and pro-metastatic behavior of IGF-IR in breast cancer cells (Jackson et al., 2001), and indeed, only IRS-2 was phosphorylated upon IGF-1 ligand stimulation in 231Br cells but not the parental cells (Figure 7B). Downstream of IGF-IR, AKT was also phosphorylated at Ser 473 upon IGF-1 ligand stimulation in 231Br cells but not 231P cells (Figure 7C). The differential AKT activation in the two cell types may be due to the serum-free medium used in this experiment. It is possible that the stimulation time (15 minutes) or IGF-1 concentration may not be high enough to induce AKT Ser 473 phosphorylation in parental cells, but the 231 Br cells were sensitive to IGF-1 ligand due to IGF-IR

overexpression. Taken together, these data suggest that the IGF-1 ligand activates IGF-IR axis signaling molecules in brain-seeking cells.

Next, we performed a transwell assay to measure the response of 231Br cells to IGF-1 ligand as a chemoattractant and found that overnight incubation with IGF-1 stimulated the migration of 231Br but not 231P cells under low serum conditions (0.2% FBS DMEM; Figure 8A with quantification in the lower panel). Similarly, 231Br cells were more invasive in a matrigel invasion assay when IGF-1 ligand was present as a chemoattractant (Figure 8B with quantification in the lower panel). In our experience, only the 231Br cells responded to IGF-1 ligand stimulation under low serum conditions. We speculate that under low serum conditions, IGF-1 ligand stimulation is not sufficient to induce migration and invasion in 231 parental cells, but 231Br cells are more sensitive to IGF-1 ligand stimulation due to their higher levels of IGF-IR expression. Thus, we concluded that the IGF-IR signaling and pro-metastatic functions of brain-seeking cells are likely mediated by IGF-1 ligand and further amplified by higher expression of IGF-IR protein.

Future studies should delve deeper into the molecular mechanisms of increased IGF-IR expression of 231Br cells in further detail. Dysregulation of IGF-IR expression in cancer is rarely a result of gene amplification or activating genetic mutations. Rather, IGF-IR protein is regulated by a variety of tumor suppressor proteins at the pre- and post-transcriptional level. For example, PTEN is known to inhibit the synthesis of IGF-IR precursor, as well as inactivate AKT (Tanno et al., 2001). Loss of PTEN results in increased AKT phosphorylation as well as increased IGF-IR protein translation (Tanno et al., 2001). Similarly, mutations of

p53 can lead to increased IGF-IR promoter activity and mRNA transcript levels (Werner, Karnieli, Rauscher, & LeRoith, 1996). The IGF-IR promoter is also repressed by BRCA1 (Maor, Abramovitch, Erdos, Brody, & Werner, 2000) and VHL protein is a post-translational regulator by sequestration of HuR protein that results in de-stabilization of IGF-IR mRNA (Yuen et al., 2007). p53, BRCA1, and VHL are all known to downregulate IGF-IR transcription through interaction with Sp1 transcription factor and disrupting its binding to the IGF-IR promoter (Abramovitch, Glaser, Ouchi, & Werner, 2003; Ohlsson, Kley, Werner, & LeRoith, 1998; Yuen et al., 2007). Furthermore, Wilms Tumor Protein 1 (WT1) can also bind the IGF-IR promoter directly on consensus sites on either side of the promoter through its zinc finger domain and repress transcription (Werner et al., 1993).

Figure 7

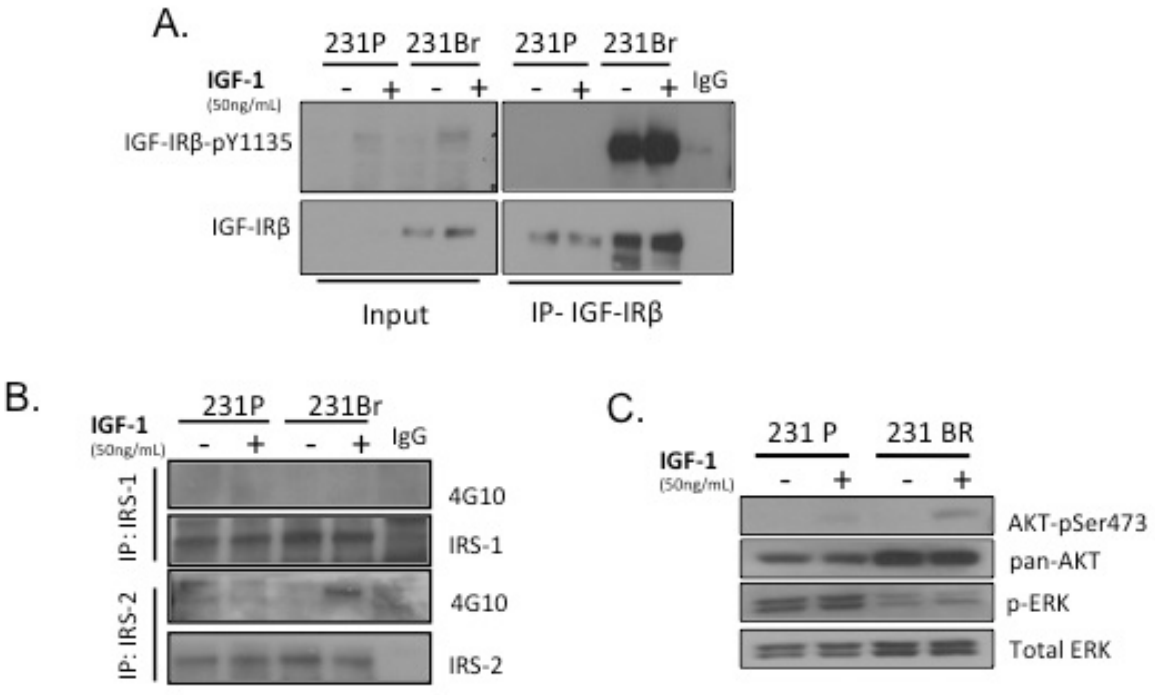
A.
231P
231Br
231P
231Br
IGF-1
(50ng/mL)
- + - + - + - +
IgG
IGF-IRβ-pY1135
IGF-IRβ
Input
IP- IGF-IRβ
B.
231P
231Br
IGF-1
(50ng/mL)
- + - +
IgG
IP: IRS-1
IP: IRS-2
4G10
IRS-1
4G10
IRS-2
C.
231 P
231 BR
IGF-1
(50ng/mL)
- + - +
AKT-pSer473
pan-AKT
p-ERK
Total ERK

Figure 7. IGF-IR activation is IGF-1 ligand-dependent in brain-seeking cells.

A, 231P and 231Br cells were serum-starved overnight, and then stimulated with 50 ng/ml IGF-1 for 15 min. IGF-IR was immunoprecipitated and then immunoblotted with phospho-Y1135-IGF-IR antibody.

B, Immunoprecipitates of IRS-1 and IRS-2 proteins from serum-starved 231P and 231Br cells, unstimulated or stimulated with 50 ng/ml IGF-1 for 15 min.

C, Western blot analysis of whole cell lysates of 231P and 231Br cells after stimulation with IGF-1.

Figure 8

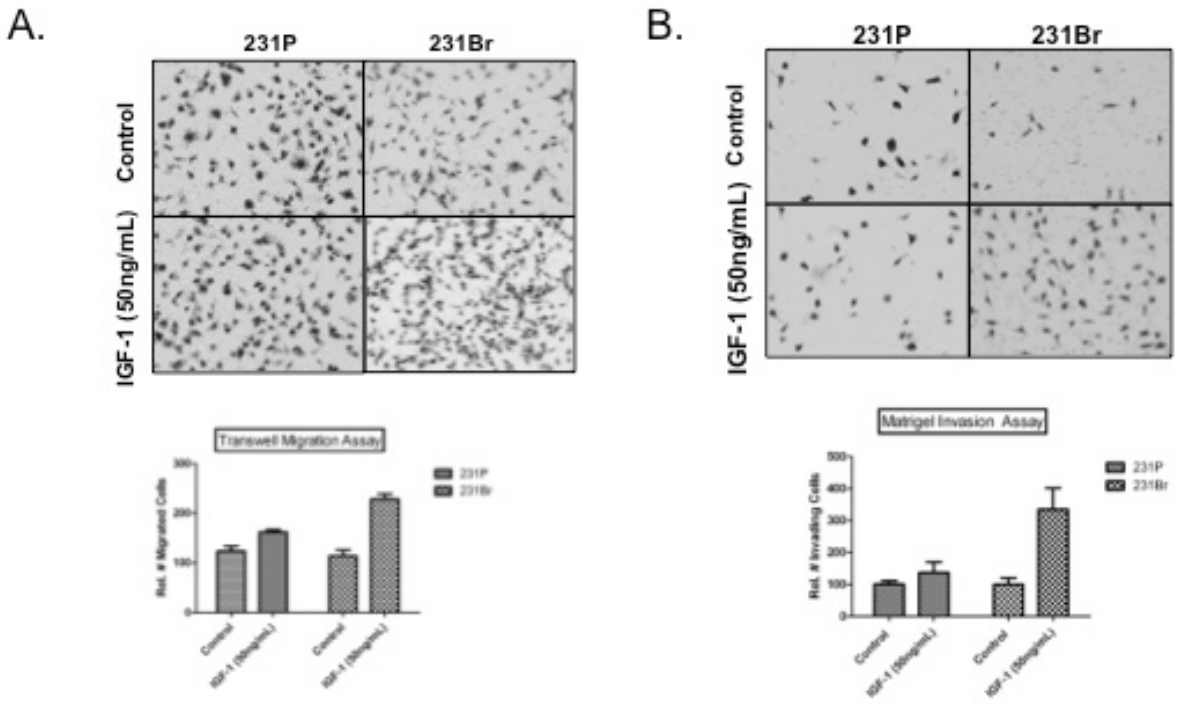
A.
231P
231Br
Control
IGF-1 (50ng/mL)
Transwell Migration Assay
231P
231Br
B.
231P
231Br
Control
IGF-1 (50ng/mL)
Matrigel Invasion Assay
231P
231Br

Figure 8. IGF-1 stimulation drives *in vitro* migration and invasion in brain-seeking breast cancer cells.

A, Transwell migration assay of cells incubated for 24h in low serum with or without IGF-1 as a chemoattractant (top panel), quantitative analysis of relative cell invasion (bottom panel).

B, Matrigel invasion assay of cells incubated for 24h in low serum with or without IGF-1 as a chemoattractant (top panel), quantitative analysis of relative cell invasion (bottom panel). Bars represent mean ± SEM.

3.4 Secreted form of IGFBP3 is overexpressed in brain-seeking cells

Since the basal level of IGF-IR autophosphorylation in 231Br and BT474Br3 cells is much higher under normal culture conditions, we asked whether the IGF-IR signaling axis is constitutively activated in an autocrine manner, either dependent or independent of IGF-1 ligand. Along with IGF-1 ligand, IGFBP3 is one of the major regulators of receptor activity in the IGF-IR signaling axis and a major binding protein of IGF-1 ligand that both potentiates and inhibits its interaction with IGF-IR in different cancers (Firth & Baxter, 2002; Martin, Lin, McGowan, & Baxter, 2009; Xi et al., 2006). In Hs578T breast cancer cells, IGFBP3 promotes attachment and survival on fibronectin (McCaig, Perks, & Holly, 2002), which is present in the perivascular space of the brain microenvironment and known to promote the growth of breast cancer cells in the brain (Carbonell, Ansorge, Sibson, & Muschel, 2009). However, IGFBP3 has also been reported to modulate IGF-IR phosphorylation independently of IGF-1 (Martin & Baxter, 2011; Schedlich & Graham, 2002). When we examined the IGFBP3 mRNA expression level in 231Br cells, we found that it is expressed 25-30 fold more than in 231P (Figure 9A). While IGFBP3 is traditionally studied as a secreted protein, it is known to carry out some of its functions intracellularly (Grkovic et al., 2012; Paharkova-Vatchkova & Lee, 2010). We first analyzed the levels of secreted IGFBP3 by collecting the conditioned medium of 231P and 231Br cells. As a secreted protein, IGFBP3 exists in a non-glycosylated form (29kDa), 2N-glycosylated (40kDa), and 3N-glycosylated (45kDa) forms (Firth & Baxter, 1999). Based on the mRNA expression levels, we expected that the protein levels of IGFBP3 would be higher in brain-seeking cells. Indeed, as shown in Figure

9B, the wide IGFBP3 band indicates that all three glycosylated forms are highly secreted in 231Br cells but were undetectable in 231P cells. We also analyzed the levels of intracellular IGFBP3 and found no difference in expression between 231P and 231Br cells (Figure 9C). These results suggest that IGFBP3 exerts its function in 231Br cells in an extracellular autocrine manner.

We did not test the molecular mechanism behind IGFBP3 observed in our model system, but it is known that IGFBP3 expression is stimulated by IGF-1 ligand (57). IGFBP3 transcription is also regulated by promoter methylation and directly by the p53 tumor suppressor binding both in the promoter region and intronically (Hanafusa et al., 2005; Torng et al., 2009). Furthermore, Vitamin D Receptor (VDR) binds the IGFBP3 promoter either alone or in association with Retinoid X, in order to enhance its transcription (Peng, Malloy, & Feldman, 2004). Interestingly, VDR expression is also closely tied to IGF-IR signaling, and its expression is regulated by IGF-1 ligand stimulation (Welsh et al., 2002). Therefore, we hypothesize that the IGFBP3 is overexpression observed in 231Br cells is a result of an autocrine positive feedback loop that is stimulated by enhanced IGF-IR pathway activation through IGF-1 signaling. Further studies should test this hypothesis and elucidate the molecular mechanism of IGFBP3 regulation in our model system.

3.5 Secreted IGFBP3 level correlates with autocrine IGF-IR activation in brain-seeking cells

In this study, we sought to measure the intrinsic properties acquired by 231Br cells that may be responsible for their enhanced ability to attach to and survive in

the brain parenchyma to a greater degree than the 231 Parental cell line. Since we observed a dramatic overexpression of IGFBP3 in 231Br cells, our goal was to determine if IGFBP3 is functionally significant in promoting IGF-IR activation. To test this, we knocked down the expression of IGFBP3 by transiently transfecting 231Br cells with two different IGFBP3 siRNAs (Figure 10A) and analyzed the receptor autophosphorylation under normal growth conditions in complete medium. Knockdown of IGFBP3 by two siRNAs potently inhibited IGF-IR Tyr phosphorylation (Figure 10B). A similar inhibitory effect was observed by flow cytometry on the phosphorylation of Tyr-1131-IGF-IR (Figure 10C), suggesting that IGFBP3 stimulates IGF-IR activation in an autocrine manner. Our study tested whether IGFBP3 confers enhanced intrinsic IGF-IR activation, which may result in a survival advantage when 231Br cells arrest in the brain parenchyma. Indeed, is possible that the properties measured in this study may be equally important for metastasis to the lymph nodes, bone, or lung for example. In order to specifically test the importance of IGFBP3/IGF-IR signaling in brain-specific metastasis, it would be of great interest to study effect of brain-derived IGF-1 ligand and IGFBP3 on IGF-IR activation and 231Br cell migration/invasion. Although our study does not rule out whether IGFBP3/IGF-IR pathway is also involved in other organ metastases of breast cancer cells, it does highlight that in a heterogeneous population of breast cancer cells that arrest in the brain parenchyma, those cells that contain IGFBP3 overexpression and subsequent IGF-IR pathway activation possess a survival advantage in the brain microenvironment, as discussed in the following Chapter.

The significance of IGFBP3/IGF-IR in the honing of breast cancer cells to the brain should be the subject of future studies.

Figure 9

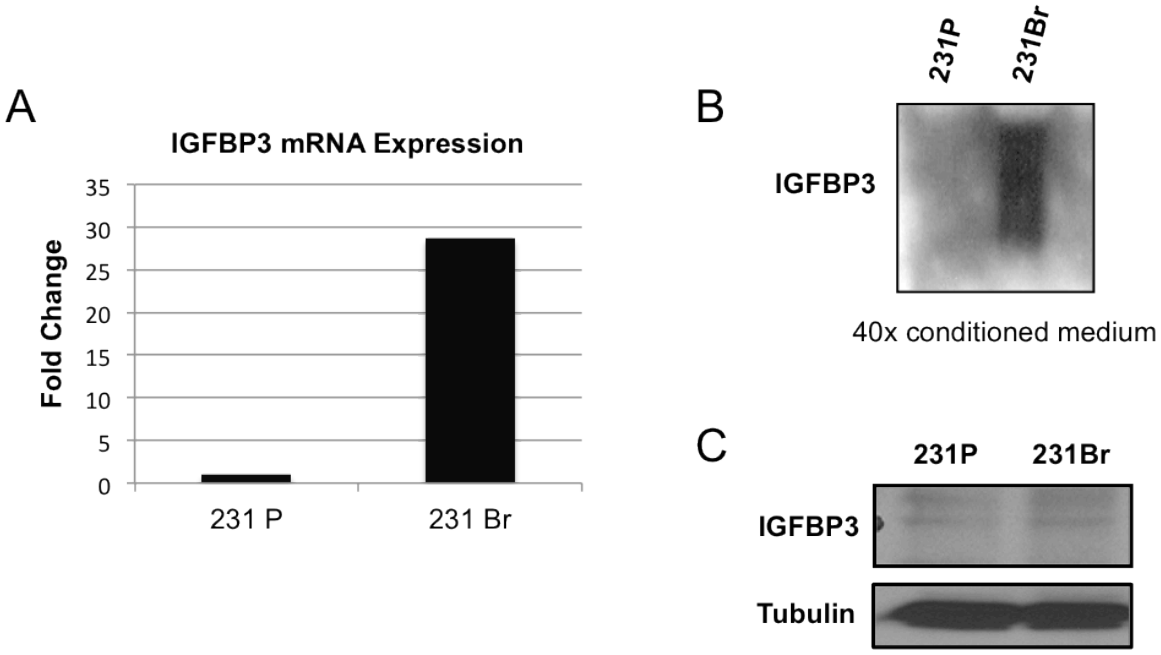
A
IGFBP3 mRNA Expression
Fold Change
35
30
25
20
15
10
5
0
231 P
231 Br
B
231P
231Br
IGFBP3
40x conditioned medium
C
231P
231Br
IGFBP3
Tubulin

Figure 9. The secreted form of IGFBP3 is overexpressed in brain-seeking breast cancer cells.

A, Real-time quantitative RT-PCR of IGFBP3 in 231P and 231Br cells. Data are expressed as relative expression as a ratio to housekeeping gene HPRT1 expression.

B, Western blot analysis of secreted IGFBP3 protein in the conditioned medium of 231P and 231Br cells. Equal cell numbers were incubated in serum-free medium for 48 hr, and then the conditioned medium was collected and concentrated by 40-fold.

C, Western blot analysis of IGFBP3 protein in lysates of 231P and 231Br cells.

Figure 10

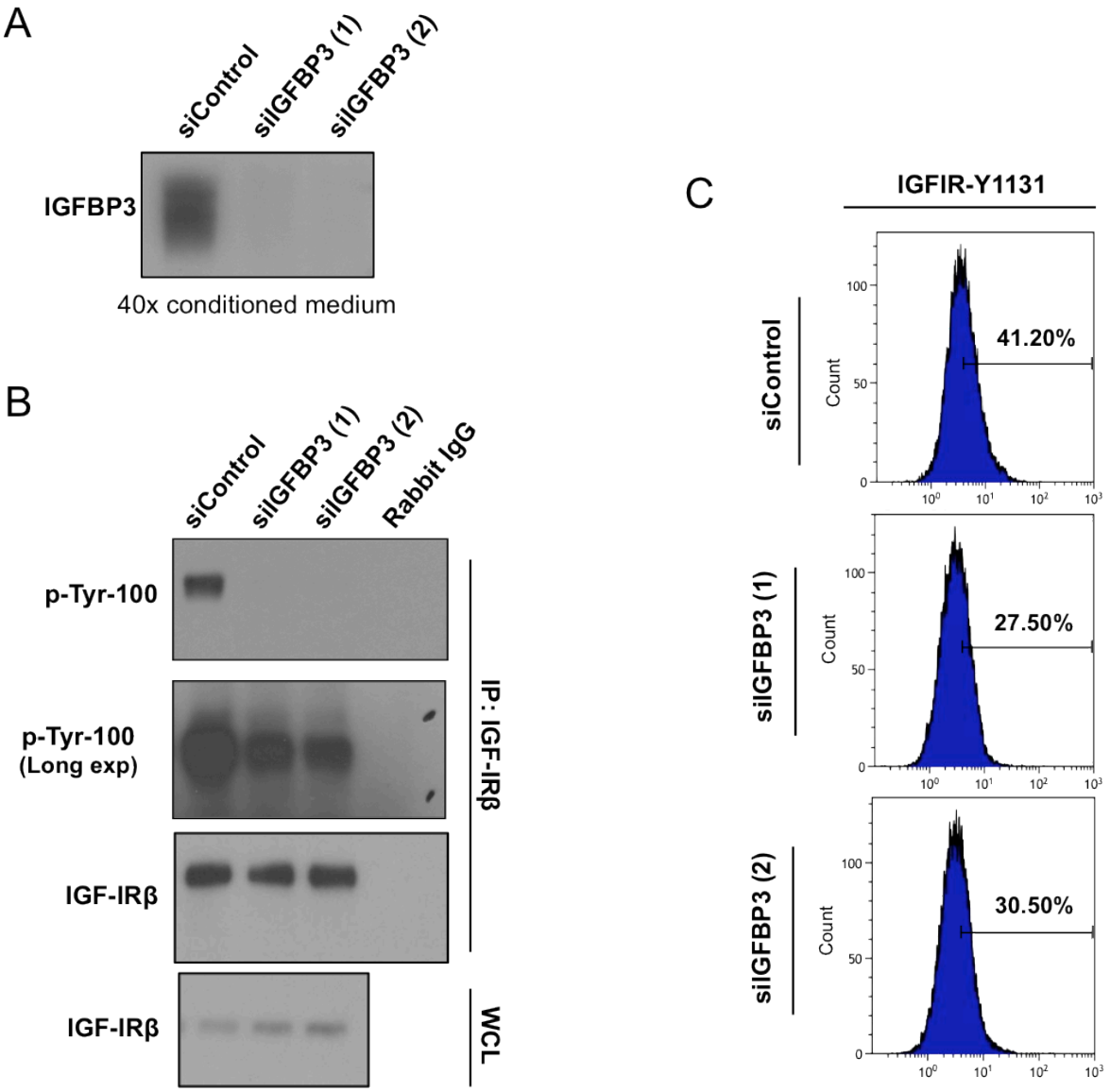
A
siControl
siIGFBP3 (1)
siIGFBP3 (2)
IGFBP3
40x conditioned medium
B
siControl
siIGFBP3 (1)
siIGFBP3 (2)
Rabbit IgG
p-Tyr-100
p-Tyr-100
(Long exp)
IGF-IRβ
IP: IGF-IRβ
IGF-IRβ
WCL
C
IGFIR-Y1131
siControl
41.20%
siIGFBP3 (1)
27.50%
siIGFBP3 (2)
30.50%
Count

Figure 10. IGFBP3 knockdown results in decreased IGF-IR activation in brain seeking cells.

A, Conditioned medium of 231Br cells transiently transfected with control or IGFBP3 siRNAs for 48 hr. Medium was concentrated by 40-fold and the protein expression of IGFBP3 was analyzed using Western blot.

B, IGFBP3 knockdown downregulates IGF-IR phosphorylation. Cells were transfected with either control or IGFBP3 siRNAs. IGF-IR was immunoprecipitated (IP) and immunoblotted with phospho-Tyr antibody. Whole cell lysate (WCL) was used as input control.

C, Flow cytometric analysis of 231Br cells after IGFBP3 knockdown. Cells were transfected with either control or IGFBP3 siRNAs, and stained with AlexaFluor 647-phospho Y1131 IGF-IR antibody. IGF-IR phosphorylation decreased in the siRNA groups.

CHAPTER 4

IN VITRO AND *IN VIVO* EFFECTS OF TYPE I INSULIN-LIKE GROWTH FACTOR RECEPTOR ABLATION IN BRAIN SEEKING BREAST CANCER CELLS

4.1 Transient knockdown of IGF-IR impairs wound healing in 231 brain-seeking cells

In order to determine the biological relevance of IGF-I Receptor in brain-seeking cells, we transiently transfected small interfering RNAs targeting the IGF-IR, and evaluated the cells' ability to close the gap in a wound healing assay. The wound-healing assay measures cell motility, as well as the degree of cell-cell and cell-matrix interactions in a cell monolayer (Rodriguez, Wu, & Guan, 2005). Figure 11A is a control showing the efficiency of IGF-IR knockdown achieved by a universal negative control siRNA, and two different IGF-IR siRNAs in both 231 parental and brain-seeking lines. Figure 11B shows time-lapse images at 0, 12, 24, and 48 hours after introduction of the wound, and the 231Br cells transfected with IGF-IR siRNAs had significantly impaired wound healing ability. The impaired ability of cells to migrate at the leading edge of the wound also suggests that IGF-IR knockdown may result in stronger cell-cell interactions between 231Br cells, and thus render them less metastatic.

4.2 Transient knockdown of IGF-IR inhibits IGF-1-mediated AKT phosphorylation in brain seeking cells.

To further validate whether IGF-IR knockdown plays a significant role in the intracellular signaling of 231 brain-seeking cells, we transfected both parental and brain-seeking 231 cells with IGF-IR siRNA and observed the effect of IGF-1 ligand stimulation at 48 hours after transfection. As in Figure 7C, IGF-1 ligand stimulation induced AKT Ser473 phosphorylation of 231Br cells but not parental cells. In

support of our hypothesis, IGF-IR siRNA inhibited AKT Ser473 phosphorylation in 231 Br cells (Figure 12). Therefore, we concluded that IGF-IR is important for intracellular signaling of brain seeking breast cancer cells.

Figure 11

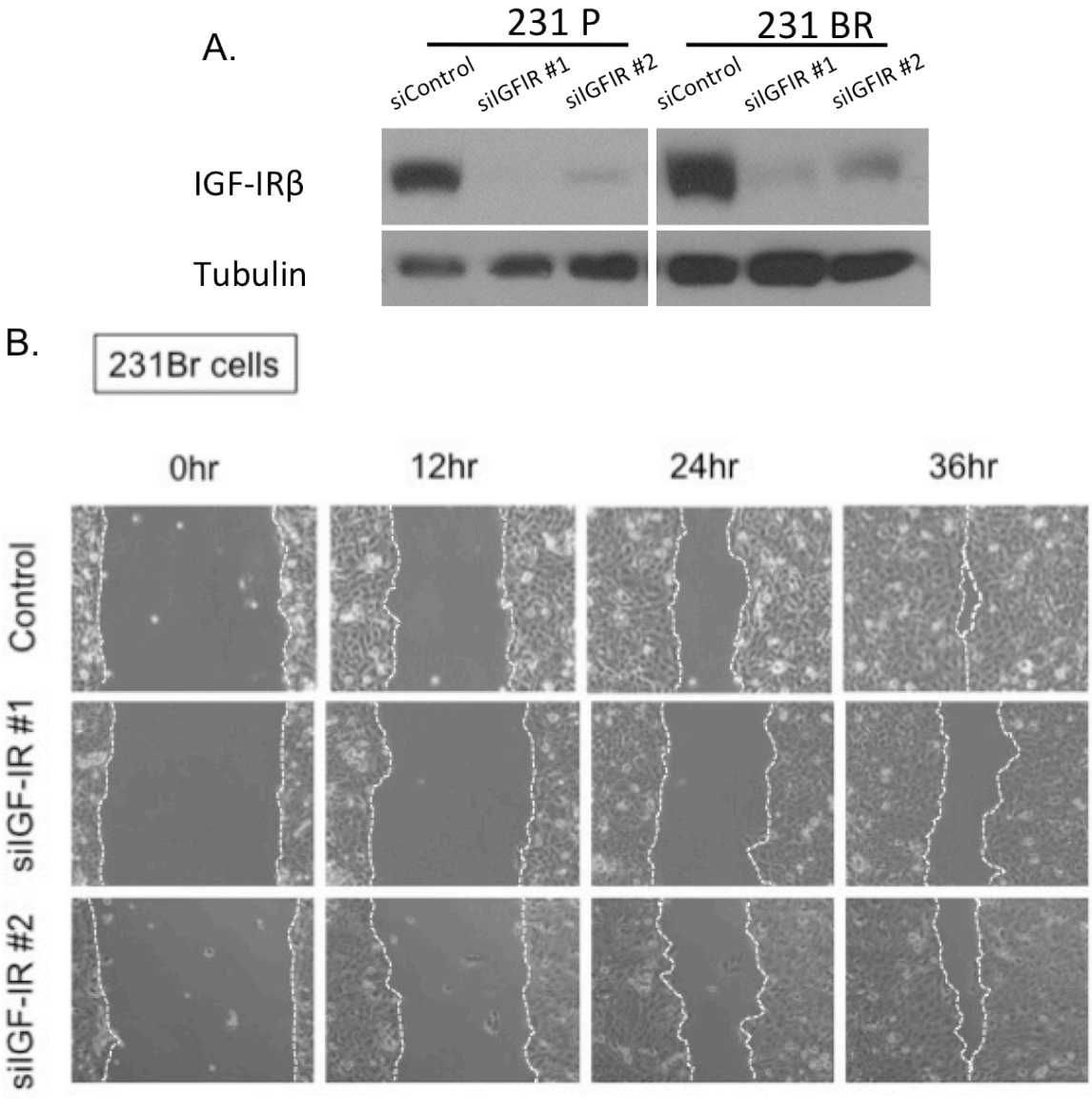
A.
231 P
231 BR
siControl
siIGFIR #1
siIGFIR #2
siControl
siIGFIR #1
siIGFIR #2
IGF-IRβ
Tubulin
B.
231Br cells
0hr
12hr
24hr
36hr
Control
siIGF-IR #1
siIGF-IR #2

Figure 11. Transient knockdown of IGF-IR inhibits migration of brain-seeking cells

A, Western blot of lysates from 231P and 231Br cells collected 72 hours after siRNA transfection, the timepoint when siRNA shows the highest knockdown efficiency.

B, Wound healing assay of 231Br cells. Cells were transfected with Control siRNA or IGF-IR siRNA #1 or #2, allowed to recover overnight and then re-seeded in a monolayer overnight in a 12-well dish for wound healing assay. Scratch wound was introduced at 48 hours after siRNA transfection, and wound closure was captured by time-lapse microscopy over the next 36 hours.

Figure 12

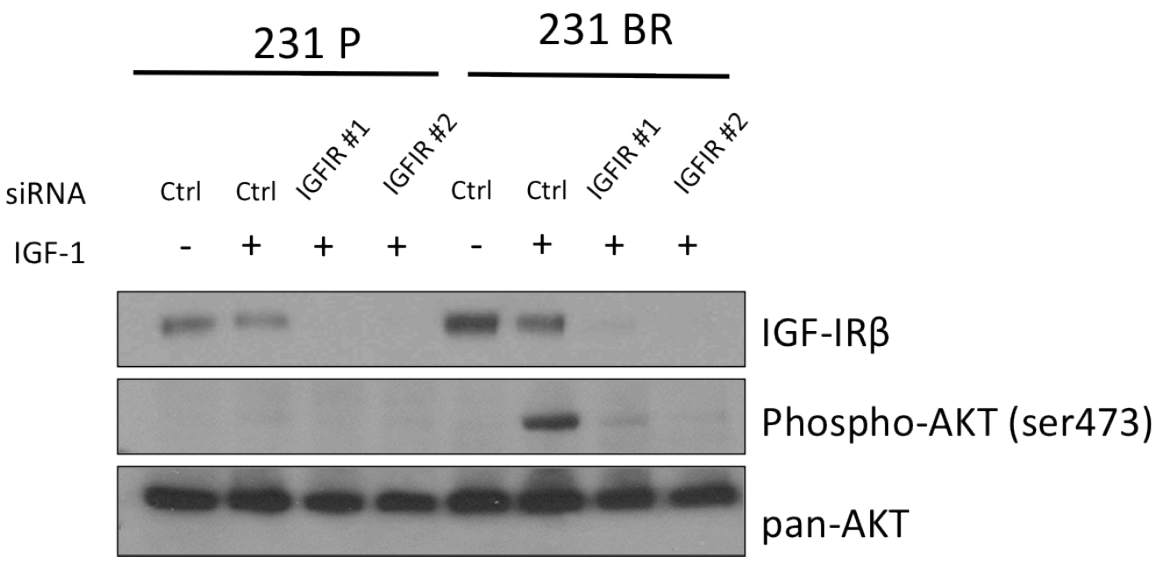
231 P
231 BR
siRNA
Ctrl
Ctrl
IGFIR #1
IGFIR #2
Ctrl
Ctrl
IGFIR #1
IGFIR #2
IGF-1
- + + + - + + +
IGF-IRβ
Phospho-AKT (ser473)
pan-AKT

Figure 12. Transient knockdown of IGF-IR downregulates IGF-1-induced AKT activation

231P and 231Br cells were transiently transfected with control, IGF-IR #1 or IGF-IR #2 siRNAs and stimulated with 50ng/mL of IGF-1 ligand for 15 minutes at 48 hours after transfection. IGF-IR knockdown efficiency and AKT Ser473 phosphorylation were observed by western blot.

4.3 Stable knockdown of IGF-IR in brain-seeking breast cancer cells inhibits cell proliferation *in vitro*

In order to study the relevance of IGF-IR in the development of brain metastasis *in vitro,* and to follow up on our transient siRNA knockdown experiments (Figures 11 and 12), we developed a model system using 231Br cells stably expressing luciferase and either empty vector (control) or IGF-IR shRNA. Of six sh-IGFR knockdown cell lines generated, two IGF-IR knockdown clones, shIGF-IR (B) and shIGF-IR (F), were selected for further characterization for comparison with the vector clone (vector). We first verified that IGF-IR was knocked down and AKT-Ser473 phosphorylation was reduced (Fig. 13A). To further assess the *in vitro* biological significance of IGF-IR knockdown in brain-seeking cells, we measured cell proliferation of knockdown and control cells using an MTT assay. As shown in Figure 13B, IGF-IR knockdown cells proliferated more slowly at all three time points. Moreover, we measured the cell growth of IGFR knockdown and vector control cells over a 72-hr period and calculated the total cell number. In agreement with the MTT assay results, IGF-IR knockdown cells grew more slowly than vector control cells (Fig. 13C).

4.4 Stable knockdown of IGF-IR in brain-seeking breast cancer cells attenuates their migratory and invasive potential *in vitro*

Next, we examined the effect of IGF-IR knockdown on the *in vitro* properties that are used as surrogate measures of metastatic potential of 231Br cells. We first

used a wound-healing assay to determine the effect of IGF-IR knockdown on migration and found that IGFR knockdown cells were less efficient at closing the wound than the vector control cells, indicating both reduced motility and an increase of cell-cell adhesion in 231Br cells (representative images shown in Figure 14A and quantification shown in Figure 14B). To determine the effect of IGF-IR knockdown on the invasive potential of 231Br cells, we performed a matrigel invasion assay. Consistent with our hypothesis, we found that IGF-IR knockdown indeed attenuated the invasiveness of 231Br cells (representative images shown in Figure 14C and quantification shown in Figure 14D). Taken together, these data demonstrate that the loss of IGF-IR expression and subsequent inactivation of its downstream signaling molecules attenuate the *vitro* invasive phenotypes, including proliferation, migration/motility and invasiveness, while enhancing *in vitro* cell-cell adhesion of the brain-seeking cells.

Figure 13

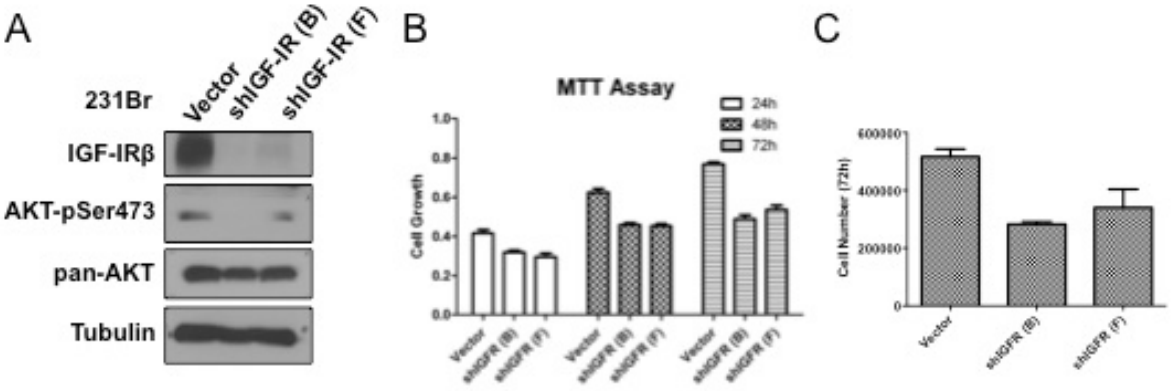
A
231Br
Vector
shIGF-IR (B)
shIGF-IR (F)
IGF-IRβ
AKT-pSer473
pan-AKT
Tubulin
B
MTT Assay
24h
48h
72h
Cell Growth
1.0
0.8
0.6
0.4
0.2
0.0
Vector
shIGFR (B)
shIGFR (F)
C
Cell Number (72h)
600000
400000
200000
0
Vector
shIGFR (B)
shIGFR (F)

Figure 13. IGF-I Receptor knockdown in brain-seeking breast cancer cells suppresses proliferation *in vitro*.

A, Immunoblot of IGF-IRβ and AKT total and phospho-Ser473 expression in 231Br cells stably transfected with control shRNA (vector) or IGF-IRβ shRNA (shIGF-IR B and F clones).

B, MTT assay of control and IGF-IR beta knockdown cells at 24, 48 and 72 hr. Values represent mean ± SEM.

C, Vector control and shIGF-IR 231Br cells were seeded 100,000 cells per well and were counted after 72 hr.

Figure 14

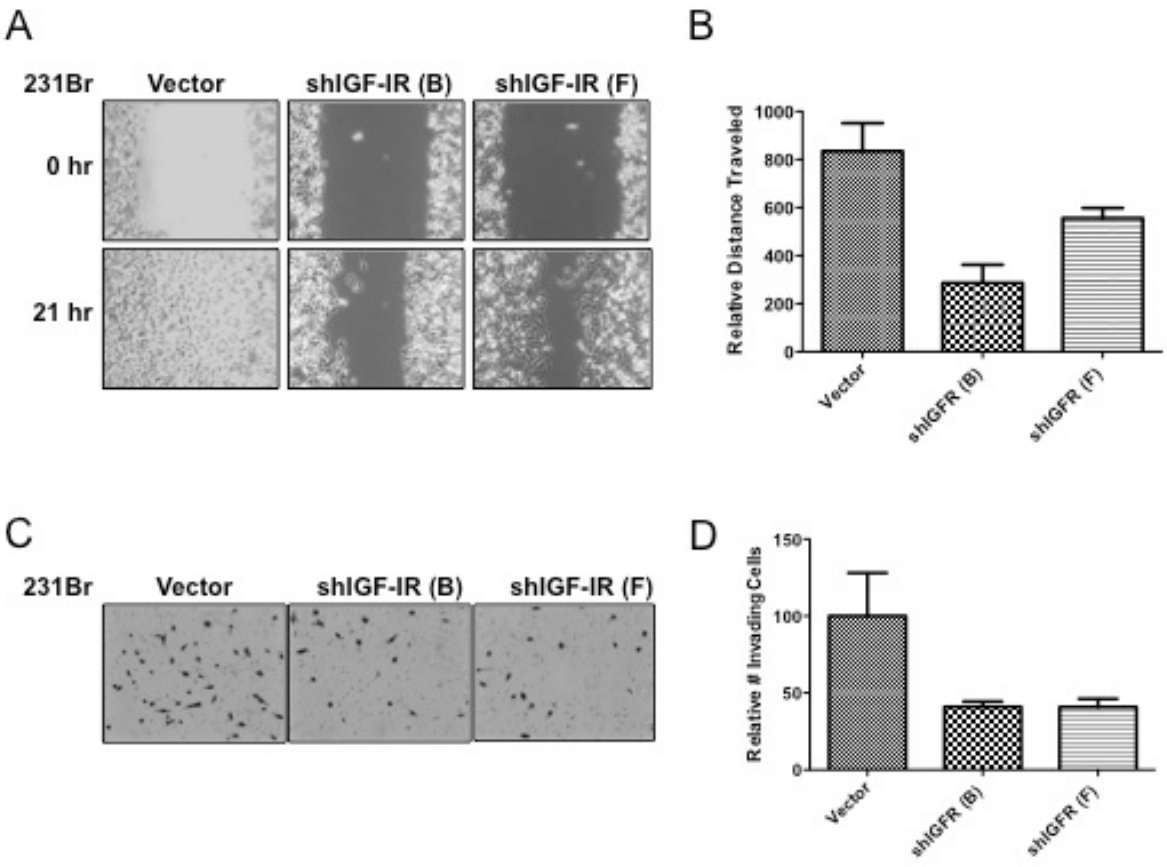
A
231Br
Vector
shIGF-IR (B)
shIGF-IR (F)
0 hr
21 hr
B
Relative Distance Traveled
1000
800
600
400
200
0
Vector
shIGFR (B)
shIGFR (F)
C
231Br
Vector
shIGF-IR (B)
shIGF-IR (F)
D
Relative # Invading Cells
150
100
50
0
Vector
shIGFR (B)
shIGFR (F)

Figure 14. IGF-I Receptor knockdown in brain-seeking breast cancer cells suppresses cell migration and invasion *in vitro*.

A, Wound-healing assay of vector and shIGF-IR 231Br cells. Images are representative of triplicates at 0 and 21 hr.

B, Quantitative measurement of wound closure area from (A). Data were calculated from one representative experiment out of three performed.

C, Matrigel invasion assay of vector and shIGF-IR 231Br cells performed in triplicate over 24 hr with complete medium as a chemoattractant.

D, Quantitative analysis results of one representative experiment out of three performed in triplicate from (C). Values represent mean ± SEM.

4.5 IGF-IR knockdown delays the outgrowth of brain metastases *in vivo*

To further characterize the functional consequences of IGF-IR knockdown on the development brain metastasis *in vivo*, we performed an experimental brain metastasis assay as described in Chapter 2. Stable 231Br-Vector, 231Br-shIGF-IR (B), and 231Br-shIGF-IR (F) cells were inoculated in the carotid artery of female swiss nu/nu mice, and brain metastasis development was monitored for 12 weeks. After the first 4 weeks, mice in the vector group developed physiological symptoms of brain metastases, such as weight loss, crouching, lethargy and/or disorientation. Figure 15 shows representative bioluminescence images of brain metastasis formation in mice from each experimental group during weeks 1-4. Mice inoculated with 231Br cells with IGF-IR knockdown demonstrated significantly longer survival than those in the vector group (Figure 16A). Mice in both knockdown groups also developed brain metastases, albeit significantly later than the vector group ($p < 0.05$). The vector group mice had a median survival of 46 days while the shIGF-IR (B) and shIGF-IR (F) groups had median survival of 77 days and 55.5 days, respectively (Figure 16B).

4.6 H&E and IHC analysis of mice that developed brain metastases

Brain sections of representative mice from each group (n=3 each Vector and shIGF-IR (B); n=2 shIGF-IR (F)) were also analyzed by H&E staining (Figure 17A) and IHC for the expression of IGF-IR (Figure 17B) and AKT-pSer473 (Figure 17C) proteins. All mice included in the analysis were sacrificed at later time points (5-10 weeks after intracarotid inoculation). H&E staining revealed visible brain

metastases in most brain sections analyzed, although metastases from the IGF-IR knockdown groups were generally smaller in size than the vector group (Figure 17A) with the exception of one sample from the shIGFR (B) group (not shown). Most metastases expressed IGF-IR protein (Table 1) although metastases in the shIGF-IR (B) and shIGF-IR (F) groups expressed lower levels of IGF-IR protein than the vector group (Figure 17B). Expression of AKT-pSer473 likewise correlated positively with IGF-IR expression levels, with the vector group expressing the highest level of AKT-pSer473 and IGF-IR knockdowns expressing the lowest (Figure 17C). These results imply that in a heterogeneous starting population of IGF-IR knockdown cells, those that retain IGF-IR and AKT-pSer473 expression are able to survive and establish tumors within the brain microenvironment in a process of positive selection.

4.7 Brain metastases induce reactive astrocytes

Furthermore, it has previously been reported that metastatic brain tumors cause the activation of astrocytes in the brain microenvironment, resulting in the support of tumor growth and vascularization (Yoshimine et al., 1985). The expression of glial fibrillary acidic protein (GFAP) is a marker of this astrocytic activation, and IHC staining revealed that the brain tissue surrounding brain metastases expressed high amounts of GFAP (80% positive cells control group, 52%-58% positive cells shIGF-IR groups, Table 1 and Figure 18). Remarkably, approximately 5-10% of GFAP positive cells infiltrated the edges of the tumor, suggesting that the activation and infiltration of astrocytes is associated with the growth of IGF-IR positive brain tumors

(Figure 18, white arrows). Interestingly, studies by Fidler et al. found that reactive astrocytes play a role in the resistance of melanoma cells to chemotherapy (Q. Lin et al., 2010). Future studies should investigate the functional significance of GFAP activation and its implications on the effect of tumor cell modulation of the brain microenvironment.

4.8 IGF-IR positive brain metastases highly express nuclear proliferation marker ki-67

In addition to IGF-IR expression, the metastases we detected also expressed the nuclear proliferation marker ki-67 (Figure 19). Tumors from the control group had an overall higher percentage of ki-67 positive cells compared with those from the shIGF-IR (B) and shIGF-IR (F) groups (Table 1). Although the IGF-IR knockdown cells eventually formed brain tumors, these metastases were less proliferative than the vector control tumors at the time of mouse morbidity.

4.9 Heterogeneous effects of IGF-IR knockdown on the growth of mammary fat pad tumors

In order to determine whether IGF-IR knockdown in 231Br cells inhibited tumor cell proliferation in vivo, we inoculated 231Br Vector and 231Br-shIGF-IR (B) and 231Br-shIGF-IR (F) into the mammary gland of nude mice. Tumors were measured bi-weekly for 8 weeks and the diameters are shown in Figure 20. The group of mice inoculated with 231Br-Vector cells behaved as expected, with tumor volumes gradually increasing over time. The 231Br-shIGF-IR (B) experimental group had

remarkably no tumor formation over the 8 weeks, while the 231Br-shIGF-IR (F) group behaved very closely to the Vector group. We hypothesized that the difference in proliferation may be due to the different levels of IGF-IR knockdown in each cell line. As shown in Figure 13A, the sh-IGFR (B) cell line had complete IGF-IR knockdown, while the shIGF-IR (F) cell line did not have complete knockdown of IGF-IR protein. This suggests that even low amount of IGF-IR is sufficient to support cell proliferation of 231Br cells *in vivo*, at least in the mammary fat pad. Indeed, the IHC staining in Figure 21 confirms that the mammary fat pad tumors from mice in the shIGF-IR (F) group expressed lower amounts of IGF-IR protein, but developed normal mammary tumors as in the Vector group.

Thus, partial IGF-IR knockdown is not sufficient to prevent *in vivo* survival of 231Br cells. This result could offer an explanation why some of the mice inoculated with both 231Br knockdown cell lines eventually developed brain metastases (Figures 16), and why the observed metastases expressed IGF-IR (Figure 17). This result also raises questions about our experimental brain metastasis model. In particular, whether factors other than IGF-IR-driven proliferation and survival of cells *in vivo* are at play in the development of brain metastasis, such as interactions with the brain microenvironment and/or MET which could be necessary for successful brain colonization.

In order to test whether the inhibition of mammary fat pad tumor formation in the shIGF-IR (B) cell line was indeed due to the complete IGF-IR knockdown achieved in this cell line, it would be useful to repeat the experiment side-by-side with additional conditions. In particular, we could test our hypothesis that incomplete

IGF-IR inhibition is insufficient for inhibition of *in vivo* cell proliferation in the mammary fat pad by adding several 231Br-Vector control groups with the addition of incremental doses of the IGF-IR inhibitor PPP. In this setting, there should be an inverse relationship between tumor volumes and PPP concentrations if our hypothesis is correct that IGF-IR expression level dictates 231Br cell survival and proliferation *in vivo*. Confirmation of our hypothesis would imply that survival of 231Br shIGF-IR (B) cells in our brain metastasis model is a result of a re-expression of IGF-IR protein in our shIGF-IR cell lines, perhaps by epigenetic modulation, since we know that we started with a population with complete IGF-IR knockdown (Figure 13A). Another possibility is that IGF-IR is not the only factor dictating in vivo cell proliferation and brain metastasis in our model, in which case microenvironmental factors such as the induction of MET may be at play. Both possibilities could account for the differences in brain metastasis development evidenced in the shIGF-IR (B) group, where 5 out of 8 mice (62.5%) eventually bypassed the barrier posed by IGF-IR knockdown, and the remaining 3 mice (37.5%) never developed brain metastases (Figure 16). We originally hypothesized that IGF-IR knockdown in shIGF-IR (B) cells would result in complete inhibition of brain metastasis, but our results suggest an epigenetic modulation of IGF-IR expression and perhaps other IGF-IR-independent mechanisms of cell survival such as MET in the brain microenvironment. Further testing using the experiment proposed in this section, and the investigation of EMT/MET markers in our brain metastasis and mammary fat pad models would help to discern between these two possibilities.

Figure 15

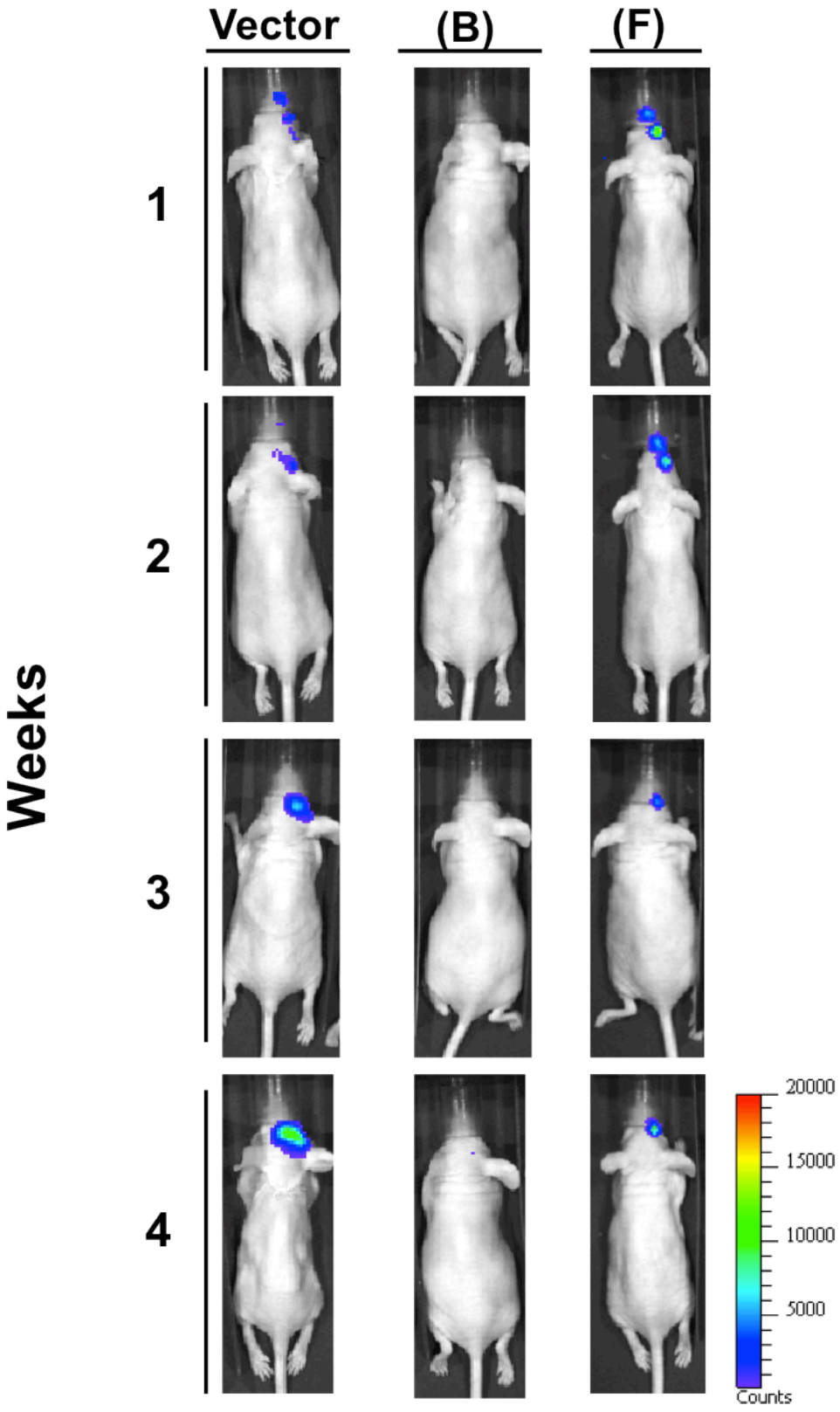

Figure 15. IGFR knockdown delays brain metastasis development *in vivo*. Mice were anesthetized and injected with 200,000 231Br cells in the carotid artery; 231Br-Luc-Vector (n=9), 231Br-Luc-shIGF-IR (B) (n=8), and 231Br-Luc-shIGF-IR (n=8). Mice were imaged the day after surgery to ensure cells were arrested in the brain capillary. Brain metastasis progression was monitored weekly by imaging with the IVIS imaging system following intraperitoneal administration of D-Luciferin.

Figure 16

A

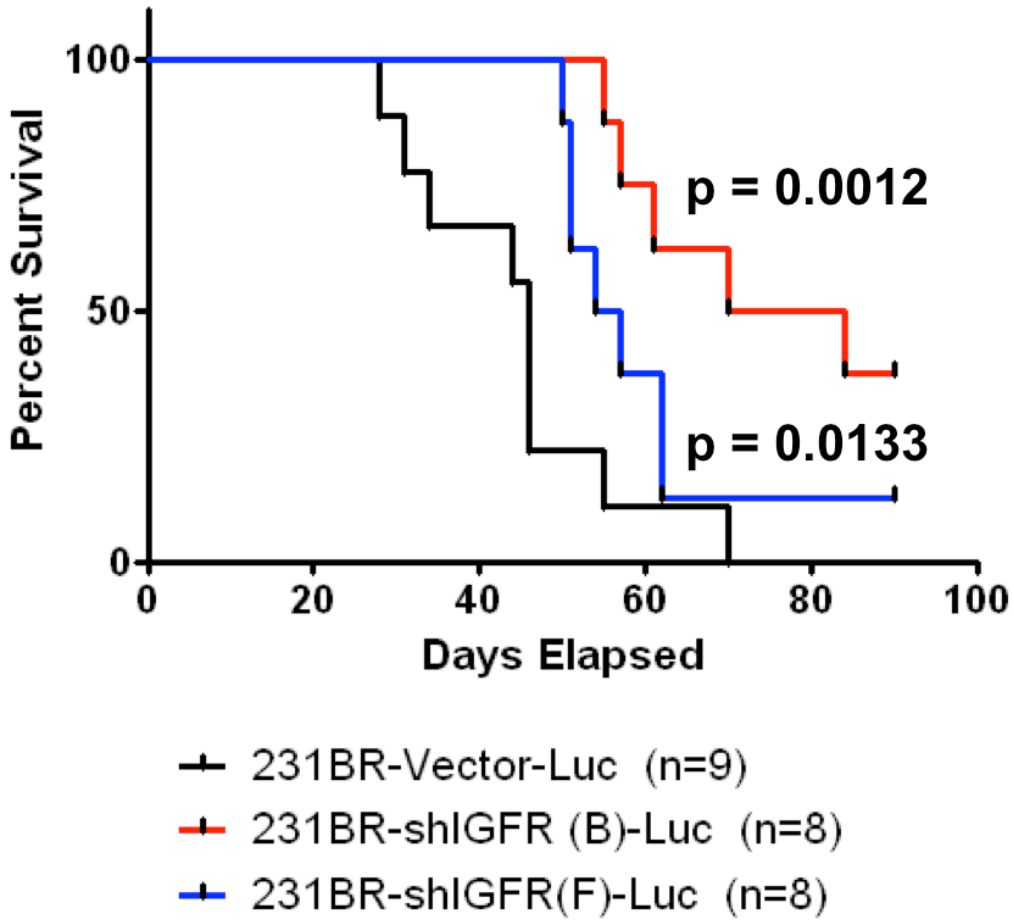

B

	Median Survival (days)
Vector	46
shIGFR (B)	77
shIGFR (F)	55.5

Figure 16. IGF-IR knockdown increases survival of mice bearing brain metastases.

A, Survival curve of mice injected with 231Br cells stably expressing IGF-IR shRNA or vector shRNA. Mice were monitored weekly and sacrificed when moribund. shIGF-IR(B) and shIGF-IR(F) groups had significantly longer survival, $p = 0.0012$ and $p = 0.0133$, respectively.

B, Median survival of each group from (A).

Figure 17

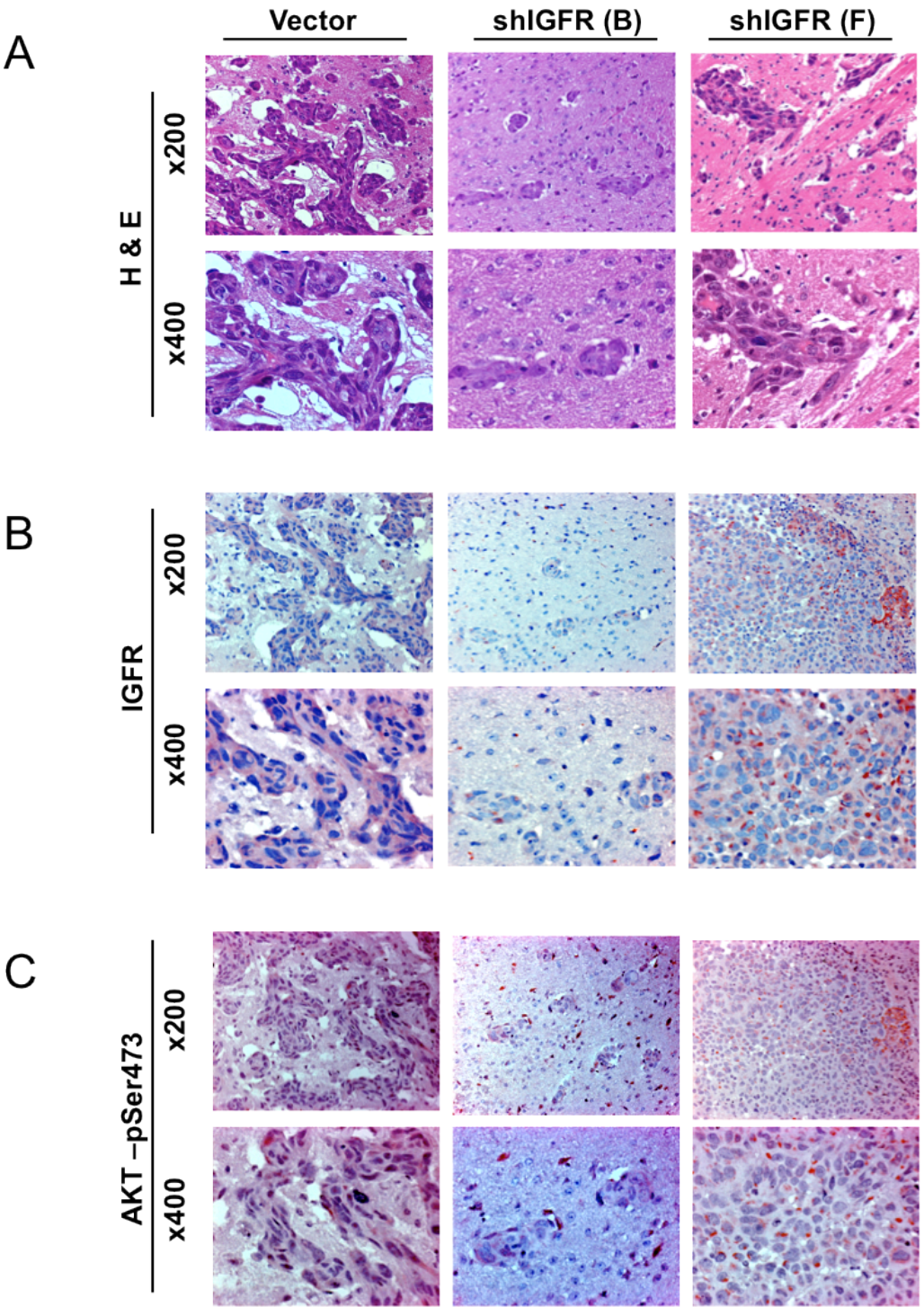
A
Vector
shIGFR (B)
shIGFR (F)
H & E
x200
x400
B
IGFR
x200
x400
C
AKT –pSer473
x200
x400

Figure 17. IGF-IR knockdown delays brain metastasis *in vivo.*

H&E and IHC staining of representative brain metastases from each group.

A, H&E panels: dark red = tumor tissue; blue = nucleus; light red = negative.

B and C, IGF-IR and AKT-pSer473 panels, respectively: red = positive; blue = nucleus. Images were taken at 200x and 400x magnification, as indicated.

Figure 18

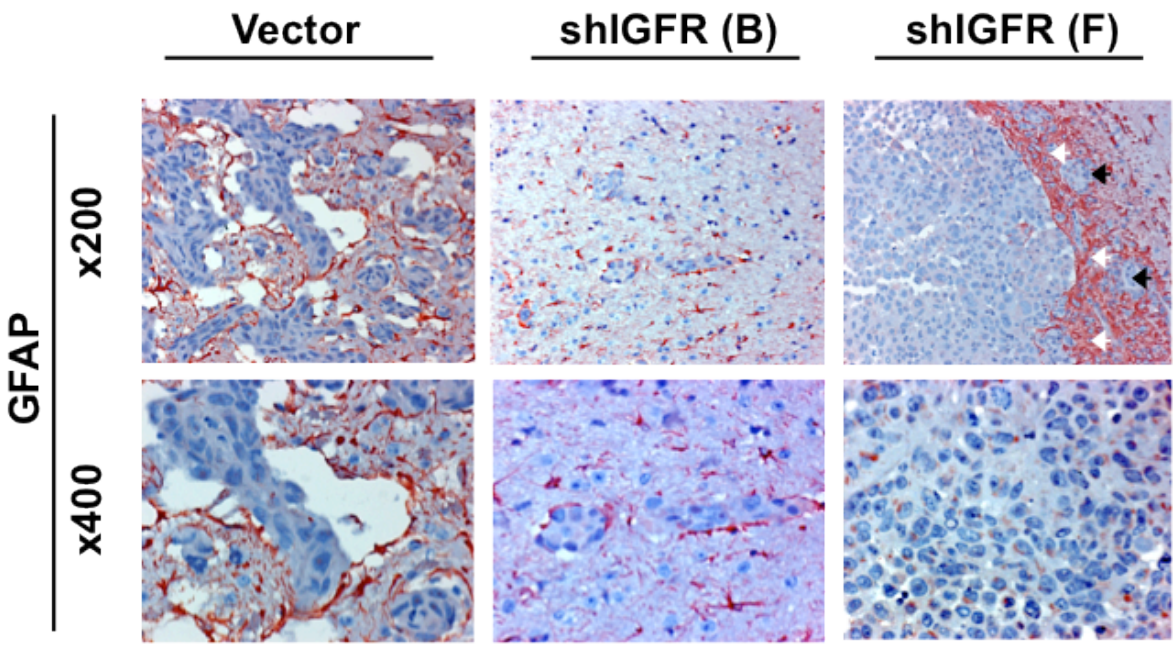

Figure 18. IHC staining of GFAP of brain metastases of mice inoculated with Vector, shIGF-IR (B) and shIGF-IR (F) 231Br cells. GFAP: dark red/brown = positive; blue = nucleus; black arrows = tumor cells; white arrows = tumor-infiltrating astrocytes. Images were taken at 200x and 400x magnification, as indicated.

Figure 19

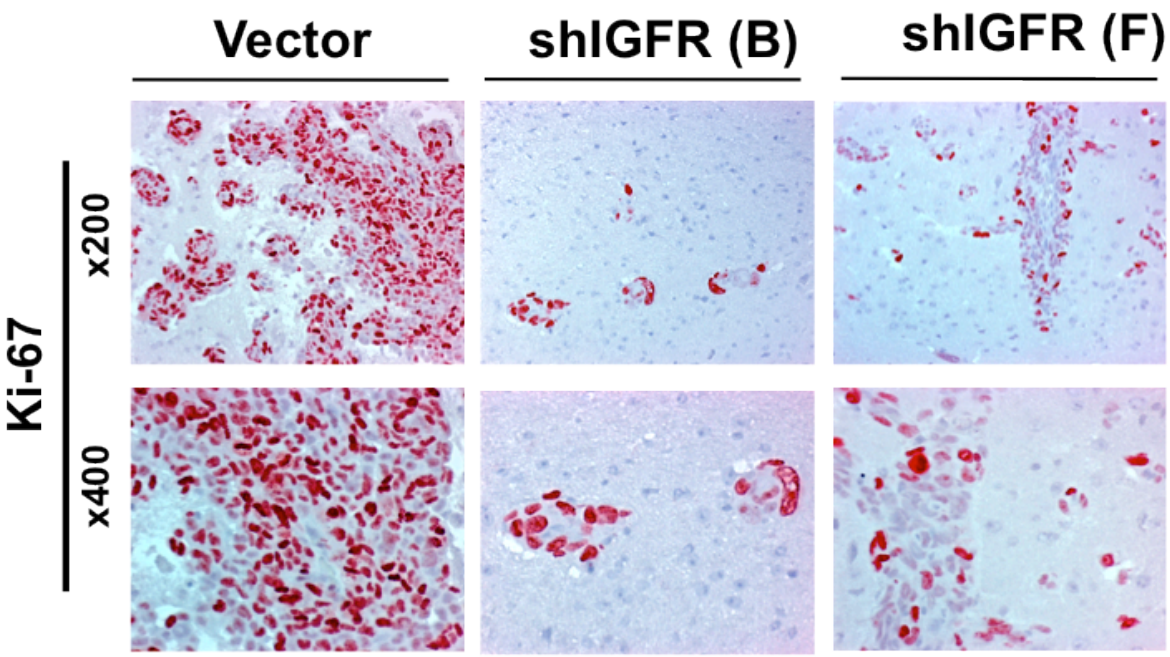

Figure 19. IHC staining of ki-67 of brain metastases of mice inoculated with Vector, shIGF-IR (B) and shIGF-IR (F) 231Br cells. Red = nuclear ki-67 staining. Images were taken at 200x and 400x magnification, as indicated.

Table 1

	Expression		
Staining	**Vector**	**shIGFIR (B)**	**shIGFIR (F)**
IGF-IR	High	Medium	Low
GFAP	High	High	High
Ki-67	N 80%	N 30%	N 22%

Legend:
High = ++/+++
Medium = +/++
Low = +
N = nucleus
GFAP = glial fibrillary acidic protein
High = cytosolic expression

Table 1. Summary of H&E and IHC staining of brain metastases of mice inoculated with Vector, shIGF-IR (B) and shIGF-IR (F) 231Br cells. Higher IGF-IR and ki-67 staining appears to correlate with formation of larger metastases.

Figure 20

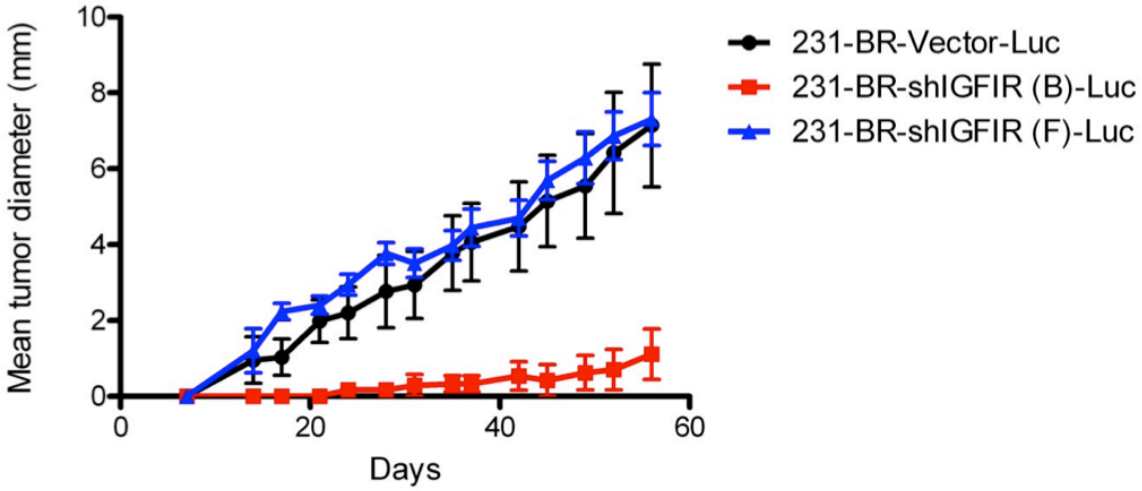
Mean tumor diameter (mm)
10
8
6
4
2
0
0
20
40
60
Days
231-BR-Vector-Luc
231-BR-shIGFIR (B)-Luc
231-BR-shIGFIR (F)-Luc

Figure 20. Tumor formation in the mammary fat pad is heterogeneous in IGF-IR knockdown cell lines.

Female nude mice were inoculated with 231Br-Vector (n=10), 231Br-shIGF-IR (B) (n=10), or 231Br-shIGF-IR (F) (n=10) cells in the mammary fat pad. Tumor growth was measured bi-weekly for eight weeks beginning on the second week, and average tumor volumes are plotted.

Figure 21

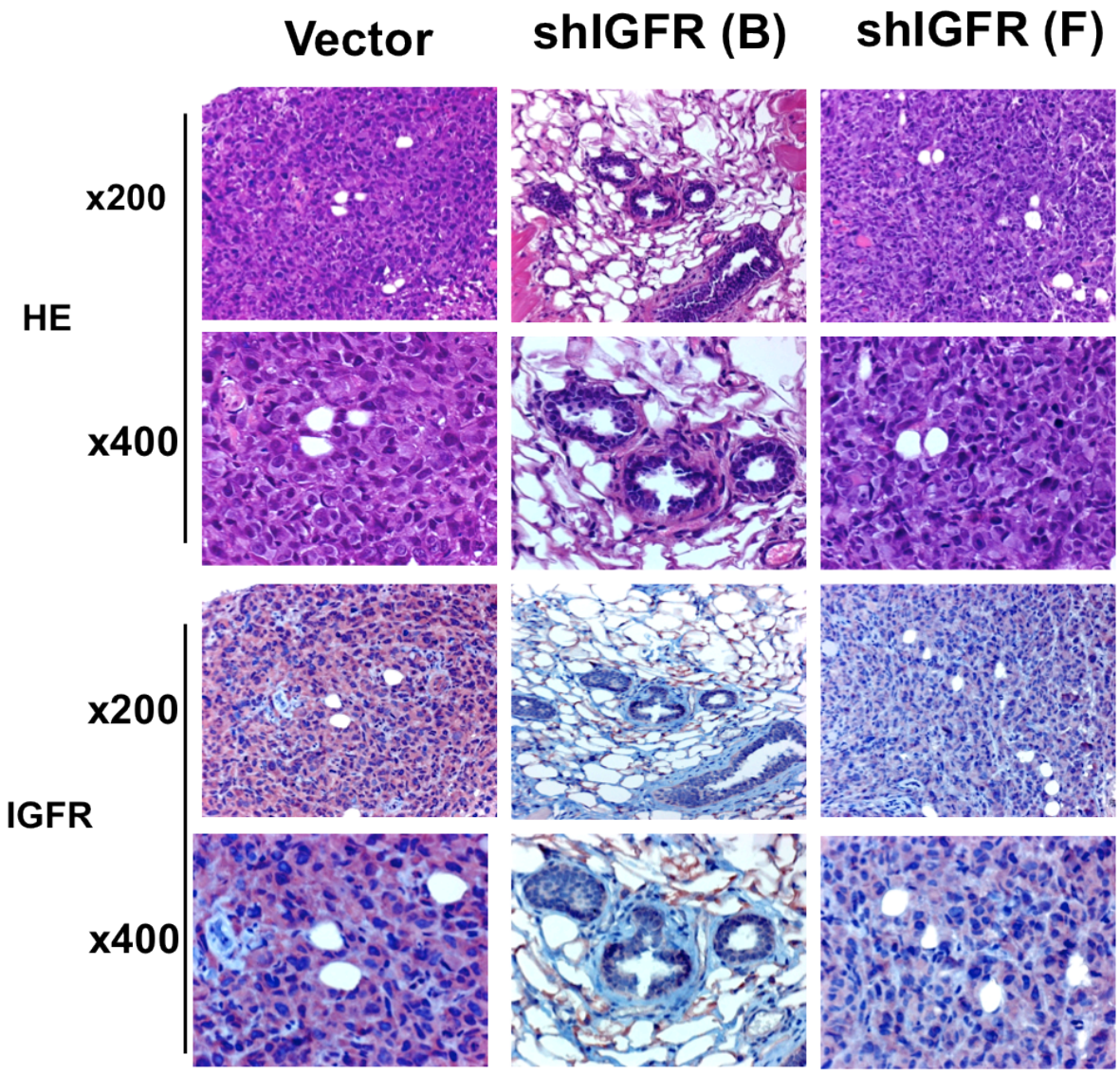

Figure 21. Tumor formation in the mammary fat pad from IGF-IR knockdown cells is heterogeneous.

H&E and IHC staining of representative mammary fat pad tumors from each group.

A, H&E panels: dark red = tumor tissue; blue = nucleus; light red = negative.

B and C, IGF-IR: red = positive; blue = nucleus. Images were taken at 200x and 400x magnification, as indicated.

4.10 Inhibition of the IGF-IR by picropodophyllin induces G2/M cell cycle arrest and inhibits downstream signaling and biological function

Several monoclonal antibodies and TKIs against IGF-IR are currently under study in the clinical setting and have shown promise in the treatment of solid tumors (Chitnis et al., 2008). Picropodophyllin (PPP) causes an induction of cell cycle arrest in the G2/M phase and is the only inhibitor that can specifically inhibit IGF-IR without affecting the insulin receptor (Stromberg et al., 2006). PPP also leads to inhibition of cell growth, migration and invasion, and metastasis in a PI3K/AKT-dependent manner (Girnita et al., 2004; Menu et al., 2006; D. Vasilcanu et al., 2004). We analyzed the effect of PPP on the cell cycle and demonstrated that PPP induces an increase of cells in G2/M phase by 86% in 231Br cells and 35% in BT474Br3 cells (Figure 22). This result is consistent with other published studies that demonstrated arrest in the G2/M transition upon PPP treatment (Stromberg et al., 2006),(Karasic, Hei, & Ivanov, 2010). However, PPP-induced G2/M cell cycle arrest is an interesting phenomenon given that the IGF-IR's major effect on the cell cycle is not primarily exerted in G2/M, but in the G1/S transition. IGF-IR regulates the G1/S transition by activation of PI-3K/Akt and/or ERK pathways, which leads to Cyclin D1 and CDK4 expression and cell cycle progression (Lavoie, L'Allemain, Brunet, Muller, & Pouyssegur, 1996). IGF-IR may also regulate the G2/M transition by upregulation of Cyclins A and B, and cdc2 synthesis, but this function is not as well documented (Furlanetto, Harwell, & Frick, 1994).

Concomitant with G2/M cell cycle arrest, PPP treatment of 231Br and BT474 Br3 cells potently blocked the activation of molecules downstream of IGF-IR in a

dose-dependent manner, in particular the phosphorylation of AKT-Ser473 and p70S6 kinase-Thr389 (Figure 23). It is unlikely that inhibition of AKT phosphorylation by PPP is responsible for the G2/M cell cycle arrest we observed, since AKT is primarily involved in the G1/S transition. It is possible that the G2/M cell cycle arrest resulted in less cycling cells and therefore a decrease in overall AKT activation. Another explanation could be off-target effects of PPP treatment, such as inhibition of the EGFR or c-Met receptors, which are both known to play a role in the G2/M transition (Baker & Yu, 2001) (Factor et al., 2010). Further studies should address whether PPP-induced G2/M arrest and AKT pathway downregulation are linked, or a result of off-target effects in our cell lines.

In addition, PPP inhibited biological functions of the 231 brain-seeking cells in which PPP-treated cells had impaired migration (Figure 24A, quantitation shown in Figure 24B) and invasion (Figure 24C, quantitation shown in Figure 24D). PPP did not significantly inhibit the migration or invasion of BT474 Br3 cells (Figure 24E), which may be due to the low baseline *in vitro* metastatic properties of this luminal-type cell line. Perhaps overexpression of IGF-IR in BT474 M1 (parental) or BT474 Br3 cells combined with PPP inhibitor experiments using IGF-1 as a chemoattractant would better address the significance of IGF-IR in these less aggressive, yet still brain-seeking, breast cancer cells. Furthermore, treatment of 231 Parental and brain-seeking breast cancer cells with different concentrations of PPP inhibited wound-healing (Figure 25A) and cell proliferation (Figure 25B), and these effects were more pronounced in the brain-seeking cells that overexpress IGF-IR. Thus, PPP inhibits cell migration and proliferation while enhancing cell-cell

adhesion, similar to the effects achieved by siRNA and shRNA ablation of IGF-IR. Taken together, these data indicate that IGF-IR-driven signaling could be potentially targeted by PPP in highly invasive brain-seeking cells. Further studies should test this hypothesis in a mouse model of experimental brain metastasis.

Figure 22

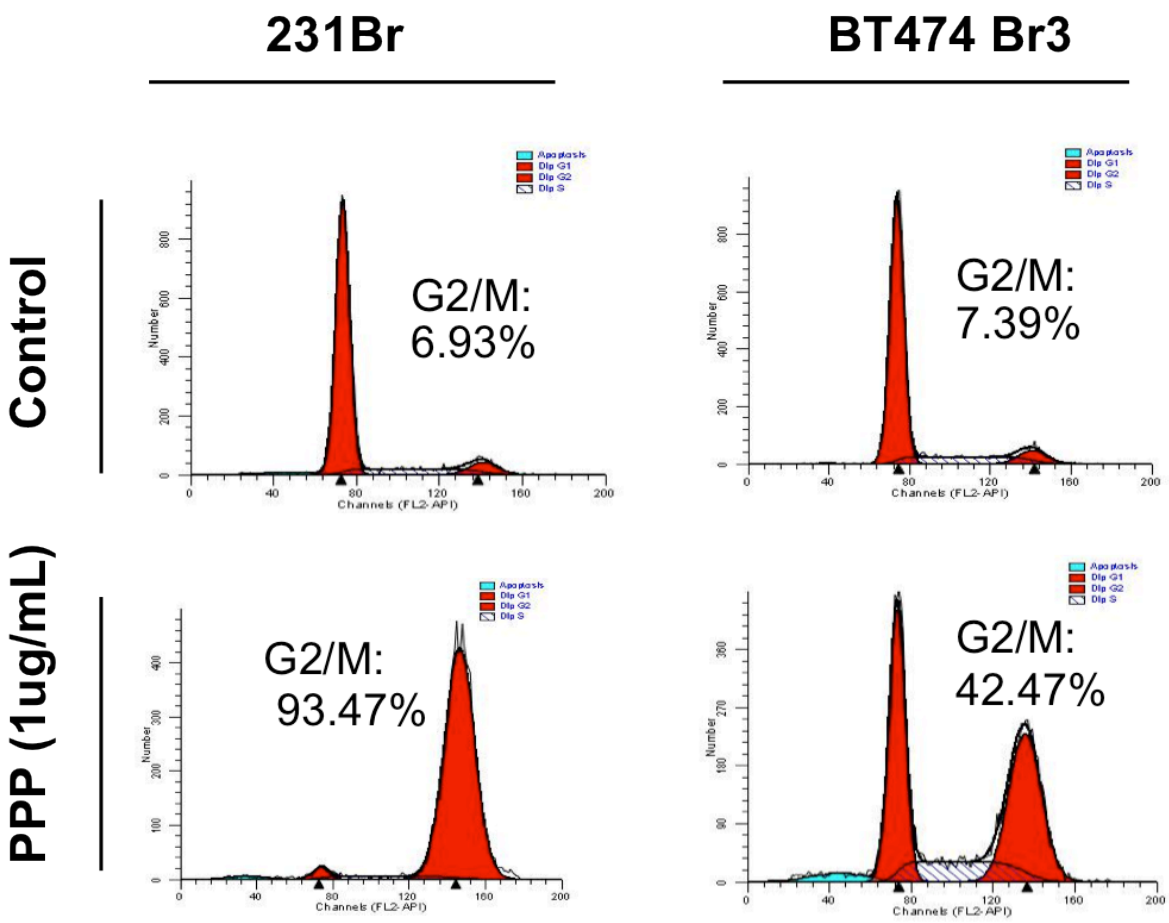
231Br
BT474 Br3
Control
PPP (1ug/mL)
G2/M:
6.93%
G2/M:
7.39%
G2/M:
93.47%
G2/M:
42.47%
Channels (FL2-API)
Number

Figure 22. Picropodophyllin induces G2/M cell cycle arrest in brain-seeking breast cancer cells.

Cell cycle analysis by propidium iodide staining of brain-seeking cells (231Br and BT474 Br3) treated with 1 μg/mL PPP for 48 hr.

Figure 23

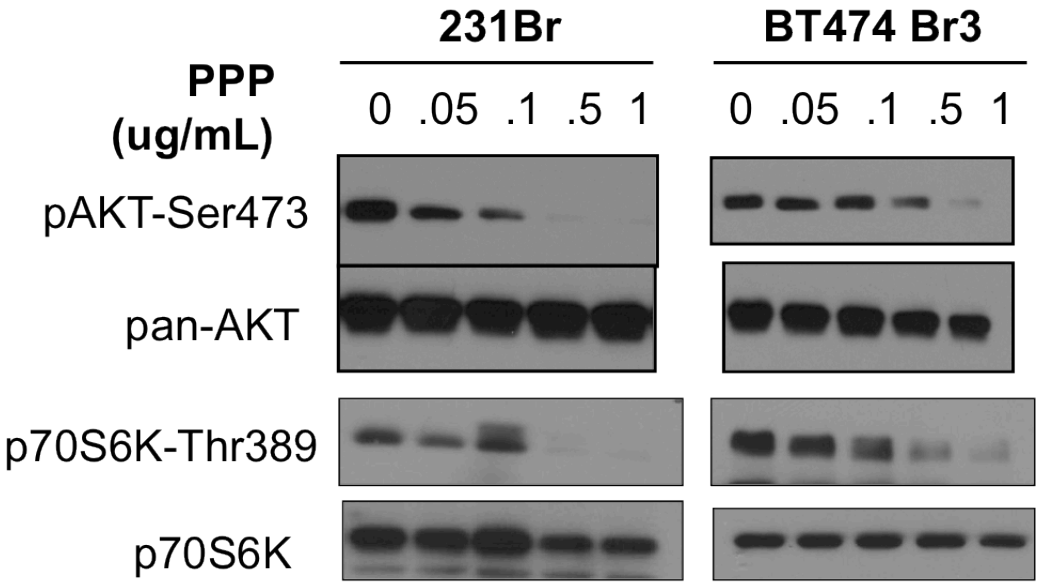
231Br
BT474 Br3
PPP
(ug/mL)
0 .05 .1 .5 1
0 .05 .1 .5 1
pAKT-Ser473
pan-AKT
p70S6K-Thr389
p70S6K

Figure 23. Picropodophyllin inhibits activation of IGF-IR downstream targets in brain-seeking breast cancer cells.

Immunoblot of phospho-proteins activation downstream of IGF-IR in brain-seeking cells treated with escalating concentrations of PPP for 24h.

Figure 24

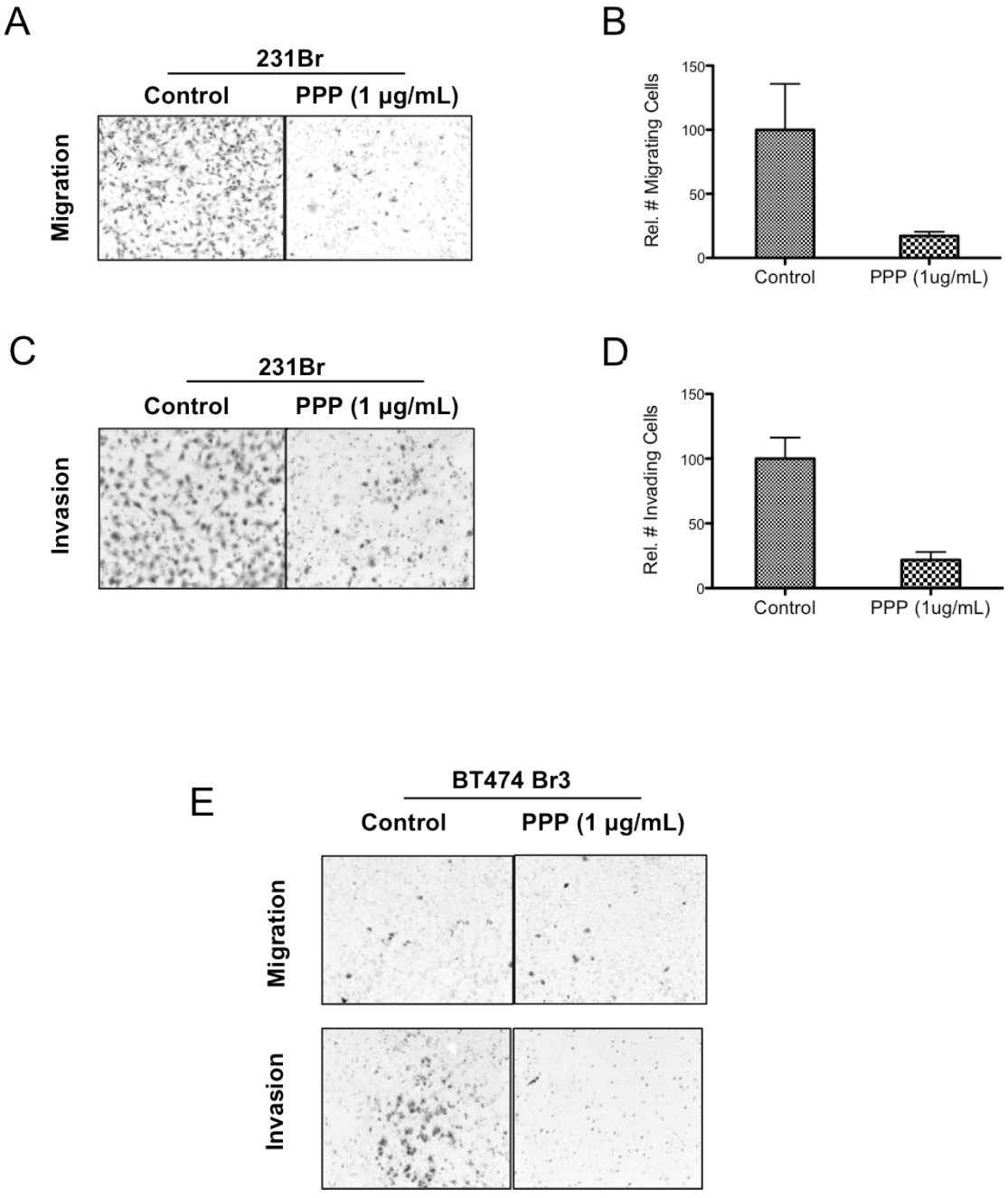
A
231Br
Control
PPP (1 µg/mL)
Migration
B
Rel. # Migrating Cells
150
100
50
0
Control
PPP (1ug/mL)
C
231Br
Control
PPP (1 µg/mL)
Invasion
D
Rel. # Invading Cells
150
100
50
0
Control
PPP (1ug/mL)
E
BT474 Br3
Control
PPP (1 µg/mL)
Migration
Invasion

Figure 24. Picropodophyllin inhibits migration and invasion in 231 brain-seeking breast cancer cells.

A, Transwell migration assay of 231Br cells treated with 1 μg/mL PPP for 24 hr.

B, Quantitative analysis of relative number of migrating cells from (A).

C, Matrigel invasion assay of 231Br cells treated with 1 μg/mL PPP for 24 hr.

D, Quantitative analysis of relative number of migrating cells from (D).

All migration and invasion assays used complete medium as a chemoattractant. Images shown are representative of one of three experiments performed. Bars represent mean ± SEM.

E, Transwell migration and matrigel invasion assay of BT474 Br3 cells.

Figure 25

A

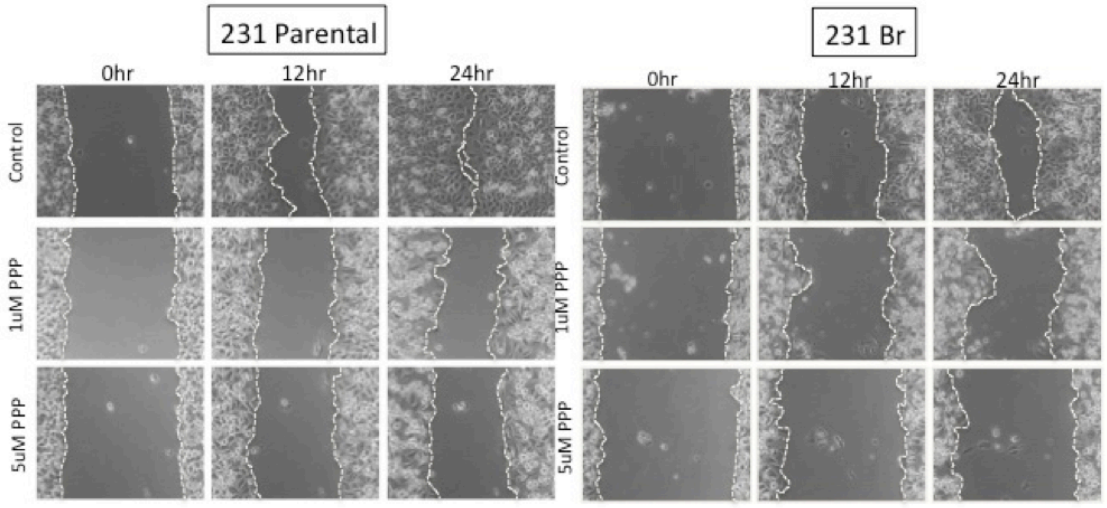
231 Parental
231 Br
0hr
12hr
24hr
0hr
12hr
24hr
Control
1uM PPP
5uM PPP
Control
1uM PPP
5uM PPP

B

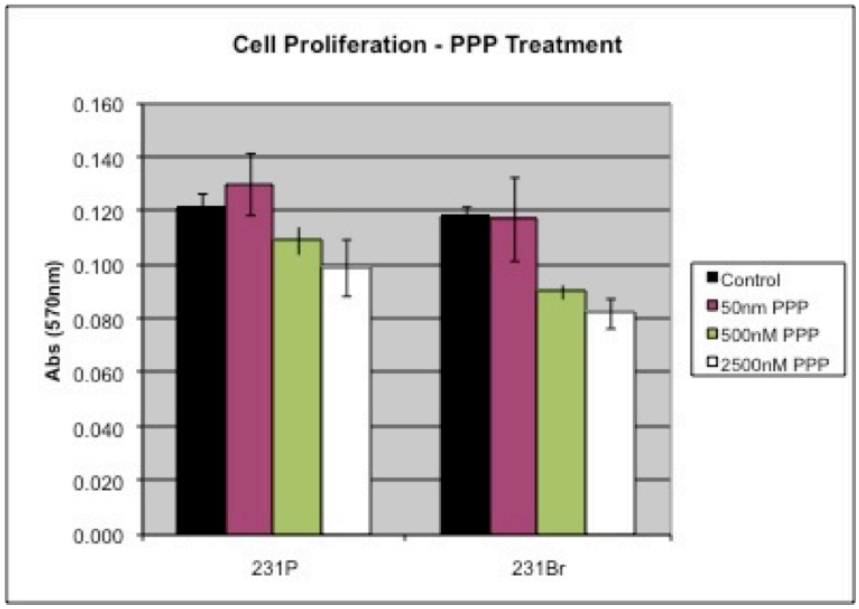
Cell Proliferation - PPP Treatment
Abs (570nm)
0.160
0.140
0.120
0.100
0.080
0.060
0.040
0.020
0.000
231P
231Br
Control
50nm PPP
500nM PPP
2500nM PPP

Figure 25. Picropodophyllin inhibits wound healing and proliferation in brain-seeking breast cancer cells.

A, Wound healing assay of parental and brain-seeking 231 cells treated with different concentrations of PPP. Brain-seeking cells have decreased wound healing ability in response to PPP.

B, MTT assay of cells treated with PPP for 48 hours. Proliferation of brain-seeking cells is more sensitive to PPP treatment than parental cells.

CHAPTER 5

SUMMARY AND DISCUSSION

5.1 Summary

The work described in this thesis is summarized in the model depicted in Figure 32. In brief, the IGF-IR signaling axis was activated both endogenously and in an IGF-1 dependent manner in brain-seeking subclones of breast cancer cell lines. IGF-IR activation is determined by the level of total tyrosine phosphorylation of the IGF-I receptor, and by the phosphorylation of specific tyrosine residues 1131 and 1135, which pertain to the kinase domain. IGF-IR activation was also evident by the tyrosine phosphorylation detected in IRS-2, the scaffold protein immediately downstream of IGF-IR that is known to activate migratory and invasive functions in metastatic breast cancer cells. AKT, but not ERK, was also phosphorylated both endogenously and upon IGF-1 stimulation of brain-seeking cells. We found that IGF-IR activation was at least partially dependent on IGFBP3 protein, which is highly secreted in 231Br cells but not in parental 231 cells. IGFBP3 knockdown resulted in significant downregulation of IGF-IR tyrosine phosphorylation.

When we experimentally ablated IGF-IR protein in brain-seeking cells, either by transient siRNA transfection or stable shRNA transfection, we observed a decrease in the proliferation, motility and invasiveness of cells. When injected into the intracarotid artery of nude mice, these IGF-IR shRNA knockdown cells displayed a delay in their colonization of the brain, which led to a significantly longer lifespan of these mice that acquired brain metastases. The IHC staining confirmed that IGF-IR expression was high in the control brain-seeking cells, but interestingly the brain metastases formed from shRNA groups had retained or partially re-expressed IGF-IR, although lower than the control groups. IGF-IR shRNA effects on mammary fat

pad tumor growth did not behave as expected, with one knockdown group completely unable to form tumors and the other producing equal tumor volumes as the control groups. The IGF-IR inhibitor PPP caused G2/M cell cycle arrest as well as dose-dependent downregulation of AKT phosphorylation and p70S6Kinase.

In a separate study aimed at better characterize the AKT activation profile between brain-seeking and parental breast cancer cells, we found that AKT is constitutively phosphorylated in the nucleus of brain-seeking cells, and this phosphorylated form is stimulated by the IGF-IR signaling axis. Nuclear phospho-AKT was enhanced upon IGF-1 stimulation and downregulated in IGF-IR shRNA knockdown cell lines. However, when stimulated with EGF-ligand or treated with the EGFR inhibitor Tarceva, nuclear phospho-AKT remained unchanged. Furthermore, we found that transient transfection with a combination of AKT1 and AKT3 are the two major isoforms of AKT that are phosphorylated in the nucleus of brain-seeking cells.

Figure 26

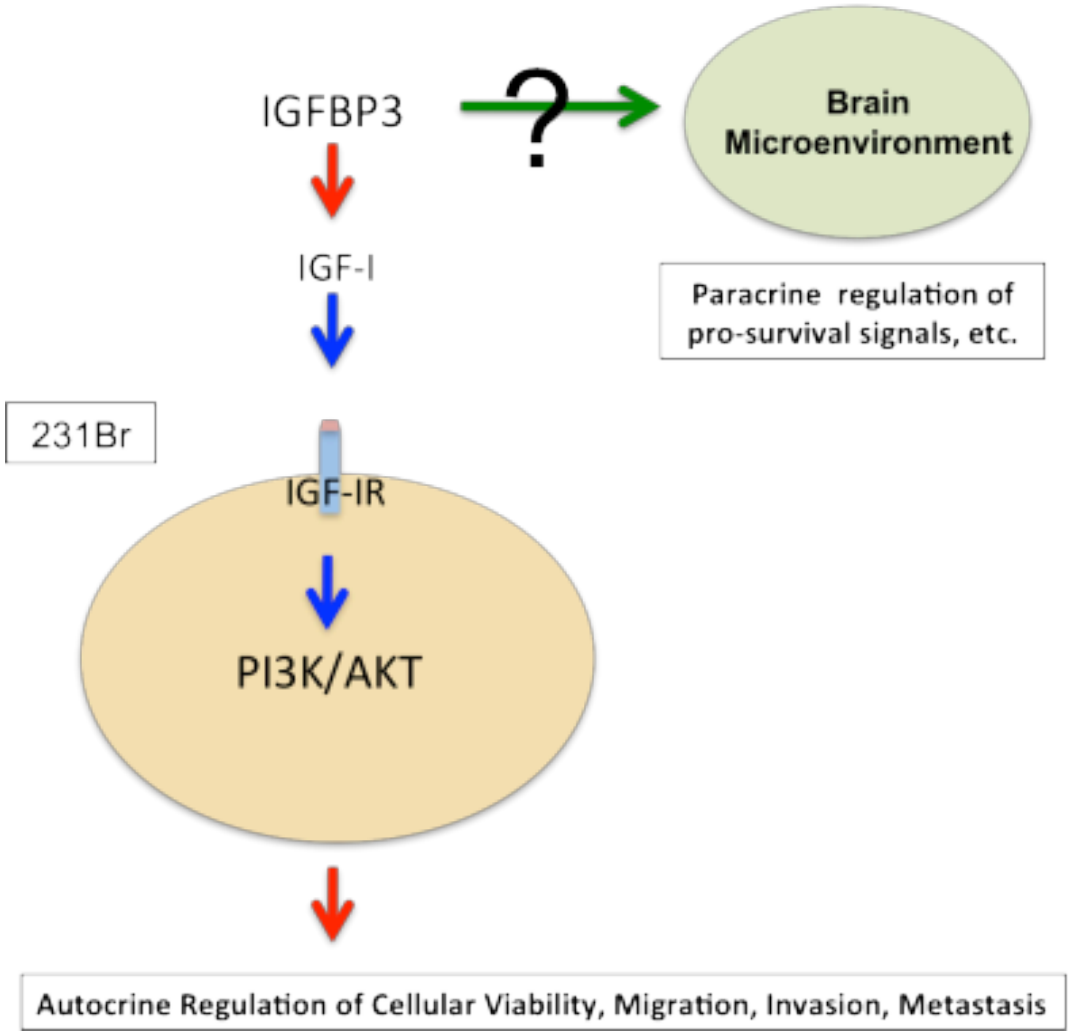
IGFBP3
?
Brain Microenvironment
IGF-I
Paracrine regulation of pro-survival signals, etc.
231Br
IGF-IR
PI3K/AKT
Autocrine Regulation of Cellular Viability, Migration, Invasion, Metastasis

5.2 Discussion

An important step in the development of rational therapies for brain-metastatic breast cancer is the identification of major molecular drivers of the disease. The study presented here supports the notion that (A) the IGF-IR signaling axis is active and mediates malignant phenotypes in brain-seeking breast cancer cells, (B) both genetic and pharmacological inhibition IGF-IR decrease the malignancy of brain-seeking cells *in vitro*, and remarkably (C) IGF-IR shRNA-expressing breast cancer cells have a decreased ability to form brain tumors in an *in vivo* model of experimental brain metastasis. The studies presented here support that IGF-IR signaling is a driver of brain metastases, with important implications in which therapeutic inhibition of this receptor may prevent or delay the establishment of IGF-IR-positive metastatic brain tumors from breast cancer.

In our model system, 231Br and BT474Br3 cells expressed more of the autophosphorylated form of IGF-IR. This result is in agreement with previous studies that found activated phospho-IGF-IR/IR and phospho-S6K are associated with poor survival in patients with invasive breast cancer (Law et al., 2008). Furthermore, phospho-IGF-IR and phospho-AKT were recently shown to correlate with metastases of breast cancer to the brain in a cohort of 42 brain metastases from breast and lung cancer patients (Improta et al., 2011). In our study, we found constitutively activated IGF-I Receptor when cells were examined in normal serum conditions (10%FBS/DMEM), concomitant with a baseline AKT phosphorylation at Ser473, suggesting constitutive IGF-IR pathway activation (Figs. 5A, 5B, 12, 26). This constitutive IGF-IR activation was abrogated when we eliminated the IGF-I

Receptor through siRNA, shRNA, or by treatment with PPP (Figs. 11-14, 22-25). Indeed, phosphorylated IGF-IR appears to be a recurrent theme in advanced breast cancers, and our results further elucidated its biological significance.

We concluded that constitutive autophosphorylation of IGF-IR is likely due to regulation by the autocrine components of the IGF-IR signaling axis, such as IGF-1 and IGFBP3. IGFBP3 was overexpressed in 231Br brain-seeking cells, and its knockdown by siRNA resulted in a significant decrease of IGF-IR Tyr phosphorylation. These findings led us to believe that IGFBP3 may enhance IGF-1 bioavailability and subsequently activate IGF-IR in our model system. Various studies suggest mechanisms of IGF-IR induction by IGFBP3, including signaling through sphingosine kinase (Sphk) and cross-activation of IGF-IR and EGFR and binding of IGFBP3 (Martin et al., 2009). However, further work is needed to confirm the IGF-1 ligand-dependent function of IGFBP3 on IGF-IR.

To address the biological significance of IGF-IR, we constructed brain-seeking 231 cells stably expressing IGF-IR shRNA. Ablation of IGF-IR diminished the proliferation, migration, and invasion of 231Br cells *in vitro*. Knocking down IGF-IR delayed the outgrowth of brain metastases and extended the survival of mice bearing brain metastases. When we examined the brains of mice bearing brain metastases of shIGF-IR 231Br cells, we were surprised to find that these metastases expressed IGF-IR, albeit at lower levels than the brain metastases from the vector 231Br group. We speculate that in our model, the brain microenvironment selected for, if not promoted, the survival of tumor cells with remaining expression of IGF-IR.

5.2.I Implications for brain metastasis in Her2+ and triple negative breast cancer

The cause of brain metastasis remains elusive although 25 to 40% of patients with Her2+ and triple-negative breast cancer (TNBC) have a significantly increased likelihood of developing brain metastases (Duchnowska et al., 2012; Steeg et al., 2011) (Hicks et al., 2006). Interestingly, the increased signaling of the IGF-IR has been shown to associate with resistance of Her2+ breast cancers to trastuzumab (Gallardo et al., 2012). A recent preclinical study showed the expression of an IGF-IR gene signature in TNBC that consequently sensitizes this cancer subtype to anti-IGF-IR therapy (Litzenburger et al., 2011). IGF-IR signaling was also shown to promote the proliferation and survival of TNBC cells, and it was associated with early tumor recurrence in TNBC patients when accompanied by PTEN loss (Davison, de Blacquiere, Westley, & May, 2011; Iqbal, Thike, Cheok, Tse, & Tan, 2012). In addition, other groups have also suggested the reliance of TNBC cell lines on IGF-1 signaling (Davison et al., 2011). It is worth noting that the 231Br cell line used in our model system is a TNBC cell line, and our results support the notion that IGF-IR might play a role in brain metastasis of TNBC. Future studies with additional TNBC models should explore the role of IGF-IR in this aggressive subset of breast cancers in further detail.

5.2.II Implications for pharmacological targeting of the IGF-IR signaling axis

We found that PPP potently inhibited IGF-IR signaling in breast cancer cells *in vitro*. A previous report identified that the major IGF-regulated process in the cell cycle is upregulation of genes involved in the G2/M transition (Litzenburger et al., 2011). Our findings confirmed that the same holds true in brain-seeking breast cancer cells. Furthermore, in an intracranial xenograft model of glioblastoma, PPP demonstrated ability to cross the blood-brain-barrier and cause tumor regression as well as downregulation of p-AKT, suggesting its potential usefulness in brain metastasis treatment (Yin et al., 2010). However, a recent study of drug delivery in mouse models of breast cancer brain metastasis found the heterogeneity of blood-tumor-barrier permeability to be a major obstacle to drug efficacy, and further validation of PPP in these mouse models is needed (Lockman et al., 2010). To our knowledge, this is the first study to establish a clear biological role of the IGF-IR and its activation in brain-specific metastases of breast cancer, suggesting that dysregulated molecules along the IGF-IR signaling pathway play a significant role in the establishment of brain metastasis. Further studies should pursue the utility of IGF-IR inhibitors for the prevention and treatment of brain metastases of breast cancer, particularly in a setting where the patient is refractory to other therapies.

5.2.III Implications of using human breast cancer cell lines in models of brain metastasis

Our model of experimental brain metastasis consisted of injection of human breast cancer cell lines that had been selected in vitro for their brain-seeking properties.

Our model, therefore, may not be the best for studies of spontaneous brain metastasis, or to study the early steps of brain metastasis when tumor cells leave their primary and/or metastatic tumor site and the characteristics that attract these cells to the brain as a metastatic site. Injection of the tumor cells into the carotid artery of mice circumvents all of these early steps, and even the major anatomical barrier of the lung that tumor cells encounter prior to reaching the brain. Therefore, it is important to note that our model primarily deals with the effect of IGF-IR knockdown in the ability of breast cancer cells to arrest and attach to the capillary bed of the brain, cross the blood-brain-barrier, survive in the brain to establish metastases and eventually cause morbidity due to tumor burden. Future studies should fine-tune exactly which of these later steps of metastasis the IGF-IR is involved in. For example, *in vitro* transendothelial migration assays using human brain microvascular endothelial cells using IGF-1 as a chemoattractant would provide clues about brain-derived IGF-1's role in inducing breast cancer cells to cross the blood-brain barrier, much like SDF-1 acts on the cell surface receptor CXCR4. Co-culture studies of astrocytes and our IGF-IR-knockdown breast cancer cells would yield more information about the crosstalk between breast cancer cells with cells of the brain parenchyma in the activation of survival cues.

5.2.IV Implications of using epithelial vs. mesenchymal cell types in modeling brain metastasis.

The MDA-MB-231 breast cancer cell line is a highly malignant and metstatic breast cancer cell line from epithelial origin. Despite its epithelial origin, the 231 cell line

behaves like an undifferentiated, mesenchymal cell type and in gene expression profiling studies it was found to express mostly mesenchymal genes (Charafe-Jauffret et al., 2006). This is in contrast to the BT-474 cell line that is also from epithelial origin but is more differentiated and has been classified into the luminal subtype. Luminal cell types are believed to be less invasive than mesenchymal or basal types due to the expression of the cell-fate differentiating factor GATA-3 (Asselin-Labat et al., 2007), although recent evidence suggests that luminal cell types also possess the ability to initiate metastatic tumors (Kim et al., 2012). It is important to note the difference in intrinsic behaviors between the 231 and BT-474 cell lines, because this may explain the differences we observed between the two cell types in *in vitro* experiments in our model of brain metastasis. In Figure 24, for instance, the migratory and invasive behavior of the 231Br cell line was inhibited by treatment with the IGF-IR inhibitor PPP, while the migration of BT474 Br3 cells was unchanged, and invasion was not as pronounced as in 231Br cells. Due to its non-invasive phenotype, the baseline metastatic potential of BT474 Br 3 cells is already very low, which presents a challenge in experiments where a decreased metastatic potential is expected. A more appropriate experiment for this cell type may be to measure the increase in *in vitro* metastatic potential under exogenous overexpression of IGF-IR.

5.2.V Role of EMT/MET and the brain microenvironment

Epithelial-to-mesenchymal transition (EMT) is the process by which tumor cells originating in the epithelium degrade the extracellular matrix and separate from the

tumor to become undifferentiated, mesenchymal-like cells with enhanced invasive and metastatic ability (Gao, Vahdat, Wong, Chang, & Mittal, 2012; Kalluri & Weinberg, 2009).

It was recently shown that mesenchymal-like 231 breast cancer cells can revert to the epithelial phenotype in the metastatic organ microenvironment in a process called MErT, or mesenchymal to epithelial reverting transition (Y. L. Chao, Shepard, & Wells, 2010). MErT was achieved by re-expression of E-cadherin in the metastatic tumor microenvironment, through a loss of methylation of the E-cadherin promoter. It would be of interest to perform IHC studies of brain metastases arising from 231Br cells, to test whether the brain microenvironment indeed induces the re-expression of E-cadherin in these cells, and whether IGF-IR has any part in this process. Since IGF-IR knockdown reduced brain metastasis in our model system, it would further strengthen our hypothesis that IGF-IR provides a survival advantage if somehow as a result of IGF-IR knockdown, E-cadherin re-expression was inhibited as well. Previous studies have found that IGF-IR overexpression in breast cancer cells promotes E-cadherin dependent cell-cell adhesion, cellular aggregation and survival (Guvakova & Surmacz, 1997). Also, IGF-IR knockdown in breast cancer cells resulted in a decrease of E-cadherin expression and destabilization of the E-cadherin-catenin complex, which is responsible for epithelial cell-cell adhesion and maintenance of the tumor architecture (Pennisi, Barr, Nunez, Stannard, & Le Roith, 2002; Wijnhoven, Dinjens, & Pignatelli, 2000).

5.3 Future Studies

This dissertation deals primarily with characterization of the intrinsic metastatic properties of brain-seeking breast cancer cells, the autocrine signaling that enhances metastatic properties, and the role of IGF-IR expression in the later stages of the metastatic process *in vivo*. Future studies should address the interactions between IGF-IR expressing breast cancer cells and other cell types in the brain microenvironment, such as vascular endothelial cells, astrocytes, and pericytes. The role of brain-derived IGF-1 and IGFBP3 in the promotion of metastatic cell survival is also of interest, as is the effect of breast cancer cells' intrinsic IGFBP3 overexpression in modulation of the brain parenchyma.

It is known that breast cancer patients differentially express IGF-1 and IGFBP3 in the circulation, but the relevance of their expression levels and their contribution to metastasis is still unknown. Therefore, the effect of circulating IGF-1 and IGFBP3 levels on the outcome of brain metastases of IGF-IR-positive breast cancers should be a subject for future studies.

We show that PPP successfully induced G2/M cell cycle arrest in both, 231Br and BT474 Br3 cells. As a next step, in vivo studies should examine the efficacy of PPP in preventing or reducing brain metastases at different doses, in order to establish whether inhibition of IGF-IR would be a good target to pursue in further pre-clinical studies.

CHAPTER 6

APPENDIX:

NUCLEAR AKT IN BRAIN SEEKING BREAST CANCER CELLS

6.1 Nuclear AKT signaling

Activated AKT has been previously shown to localize in the nucleus of cancer cells and correlates with poor progression in several cancers. In myocardial cells, for example, targeting of AKT to the nucleus resulted in enhanced cell survival and increased kinase activity (Shiraishi et al., 2004). Furthermore, myocardial epithelial cells that overexpress IGF-IR have an enrichment of nuclear phospho-AKT Ser47, which is also associated with enhanced cell survival (Camper-Kirby et al., 2001).

We previously observed that AKT signaling is stimulated by IGF-IR signaling in our model system (Figures 7 and 12). When we looked at the subcellular activation profile of AKT, we were surprised to find that AKT was constitutively phosphorylated in the nucleus of 231Br cells (Figure 26). Importantly, nuclear phospho-AKT observed most likely has active kinase function, since we also detected enhanced endogenous phosphorylation of AKT nuclear substrates, compared to 231 parental cells which did not express nuclear phospho-AKT (Figure 26). Furthermore, AKT phosphorylation was further enhanced by stimulation with IGF-1 ligand, which suggests that constitutive IGF-IR signaling may be at least partially responsible for enhanced nuclear AKT signaling.

In order to test the hypothesis that IGF-IR increases nuclear AKT signaling, we obtained nuclear lysates from the 231Br-Vector, 231Br-shIGF-IR (B) and 231Br-shIGF-IR (F) cell lines. 231Br Vector cells had Ser473 and Thr307 AKT phosphorylation, as expected. Ser473 phosphorylation was unaffected by IGF-IR knockdown in the shIGFR cells, however, AKT phosphorylation at Thr308 was

downregulated. The phosphorylation of nuclear AKT ser/thr substrates at the RXXS/T motif was also partially downregulated in the IGF-IR knockdown cell lines, although not dramatically, perhaps due to the residual Ser473 phosphorylation.

Next, we were interested in discerning which of the three AKT isoforms is phosphorylated in the nucleus of 231Br cells. We transiently transfected 231Br cells with control siRNA, or siRNAs targeting a combination of two or three AKT isoforms. We then isolated nuclear lysates from siRNA-transfected cells, and assessed the resulting AKT phosphorylation. AKT1 and AKT3 knockdown contributed the most significant decrease in phospho-AKT at both Ser473 and Thr308. This is an important result since both AKT1 and AKT3, have been implicated in metastasis and/or in vitro metastatic properties. In thyroid cancer, for example, it was shown that AKT1 and activated AKT co-localize in the nucleus of malignant cells, but not normal thyroid cells, and correlates with increased malignancy and migration (Vasko et al., 2004). Interestingly, it was also shown that an AKT1 mutant lacking a nuclear export sequence is sufficient to cause increased in vitro migration of Akt1 -/- fibroblasts (Saji et al., 2005). Akt3 deregulation was found to correlate with melanoma malignancy, and AKT3 expression progressively increases in more advanced stages of metastasis (Stahl et al., 2004). Taken together, our data suggest that IGF-IR signaling axis activation in brain-seeking breast cancer cells may lead to an enrichment of phosphorylated and kinase-active nuclear AKT, primarily AKT1 and AKT3, which then may activate nuclear substrates that promote migration and metastasis. Further studies should validate specific targets enhanced by this signaling axis, and further clarify the functional significance of nuclear AKT *in*

vivo.

Figure 27

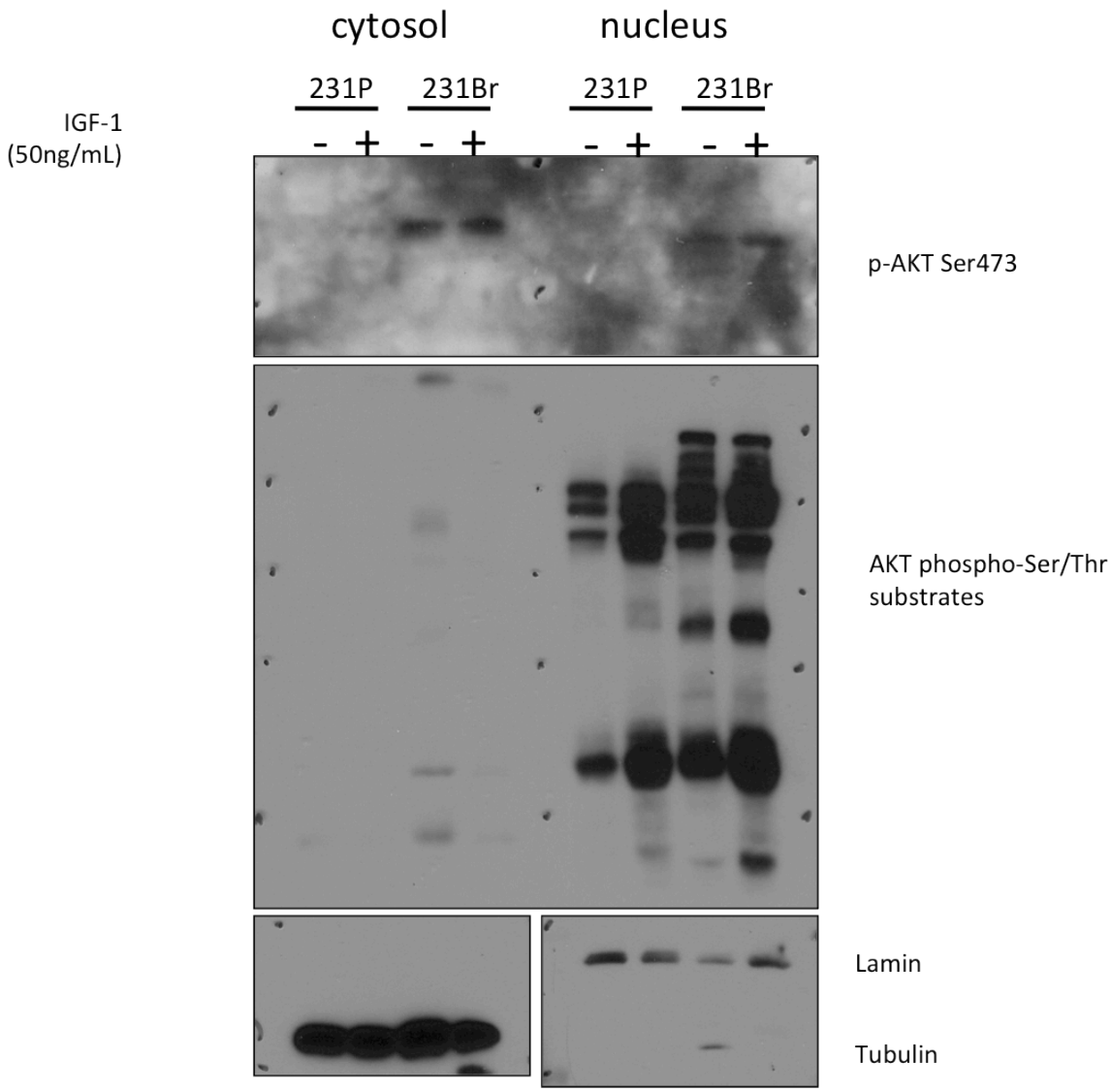
cytosol
nucleus
231P
231Br
231P
231Br
IGF-1
(50ng/mL)
- + - + - + - +
p-AKT Ser473
AKT phospho-Ser/Thr
substrates
Lamin
Tubulin

Figure 27. Nuclear localization of phospho-AKT and enhanced AKT nuclear substrate activation in brain-seeking breast cancer cells

Lysates of cytosolic and nuclear compartments of 231 and 231Br cells were obtained. Cytosolic fraction on the left is confirmed by Tubulin expression, and purity of the nuclear fraction on the right is confirmed by Lamin-B expression. Nuclear phospho-AKT is found in 231Br cells, but not parental cells. Constitutive AKT kinase activation is confirmed by serine/threonine phosphorylation of AKT substrates on the RXXS/T motif. Nuclear AKT and nuclear AKT substrate Ser/Thr phosphorylation are further stimulated by IGF-1 ligand.

Figure 28

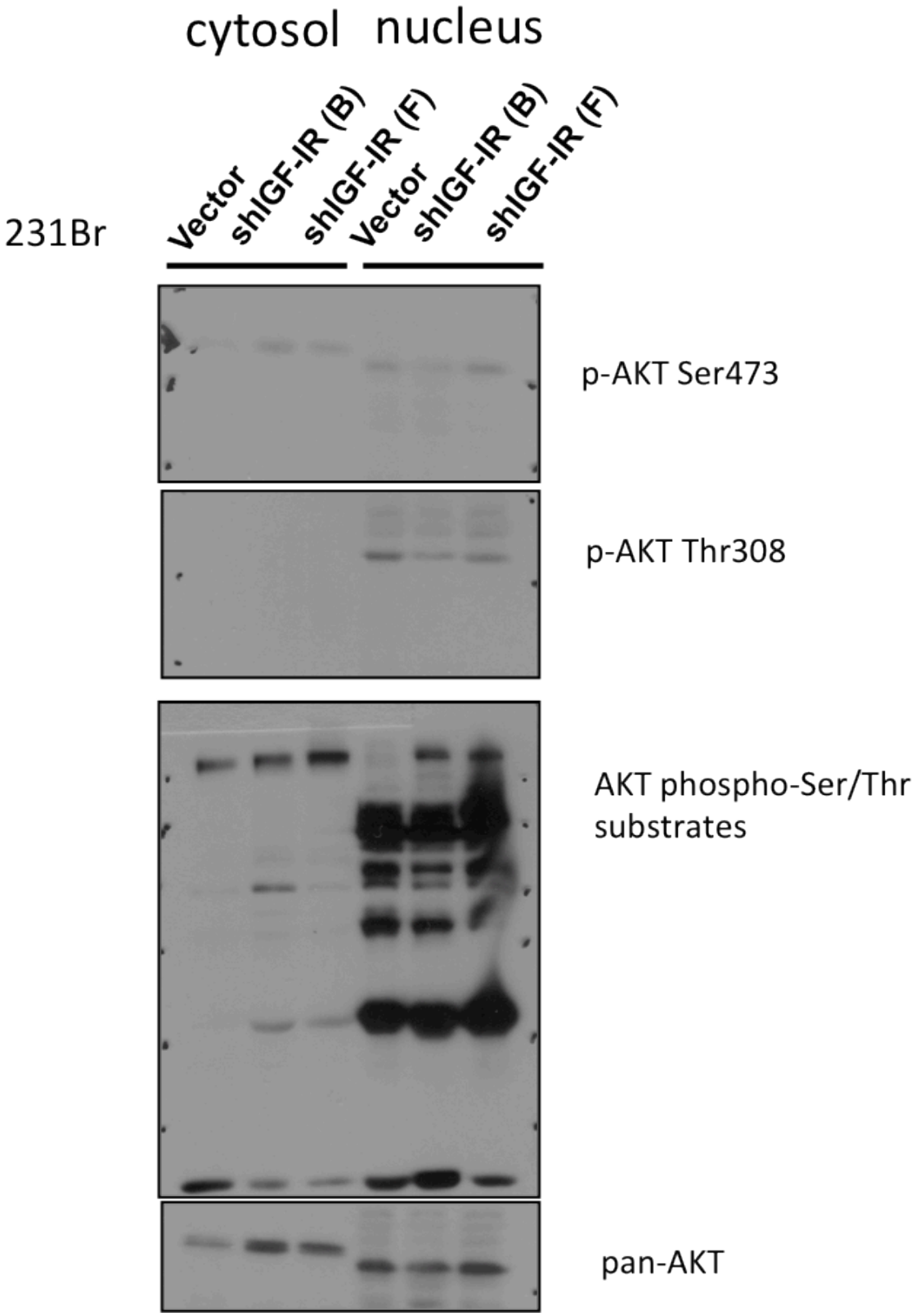
cytosol
nucleus
231Br
Vector
shIGF-IR (B)
shIGF-IR (F)
Vector
shIGF-IR (B)
shIGF-IR (F)
p-AKT Ser473
p-AKT Thr308
AKT phospho-Ser/Thr substrates
pan-AKT

Figure 28. Nuclear phospho-AKT and nuclear substrate activation are downregulated in IGF-IR knockdown brain-seeking breast cancer cells

Lysates of cytosolic and nuclear compartments of 231Br-Vector, 231Br-shIGF-IR (B) and 231Br-shIGF-IR (F) were obtained. Nuclear AKT phosphorylation at Ser473 is found in 231Br Vector cells and unaffected by IGF-IR knockdown. AKT phosphorylation at Thr308 is downregulated in IGF-IR knockdown cells. Phosphorylation of nuclear AKT serine/threonine substrates on the RXXS/T motif is partially downregulated in the IGF-IR knockdown cell lines.

Figure 29

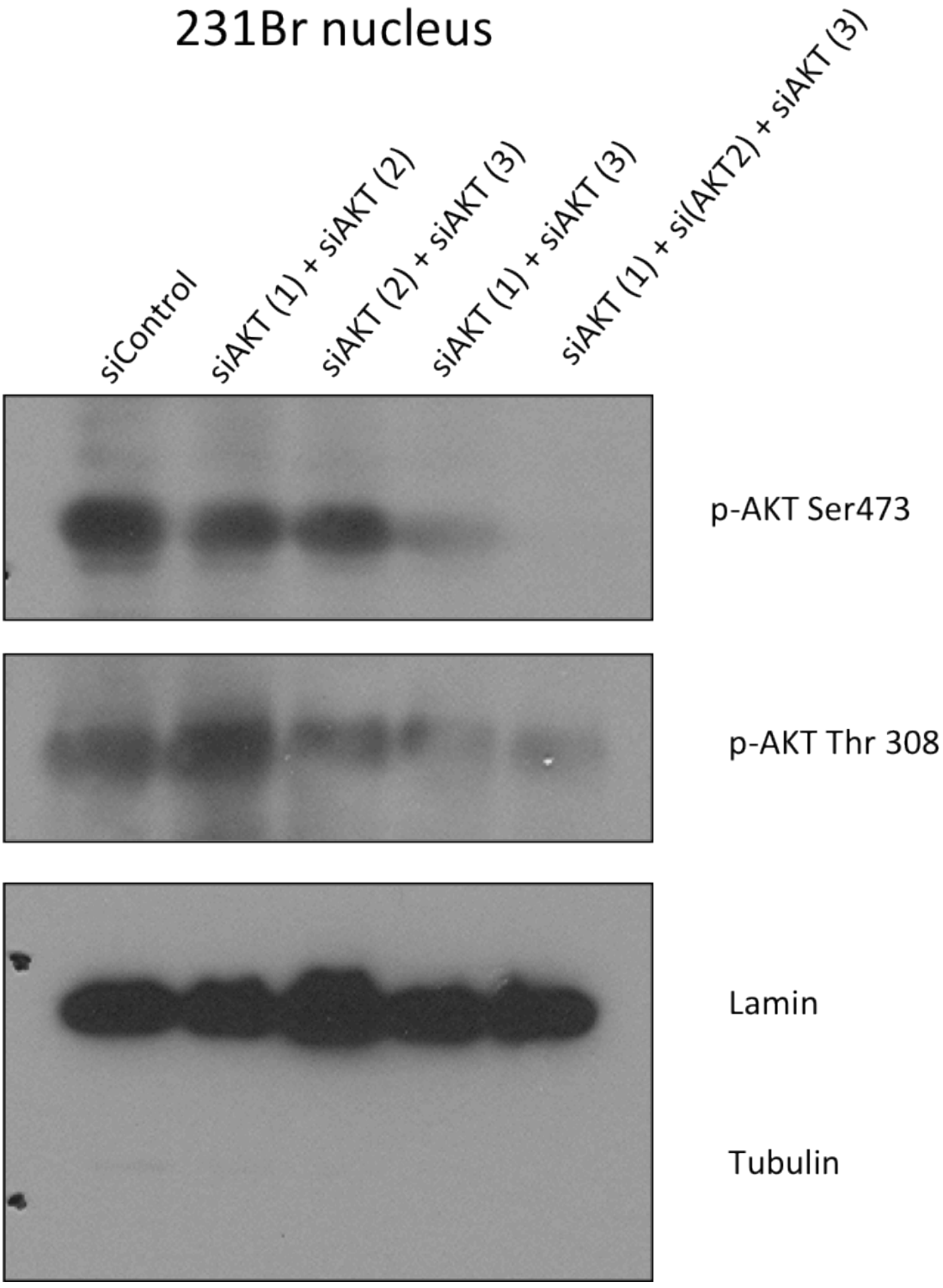
231Br nucleus
siControl
siAKT (1) + siAKT (2)
siAKT (2) + siAKT (3)
siAKT (1) + siAKT (3)
siAKT (1) + si(AKT2) + siAKT (3)
p-AKT Ser473
p-AKT Thr 308
Lamin
Tubulin

Figure 29. Nuclear phospho-AKT signal observed is primarily from AKT1 and AKT3 isoforms.

231Br cells were transiently transfected with control siRNA, or siRNAs targeting a combination of two or three AKT isoforms. Nuclear lysates from siRNA-transfected cells were isolated, and AKT phosphorylation was assessed. AKT1 and AKT3 knockdown contributed the most significant decrease in phospho-AKT at both Ser473 and Thr308.

CHAPTER 7

REFERENCES

Abramovitch, S., Glaser, T., Ouchi, T., & Werner, H. (2003). BRCA1-Sp1 interactions in transcriptional regulation of the IGF-IR gene. [Research Support, Non-U.S. Gov't

Research Support, U.S. Gov't, P.H.S.]. *FEBS Lett, 541*(1-3), 149-154.

Adelaide, J., Finetti, P., Bekhouche, I., Repellini, L., Geneix, J., Sircoulomb, F., . . . Chaffanet, M. (2007). Integrated profiling of basal and luminal breast cancers. [Research Support, Non-U.S. Gov't]. *Cancer Res, 67*(24), 11565-11575. doi: 10.1158/0008-5472.CAN-07-2536

Andrews, D. W., Scott, C. B., Sperduto, P. W., Flanders, A. E., Gaspar, L. E., Schell, M. C., . . . Curran, W. J., Jr. (2004). Whole brain radiation therapy with or without stereotactic radiosurgery boost for patients with one to three brain metastases: phase III results of the RTOG 9508 randomised trial. [Clinical Trial

Clinical Trial, Phase III

Multicenter Study

Randomized Controlled Trial

Research Support, U.S. Gov't, P.H.S.]. *Lancet, 363*(9422), 1665-1672. doi: 10.1016/S0140-6736(04)16250-8

Asselin-Labat, M. L., Sutherland, K. D., Barker, H., Thomas, R., Shackleton, M., Forrest, N. C., . . . Visvader, J. E. (2007). Gata-3 is an essential regulator of

mammary-gland morphogenesis and luminal-cell differentiation. [Research Support, Non-U.S. Gov't]. *Nat Cell Biol, 9*(2), 201-209. doi: 10.1038/ncb1530

Bachelot, T., Romieu, G., Campone, M., Dieras, V., Cropet, C., Dalenc, F., . . . Labbe-Devilliers, C. (2013). Lapatinib plus capecitabine in patients with previously untreated brain metastases from HER2-positive metastatic breast cancer (LANDSCAPE): a single-group phase 2 study. [Research Support, Non-U.S. Gov't]. *Lancet Oncol, 14*(1), 64-71. doi: 10.1016/S1470-2045(12)70432-1

Baker, N. E., & Yu, S. Y. (2001). The EGF receptor defines domains of cell cycle progression and survival to regulate cell number in the developing Drosophila eye. [Research Support, U.S. Gov't, P.H.S.]. *Cell, 104*(5), 699-708.

Barnholtz-Sloan, J. S., Sloan, A. E., Davis, F. G., Vigneau, F. D., Lai, P., & Sawaya, R. E. (2004). Incidence proportions of brain metastases in patients diagnosed (1973 to 2001) in the Metropolitan Detroit Cancer Surveillance System. [Research Support, Non-U.S. Gov't

Research Support, U.S. Gov't, P.H.S.]. *J Clin Oncol, 22*(14), 2865-2872. doi: 10.1200/JCO.2004.12.149

Bos, P. D., Zhang, X. H., Nadal, C., Shu, W., Gomis, R. R., Nguyen, D. X., . . . Massague, J. (2009). Genes that mediate breast cancer metastasis to the brain. [Research Support, N.I.H., Extramural

Research Support, Non-U.S. Gov't]. *Nature, 459*(7249), 1005-1009. doi: 10.1038/nature08021

Buijs, J. T., Stayrook, K. R., & Guise, T. A. (2011). TGF-beta in the Bone Microenvironment: Role in Breast Cancer Metastases. *Cancer Microenviron, 4*(3), 261-281. doi: 10.1007/s12307-011-0075-6

Camper-Kirby, D., Welch, S., Walker, A., Shiraishi, I., Setchell, K. D., Schaefer, E., . . . Sussman, M. A. (2001). Myocardial Akt activation and gender: increased nuclear activity in females versus males. [Research Support, Non-U.S. Gov't

Research Support, U.S. Gov't, P.H.S.]. *Circ Res, 88*(10), 1020-1027.

Carbonell, W. S., Ansorge, O., Sibson, N., & Muschel, R. (2009). The vascular basement membrane as "soil" in brain metastasis. [Research Support, N.I.H., Extramural

Research Support, Non-U.S. Gov't

Research Support, U.S. Gov't, Non-P.H.S.]. *PLoS One, 4*(6), e5857. doi: 10.1371/journal.pone.0005857

Chaffer, C. L., Brennan, J. P., Slavin, J. L., Blick, T., Thompson, E. W., & Williams, E. D. (2006). Mesenchymal-to-epithelial transition facilitates bladder cancer metastasis: role of fibroblast growth factor receptor-2. [Research Support, Non-U.S. Gov't

Research Support, U.S. Gov't, Non-P.H.S.]. *Cancer Res, 66*(23), 11271-11278. doi: 10.1158/0008-5472.CAN-06-2044

Chao, Y., Wu, Q., Acquafondata, M., Dhir, R., & Wells, A. (2012). Partial mesenchymal to epithelial reverting transition in breast and prostate cancer metastases. *Cancer Microenviron, 5*(1), 19-28. doi: 10.1007/s12307-011-0085-4

Chao, Y. L., Shepard, C. R., & Wells, A. (2010). Breast carcinoma cells re-express E-cadherin during mesenchymal to epithelial reverting transition. [Research Support, U.S. Gov't, Non-P.H.S.]. *Mol Cancer, 9*, 179. doi: 10.1186/1476-4598-9-179

Charafe-Jauffret, E., Ginestier, C., Monville, F., Finetti, P., Adelaide, J., Cervera, N., . . . Bertucci, F. (2006). Gene expression profiling of breast cell lines identifies potential new basal markers. [Comparative Study

Research Support, Non-U.S. Gov't]. *Oncogene, 25*(15), 2273-2284. doi: 10.1038/sj.onc.1209254

Cheng, X., & Hung, M. C. (2007). Breast cancer brain metastases. [Research Support, N.I.H., Extramural

Research Support, U.S. Gov't, Non-P.H.S.

Review]. *Cancer Metastasis Rev, 26*(3-4), 635-643. doi: 10.1007/s10555-007-9083-x

Chitnis, M. M., Yuen, J. S., Protheroe, A. S., Pollak, M., & Macaulay, V. M. (2008). The type 1 insulin-like growth factor receptor pathway. [Research Support, Non-U.S. Gov't

Review]. *Clin Cancer Res, 14*(20), 6364-6370. doi: 10.1158/1078-0432.CCR-07-4879

Davison, Z., de Blacquiere, G. E., Westley, B. R., & May, F. E. (2011). Insulin-like growth factor-dependent proliferation and survival of triple-negative breast cancer cells: implications for therapy. [Research Support, Non-U.S. Gov't]. *Neoplasia, 13*(6), 504-515.

Duchnowska, R., Biernat, W., Szostakiewicz, B., Sperinde, J., Piette, F., Haddad, M., . . . Jassem, J. (2012). Correlation between quantitative HER-2 protein expression and risk for brain metastases in HER-2+ advanced breast cancer patients receiving trastuzumab-containing therapy. *Oncologist, 17*(1), 26-35. doi: 10.1634/theoncologist.2011-0212

Dyer, M. A., Kelly, P. J., Chen, Y. H., Pinnell, N. E., Claus, E. B., Lee, E. Q., . . . Alexander, B. M. (2012). Importance of extracranial disease status and tumor subtype for patients undergoing radiosurgery for breast cancer brain metastases. *Int J Radiat Oncol Biol Phys, 83*(4), e479-486. doi: 10.1016/j.ijrobp.2012.01.054

Eichler, A. F., Chung, E., Kodack, D. P., Loeffler, J. S., Fukumura, D., & Jain, R. K. (2011). The biology of brain metastases-translation to new therapies. [Research Support, N.I.H., Extramural

Research Support, Non-U.S. Gov't

Research Support, U.S. Gov't, Non-P.H.S.

Review]. *Nat Rev Clin Oncol, 8*(6), 344-356. doi: 10.1038/nrclinonc.2011.58

Factor, V. M., Seo, D., Ishikawa, T., Kaposi-Novak, P., Marquardt, J. U., Andersen, J. B., . . . Thorgeirsson, S. S. (2010). Loss of c-Met disrupts gene expression program required for G2/M progression during liver regeneration in mice. [Research Support, N.I.H., Intramural]. *PLoS One, 5*(9). doi: 10.1371/journal.pone.0012739

Fernandez, A. M., & Torres-Aleman, I. (2012). The many faces of insulin-like peptide signalling in the brain. [Review]. *Nat Rev Neurosci, 13*(4), 225-239. doi: 10.1038/nrn3209

Firth, S. M., & Baxter, R. C. (1999). Characterisation of recombinant glycosylation variants of insulin-like growth factor binding protein-3. [Research Support, Non-U.S. Gov't]. *J Endocrinol, 160*(3), 379-387.

Firth, S. M., & Baxter, R. C. (2002). Cellular actions of the insulin-like growth factor binding proteins. [Review]. *Endocr Rev, 23*(6), 824-854.

Fitzgerald, D. P., Subramanian, P., Deshpande, M., Graves, C., Gordon, I., Qian, Y., . . . Steeg, P. S. (2012). Opposing effects of pigment epithelium-derived factor on breast cancer cell versus neuronal survival: implication for brain metastasis and metastasis-induced brain damage. [Research Support, N.I.H., Intramural

Research Support, U.S. Gov't, Non-P.H.S.]. *Cancer Res, 72*(1), 144-153. doi: 10.1158/0008-5472.CAN-11-1904

Fujita-Yamaguchi, Y., LeBon, T. R., Tsubokawa, M., Henzel, W., Kathuria, S., Koyal, D., & Ramachandran, J. (1986). Comparison of insulin-like growth factor I receptor and insulin receptor purified from human placental membranes. [Comparative Study

Research Support, U.S. Gov't, P.H.S.]. *J Biol Chem, 261*(35), 16727-16731.

Furlanetto, R. W., Harwell, S. E., & Frick, K. K. (1994). Insulin-like growth factor-I induces cyclin-D1 expression in MG63 human osteosarcoma cells in vitro. [Research Support, U.S. Gov't, P.H.S.]. *Mol Endocrinol, 8*(4), 510-517.

Gallardo, A., Lerma, E., Escuin, D., Tibau, A., Munoz, J., Ojeda, B., . . . Peiro, G. (2012). Increased signalling of EGFR and IGF1R, and deregulation of PTEN/PI3K/Akt pathway are related with trastuzumab resistance in HER2 breast carcinomas. [Research Support, Non-U.S. Gov't]. *Br J Cancer, 106*(8), 1367-1373. doi: 10.1038/bjc.2012.85

Gao, D., Vahdat, L. T., Wong, S., Chang, J. C., & Mittal, V. (2012). Microenvironmental regulation of epithelial-mesenchymal transitions in cancer. [Research Support, N.I.H., Extramural

Review]. *Cancer Res, 72*(19), 4883-4889. doi: 10.1158/0008-5472.CAN-12-1223

Gibson, S. L., Ma, Z., & Shaw, L. M. (2007). Divergent roles for IRS-1 and IRS-2 in breast cancer metastasis. [Comparative Study

Research Support, N.I.H., Extramural

Review]. *Cell Cycle, 6*(6), 631-637.

Girnita, A., Girnita, L., del Prete, F., Bartolazzi, A., Larsson, O., & Axelson, M. (2004). Cyclolignans as inhibitors of the insulin-like growth factor-1 receptor and malignant cell growth. [Research Support, Non-U.S. Gov't]. *Cancer Res, 64*(1), 236-242.

Gombos, A., Metzger-Filho, O., Dal Lago, L., & Awada-Hussein, A. (2012). Clinical development of insulin-like growth factor receptor--1 (IGF-1R) inhibitors: at the crossroad? *Invest New Drugs, 30*(6), 2433-2442. doi: 10.1007/s10637-012-9811-0

Grkovic, S., O'Reilly, V. C., Han, S., Hong, M., Baxter, R. C., & Firth, S. M. (2012). IGFBP-3 binds GRP78, stimulates autophagy and promotes the survival of breast cancer cells exposed to adverse microenvironments. *Oncogene*. doi: 10.1038/onc.2012.264

Guvakova, M. A., & Surmacz, E. (1997). Overexpressed IGF-I receptors reduce estrogen growth requirements, enhance survival, and promote E-cadherin-mediated cell-cell adhesion in human breast cancer cells. [Research Support, U.S. Gov't, Non-P.H.S.

Research Support, U.S. Gov't, P.H.S.]. *Exp Cell Res, 231*(1), 149-162. doi: 10.1006/excr.1996.3457

Hanafusa, T., Shinji, T., Shiraha, H., Nouso, K., Iwasaki, Y., Yumoto, E., . . . Koide, N. (2005). Functional promoter upstream p53 regulatory sequence of IGFBP3 that is silenced by tumor specific methylation. [Research Support, Non-U.S. Gov't]. *BMC Cancer, 5*, 9. doi: 10.1186/1471-2407-5-9

Hicks, D. G., Short, S. M., Prescott, N. L., Tarr, S. M., Coleman, K. A., Yoder, B. J., . . . Weil, R. J. (2006). Breast cancers with brain metastases are more likely to be estrogen receptor negative, express the basal cytokeratin CK5/6, and overexpress HER2 or EGFR. [Research Support, Non-U.S. Gov't]. *Am J Surg Pathol, 30*(9), 1097-1104. doi: 10.1097/01.pas.0000213306.05811.b9

Hiraga, T., Myoui, A., Hashimoto, N., Sasaki, A., Hata, K., Morita, Y., . . . Yoneda, T. (2012). Bone-derived IGF mediates crosstalk between bone and breast cancer cells in bony metastases. *Cancer Res*. doi: 10.1158/0008-5472.CAN-11-3061

Improta, G., Zupa, A., Fillmore, H., Deng, J., Aieta, M., Musto, P., . . . Wulfkuhle, J. D. (2011). Protein pathway activation mapping of brain metastasis from lung

and breast cancers reveals organ type specific drug target activation. [Research Support, Non-U.S. Gov't

Research Support, U.S. Gov't, P.H.S.]. *J Proteome Res, 10*(7), 3089-3097. doi: 10.1021/pr200065t

Iqbal, J., Thike, A. A., Cheok, P. Y., Tse, G. M., & Tan, P. H. (2012). Insulin growth factor receptor-1 expression and loss of PTEN protein predict early recurrence in triple-negative breast cancer. *Histopathology*. doi: 10.1111/j.1365-2559.2012.04255.x

Jackson, J. G., Zhang, X., Yoneda, T., & Yee, D. (2001). Regulation of breast cancer cell motility by insulin receptor substrate-2 (IRS-2) in metastatic variants of human breast cancer cell lines. [Research Support, U.S. Gov't, P.H.S.]. *Oncogene, 20*(50), 7318-7325. doi: 10.1038/sj.onc.1204920

Joyce, J. A., & Pollard, J. W. (2009). Microenvironmental regulation of metastasis. [Research Support, N.I.H., Extramural

Research Support, Non-U.S. Gov't

Review]. *Nat Rev Cancer, 9*(4), 239-252. doi: 10.1038/nrc2618

Kalluri, R., & Weinberg, R. A. (2009). The basics of epithelial-mesenchymal transition. [Research Support, N.I.H., Extramural

Research Support, Non-U.S. Gov't

Review]. *J Clin Invest, 119*(6), 1420-1428. doi: 10.1172/JCI39104

Kang, Y., Siegel, P. M., Shu, W., Drobnjak, M., Kakonen, S. M., Cordon-Cardo, C., . . . Massague, J. (2003). A multigenic program mediating breast cancer metastasis to bone. [Comparative Study

Research Support, Non-U.S. Gov't

Research Support, U.S. Gov't, P.H.S.]. *Cancer Cell, 3*(6), 537-549.

Kaplan, M. A., Isikdogan, A., Koca, D., Kucukoner, M., Gumusay, O., Yildiz, R., . . . Urakci, Z. (2013). Clinical outcomes in patients who received lapatinib plus capecitabine combination therapy for HER2-positive breast cancer with brain metastasis and a comparison of survival with those who received trastuzumab-based therapy: a study by the Anatolian Society of Medical Oncology. *Breast Cancer*. doi: 10.1007/s12282-013-0441-y

Karasic, T. B., Hei, T. K., & Ivanov, V. N. (2010). Disruption of IGF-1R signaling increases TRAIL-induced apoptosis: a new potential therapy for the treatment of melanoma. [Research Support, N.I.H., Extramural]. *Exp Cell Res, 316*(12), 1994-2007. doi: 10.1016/j.yexcr.2010.04.014

Kato, H., Faria, T. N., Stannard, B., Roberts, C. T., Jr., & LeRoith, D. (1994). Essential role of tyrosine residues 1131, 1135, and 1136 of the insulin-like growth factor-I (IGF-I) receptor in IGF-I action. [Research Support, Non-U.S. Gov't]. *Mol Endocrinol, 8*(1), 40-50.

Kim, J., Villadsen, R., Sorlie, T., Fogh, L., Gronlund, S. Z., Fridriksdottir, A. J., . . . Petersen, O. W. (2012). Tumor initiating but differentiated luminal-like breast

cancer cells are highly invasive in the absence of basal-like activity. [Research Support, N.I.H., Extramural

Research Support, Non-U.S. Gov't

Research Support, U.S. Gov't, Non-P.H.S.]. *Proc Natl Acad Sci U S A, 109*(16), 6124-6129. doi: 10.1073/pnas.1203203109

Krutzik, P. O., & Nolan, G. P. (2003). Intracellular phospho-protein staining techniques for flow cytometry: monitoring single cell signaling events. [Comparative Study

Research Support, U.S. Gov't, P.H.S.]. *Cytometry A, 55*(2), 61-70. doi: 10.1002/cyto.a.10072

Langley, R. R., & Fidler, I. J. (2011). The seed and soil hypothesis revisited--the role of tumor-stroma interactions in metastasis to different organs. [Research Support, N.I.H., Extramural

Review]. *Int J Cancer, 128*(11), 2527-2535. doi: 10.1002/ijc.26031

Lavoie, J. N., L'Allemain, G., Brunet, A., Muller, R., & Pouyssegur, J. (1996). Cyclin D1 expression is regulated positively by the p42/p44MAPK and negatively by the p38/HOGMAPK pathway. [Research Support, Non-U.S. Gov't]. *J Biol Chem, 271*(34), 20608-20616.

Law, J. H., Habibi, G., Hu, K., Masoudi, H., Wang, M. Y., Stratford, A. L., . . . Dunn, S. E. (2008). Phosphorylated insulin-like growth factor-i/insulin receptor is

present in all breast cancer subtypes and is related to poor survival. [Research Support, Non-U.S. Gov't]. *Cancer Res, 68*(24), 10238-10246. doi: 10.1158/0008-5472.CAN-08-2755

Ledford, H. (2011). Cancer theory faces doubts. [News]. *Nature, 472*(7343), 273. doi: 10.1038/472273a

Lee, B. C., Lee, T. H., Avraham, S., & Avraham, H. K. (2004). Involvement of the chemokine receptor CXCR4 and its ligand stromal cell-derived factor 1alpha in breast cancer cell migration through human brain microvascular endothelial cells. [Research Support, Non-U.S. Gov't

Research Support, U.S. Gov't, P.H.S.]. *Mol Cancer Res, 2*(6), 327-338.

Lee, S. S., Ahn, J. H., Kim, M. K., Sym, S. J., Gong, G., Ahn, S. D., . . . Kim, W. K. (2008). Brain metastases in breast cancer: prognostic factors and management. *Breast Cancer Res Treat, 111*(3), 523-530. doi: 10.1007/s10549-007-9806-2

Lin, N. U., & Winer, E. P. (2007). Brain metastases: the HER2 paradigm. [Research Support, Non-U.S. Gov't

Review]. *Clin Cancer Res, 13*(6), 1648-1655. doi: 10.1158/1078-0432.CCR-06-2478

Lin, Q., Balasubramanian, K., Fan, D., Kim, S. J., Guo, L., Wang, H., . . . Fidler, I. J. (2010). Reactive astrocytes protect melanoma cells from chemotherapy by

sequestering intracellular calcium through gap junction communication channels. [Research Support, N.I.H., Extramural

Research Support, Non-U.S. Gov't]. *Neoplasia, 12*(9), 748-754.

Litzenburger, B. C., Creighton, C. J., Tsimelzon, A., Chan, B. T., Hilsenbeck, S. G., Wang, T., . . . Lee, A. V. (2011). High IGF-IR activity in triple-negative breast cancer cell lines and tumorgrafts correlates with sensitivity to anti-IGF-IR therapy. [Research Support, N.I.H., Extramural

Research Support, U.S. Gov't, Non-P.H.S.]. *Clin Cancer Res, 17*(8), 2314-2327. doi: 10.1158/1078-0432.CCR-10-1903

Lockman, P. R., Mittapalli, R. K., Taskar, K. S., Rudraraju, V., Gril, B., Bohn, K. A., . . . Smith, Q. R. (2010). Heterogeneous blood-tumor barrier permeability determines drug efficacy in experimental brain metastases of breast cancer. [Research Support, N.I.H., Extramural

Research Support, N.I.H., Intramural

Research Support, U.S. Gov't, Non-P.H.S.]. *Clin Cancer Res, 16*(23), 5664-5678. doi: 10.1158/1078-0432.CCR-10-1564

Lopez, T., & Hanahan, D. (2002). Elevated levels of IGF-1 receptor convey invasive and metastatic capability in a mouse model of pancreatic islet tumorigenesis. [Research Support, U.S. Gov't, P.H.S.]. *Cancer Cell, 1*(4), 339-353.

Lorger, M., Lee, H., Forsyth, J. S., & Felding-Habermann, B. (2011). Comparison of in vitro and in vivo approaches to studying brain colonization by breast cancer cells. [Comparative Study

In Vitro

Research Support, N.I.H., Extramural

Research Support, Non-U.S. Gov't]. *J Neurooncol, 104*(3), 689-696. doi: 10.1007/s11060-011-0550-4

Luga, V., Zhang, L., Viloria-Petit, A. M., Ogunjimi, A. A., Inanlou, M. R., Chiu, E., . . . Wrana, J. L. (2012). Exosomes mediate stromal mobilization of autocrine Wnt-PCP signaling in breast cancer cell migration. [Research Support, Non-U.S. Gov't]. *Cell, 151*(7), 1542-1556. doi: 10.1016/j.cell.2012.11.024

Maor, S. B., Abramovitch, S., Erdos, M. R., Brody, L. C., & Werner, H. (2000). BRCA1 suppresses insulin-like growth factor-I receptor promoter activity: potential interaction between BRCA1 and Sp1. [Research Support, Non-U.S. Gov't]. *Mol Genet Metab, 69*(2), 130-136. doi: 10.1006/mgme.1999.2958

Mardilovich, K., Pankratz, S. L., & Shaw, L. M. (2009). Expression and function of the insulin receptor substrate proteins in cancer. *Cell Commun Signal, 7*, 14. doi: 10.1186/1478-811X-7-14

Martin, J. L., & Baxter, R. C. (2011). Signalling pathways of insulin-like growth factors (IGFs) and IGF binding protein-3. [Review]. *Growth Factors, 29*(6), 235-244. doi: 10.3109/08977194.2011.614237

Martin, J. L., Lin, M. Z., McGowan, E. M., & Baxter, R. C. (2009). Potentiation of growth factor signaling by insulin-like growth factor-binding protein-3 in breast epithelial cells requires sphingosine kinase activity. [Research Support, Non-U.S. Gov't]. *J Biol Chem, 284*(38), 25542-25552. doi: 10.1074/jbc.M109.007120

McCaig, C., Perks, C. M., & Holly, J. M. (2002). Intrinsic actions of IGFBP-3 and IGFBP-5 on Hs578T breast cancer epithelial cells: inhibition or accentuation of attachment and survival is dependent upon the presence of fibronectin. [Research Support, Non-U.S. Gov't]. *J Cell Sci, 115*(Pt 22), 4293-4303.

Mehta, A. I., Brufsky, A. M., & Sampson, J. H. (2012). Therapeutic approaches for HER2-positive brain metastases: Circumventing the blood-brain barrier. *Cancer Treat Rev*. doi: 10.1016/j.ctrv.2012.05.006

Menu, E., Jernberg-Wiklund, H., Stromberg, T., De Raeve, H., Girnita, L., Larsson, O., . . . Vanderkerken, K. (2006). Inhibiting the IGF-1 receptor tyrosine kinase with the cyclolignan PPP: an in vitro and in vivo study in the 5T33MM mouse model. [Comparative Study

In Vitro

Research Support, Non-U.S. Gov't]. *Blood, 107*(2), 655-660. doi: 10.1182/blood-2005-01-0293

Nguyen, D. X., Bos, P. D., & Massague, J. (2009). Metastasis: from dissemination to organ-specific colonization. [Research Support, N.I.H., Extramural

Research Support, Non-U.S. Gov't

Review]. *Nat Rev Cancer, 9*(4), 274-284. doi: 10.1038/nrc2622

O'Han, M. K., Baxter, R. C., & Schedlich, L. J. (2009). Effects of endogenous insulin-like growth factor binding protein-3 on cell cycle regulation in breast cancer cells. [Research Support, Non-U.S. Gov't]. *Growth Factors, 27*(6), 394-408. doi: 10.3109/08977190903185032

Ocana, O. H., Corcoles, R., Fabra, A., Moreno-Bueno, G., Acloque, H., Vega, S., . . . Nieto, M. A. (2012). Metastatic colonization requires the repression of the epithelial-mesenchymal transition inducer Prrx1. [Research Support, Non-U.S. Gov't]. *Cancer Cell, 22*(6), 709-724. doi: 10.1016/j.ccr.2012.10.012

Ohlsson, C., Kley, N., Werner, H., & LeRoith, D. (1998). p53 regulates insulin-like growth factor-I (IGF-I) receptor expression and IGF-I-induced tyrosine phosphorylation in an osteosarcoma cell line: interaction between p53 and Sp1. *Endocrinology, 139*(3), 1101-1107.

Okuda, H., Xing, F., Pandey, P. R., Sharma, S., Watabe, M., Pai, S. K., . . . Watabe, K. (2013). miR-7 Suppresses Brain Metastasis of Breast Cancer Stem-Like

Cells By Modulating KLF4. *Cancer Res*. doi: 10.1158/0008-5472.CAN-12-2037

Padovani, L., Muracciole, X., & Regis, J. (2012). gamma knife radiosurgery of brain metastasis from breast cancer. [Review]. *Prog Neurol Surg, 25*, 156-162. doi: 10.1159/000331189

Paget, S. (1989). The distribution of secondary growths in cancer of the breast. 1889. [Biography

Classical Article

Historical Article]. *Cancer Metastasis Rev, 8*(2), 98-101.

Paharkova-Vatchkova, V., & Lee, K. W. (2010). Nuclear export and mitochondrial and endoplasmic reticulum localization of IGF-binding protein 3 regulate its apoptotic properties. [Research Support, N.I.H., Extramural

Research Support, Non-U.S. Gov't

Research Support, U.S. Gov't, Non-P.H.S.]. *Endocr Relat Cancer, 17*(2), 293-302. doi: 10.1677/ERC-09-0106

Palmieri, D., Bronder, J. L., Herring, J. M., Yoneda, T., Weil, R. J., Stark, A. M., . . . Steeg, P. S. (2007). Her-2 overexpression increases the metastatic outgrowth of breast cancer cells in the brain. [Research Support, Non-U.S. Gov't]. *Cancer Res, 67*(9), 4190-4198. doi: 10.1158/0008-5472.CAN-06-3316

Park, E. J., Zhang, Y. Z., Vykhodtseva, N., & McDannold, N. (2012). Ultrasound-mediated blood-brain/blood-tumor barrier disruption improves outcomes with trastuzumab in a breast cancer brain metastasis model. [Research Support, N.I.H., Extramural

Research Support, Non-U.S. Gov't]. *J Control Release, 163*(3), 277-284. doi: 10.1016/j.jconrel.2012.09.007

Peng, L., Malloy, P. J., & Feldman, D. (2004). Identification of a functional vitamin D response element in the human insulin-like growth factor binding protein-3 promoter. [Research Support, Non-U.S. Gov't

Research Support, U.S. Gov't, Non-P.H.S.

Research Support, U.S. Gov't, P.H.S.]. *Mol Endocrinol, 18*(5), 1109-1119. doi: 10.1210/me.2003-0344

Pennisi, P. A., Barr, V., Nunez, N. P., Stannard, B., & Le Roith, D. (2002). Reduced expression of insulin-like growth factor I receptors in MCF-7 breast cancer cells leads to a more metastatic phenotype. *Cancer Res, 62*(22), 6529-6537.

Quigley, M. R., Fukui, O., Chew, B., Bhatia, S., & Karlovits, S. (2012). The shifting landscape of metastatic breast cancer to the CNS. *Neurosurg Rev*. doi: 10.1007/s10143-012-0446-6

Rodon, J., DeSantos, V., Ferry, R. J., Jr., & Kurzrock, R. (2008). Early drug development of inhibitors of the insulin-like growth factor-I receptor pathway: lessons from the first clinical trials. [Research Support, Non-U.S. Gov't

Review]. *Mol Cancer Ther, 7*(9), 2575-2588. doi: 10.1158/1535-7163.MCT-08-0265

Rodriguez, L. G., Wu, X., & Guan, J. L. (2005). Wound-healing assay. [Research Support, U.S. Gov't, P.H.S.]. *Methods Mol Biol, 294*, 23-29.

Sacanna, E., Ibrahim, T., Gaudio, M., Mercatali, L., Scarpi, E., Zoli, W., . . . Amadori, D. (2011). The role of CXCR4 in the prediction of bone metastases from breast cancer: a pilot study. *Oncology, 80*(3-4), 225-231. doi: 10.1159/000327585

Sachdev, D., Zhang, X., Matise, I., Gaillard-Kelly, M., & Yee, D. (2010). The type I insulin-like growth factor receptor regulates cancer metastasis independently of primary tumor growth by promoting invasion and survival. [Research Support, N.I.H., Extramural

Research Support, U.S. Gov't, P.H.S.]. *Oncogene, 29*(2), 251-262. doi: 10.1038/onc.2009.316

Saji, M., Vasko, V., Kada, F., Allbritton, E. H., Burman, K. D., & Ringel, M. D. (2005). Akt1 contains a functional leucine-rich nuclear export sequence. [Research Support, Non-U.S. Gov't]. *Biochem Biophys Res Commun, 332*(1), 167-173. doi: 10.1016/j.bbrc.2005.04.109

Saunus, J. M., Momeny, M., Simpson, P. T., Lakhani, S. R., & Da Silva, L. (2011). Molecular aspects of breast cancer metastasis to the brain. *Genet Res Int, 2011*, 219189. doi: 10.4061/2011/219189

Schedlich, L. J., & Graham, L. D. (2002). Role of insulin-like growth factor binding protein-3 in breast cancer cell growth. [Research Support, Non-U.S. Gov't

Review]. *Microsc Res Tech, 59*(1), 12-22. doi: 10.1002/jemt.10173

Scheel, C., Onder, T., Karnoub, A., & Weinberg, R. A. (2007). Adaptation versus selection: the origins of metastatic behavior. [Research Support, N.I.H., Extramural

Research Support, Non-U.S. Gov't

Research Support, U.S. Gov't, Non-P.H.S.

Review]. *Cancer Res, 67*(24), 11476-11479; discussion 11479-11480. doi: 10.1158/0008-5472.CAN-07-1653

Shaw, L. M. (2011). The insulin receptor substrate (IRS) proteins: at the intersection of metabolism and cancer. [Research Support, N.I.H., Extramural

Research Support, Non-U.S. Gov't

Review]. *Cell Cycle, 10*(11), 1750-1756.

Shiraishi, I., Melendez, J., Ahn, Y., Skavdahl, M., Murphy, E., Welch, S., . . . Sussman, M. A. (2004). Nuclear targeting of Akt enhances kinase activity and survival of cardiomyocytes. [Research Support, Non-U.S. Gov't

Research Support, U.S. Gov't, P.H.S.]. *Circ Res, 94*(7), 884-891. doi: 10.1161/01.RES.0000124394.01180.BE

Sierra, A., Price, J. E., Garcia-Ramirez, M., Mendez, O., Lopez, L., & Fabra, A. (1997). Astrocyte-derived cytokines contribute to the metastatic brain specificity of breast cancer cells. [Research Support, Non-U.S. Gov't]. *Lab Invest, 77*(4), 357-368.

Sivaprasad, U., Fleming, J., Verma, P. S., Hogan, K. A., Desury, G., & Cohick, W. S. (2004). Stimulation of insulin-like growth factor (IGF) binding protein-3 synthesis by IGF-I and transforming growth factor-alpha is mediated by both phosphatidylinositol-3 kinase and mitogen-activated protein kinase pathways in mammary epithelial cells. [Research Support, Non-U.S. Gov't

Research Support, U.S. Gov't, Non-P.H.S.]. *Endocrinology, 145*(9), 4213-4221. doi: 10.1210/en.2003-1377

Sperduto, P. W., Chao, S. T., Sneed, P. K., Luo, X., Suh, J., Roberge, D., . . . Mehta, M. (2010). Diagnosis-specific prognostic factors, indexes, and treatment outcomes for patients with newly diagnosed brain metastases: a multi-institutional analysis of 4,259 patients. [Multicenter Study]. *Int J Radiat Oncol Biol Phys, 77*(3), 655-661. doi: 10.1016/j.ijrobp.2009.08.025

Stahl, J. M., Sharma, A., Cheung, M., Zimmerman, M., Cheng, J. Q., Bosenberg, M. W., . . . Robertson, G. P. (2004). Deregulated Akt3 activity promotes development of malignant melanoma. [Research Support, Non-U.S. Gov't]. *Cancer Res, 64*(19), 7002-7010. doi: 10.1158/0008-5472.CAN-04-1399

Steeg, P. S., Camphausen, K. A., & Smith, Q. R. (2011). Brain metastases as preventive and therapeutic targets. [Research Support, N.I.H., Intramural

Research Support, U.S. Gov't, Non-P.H.S.

Review]. *Nat Rev Cancer, 11*(5), 352-363. doi: 10.1038/nrc3053

Stromberg, T., Ekman, S., Girnita, L., Dimberg, L. Y., Larsson, O., Axelson, M., . . . Jernberg-Wiklund, H. (2006). IGF-1 receptor tyrosine kinase inhibition by the cyclolignan PPP induces G2/M-phase accumulation and apoptosis in multiple myeloma cells. [Research Support, Non-U.S. Gov't]. *Blood, 107*(2), 669-678. doi: 10.1182/blood-2005-01-0306

Su, X., Chakravarti, D., Cho, M. S., Liu, L., Gi, Y. J., Lin, Y. L., . . . Flores, E. R. (2010). TAp63 suppresses metastasis through coordinate regulation of Dicer and miRNAs. [Research Support, N.I.H., Extramural

Research Support, Non-U.S. Gov't]. *Nature, 467*(7318), 986-990. doi: 10.1038/nature09459

Takata, Y., & Kobayashi, M. (1994). Insulin-like growth factor I signalling through heterodimers of insulin and insulin-like growth factor I receptors. [Research Support, Non-U.S. Gov't]. *Diabete Metab, 20*(1), 31-36.

Taniguchi, C. M., Ueki, K., & Kahn, R. (2005). Complementary roles of IRS-1 and IRS-2 in the hepatic regulation of metabolism. [Research Support, N.I.H., Extramural

Research Support, Non-U.S. Gov't

Research Support, U.S. Gov't, P.H.S.]. *J Clin Invest, 115*(3), 718-727. doi: 10.1172/JCI23187

Tanno, S., Tanno, S., Mitsuuchi, Y., Altomare, D. A., Xiao, G. H., & Testa, J. R. (2001). AKT activation up-regulates insulin-like growth factor I receptor expression and promotes invasiveness of human pancreatic cancer cells. [Research Support, Non-U.S. Gov't

Research Support, U.S. Gov't, P.H.S.]. *Cancer Res, 61*(2), 589-593.

Thiery, J. P. (2002). Epithelial-mesenchymal transitions in tumour progression. [Review]. *Nat Rev Cancer, 2*(6), 442-454. doi: 10.1038/nrc822

Torng, P. L., Lin, C. W., Chan, M. W., Yang, H. W., Huang, S. C., & Lin, C. T. (2009). Promoter methylation of IGFBP-3 and p53 expression in ovarian endometrioid carcinoma. [Research Support, Non-U.S. Gov't]. *Mol Cancer, 8*, 120. doi: 10.1186/1476-4598-8-120

Tran, M. N., Choi, W., Wszolek, M. F., Navai, N., Lee, I. L., Nitti, G., . . . McConkey, D. J. (2013). The p63 protein isoform DeltaNp63alpha inhibits epithelial-mesenchymal transition in human bladder cancer cells: role of MIR-205. [Research Support, N.I.H., Extramural

Research Support, Non-U.S. Gov't]. *J Biol Chem, 288*(5), 3275-3288. doi: 10.1074/jbc.M112.408104

Tsai, J. H., Donaher, J. L., Murphy, D. A., Chau, S., & Yang, J. (2012). Spatiotemporal regulation of epithelial-mesenchymal transition is essential for squamous cell carcinoma metastasis. [Research Support, N.I.H., Extramural

Research Support, Non-U.S. Gov't]. *Cancer Cell, 22*(6), 725-736. doi: 10.1016/j.ccr.2012.09.022

Tsao, M. N., Lloyd, N., Wong, R. K., Chow, E., Rakovitch, E., Laperriere, N., . . . Sahgal, A. (2012). Whole brain radiotherapy for the treatment of newly diagnosed multiple brain metastases. [Meta-Analysis

Research Support, Non-U.S. Gov't

Review]. *Cochrane Database Syst Rev, 4*, CD003869. doi: 10.1002/14651858.CD003869.pub3

Vashisth, H., & Abrams, C. F. (2010). All-atom structural models for complexes of insulin-like growth factors IGF1 and IGF2 with their cognate receptor.

[Research Support, U.S. Gov't, Non-P.H.S.]. *J Mol Biol, 400*(3), 645-658. doi: 10.1016/j.jmb.2010.05.025

Vasilcanu, D., Girnita, A., Girnita, L., Vasilcanu, R., Axelson, M., & Larsson, O. (2004). The cyclolignan PPP induces activation loop-specific inhibition of tyrosine phosphorylation of the insulin-like growth factor-1 receptor. Link to the phosphatidyl inositol-3 kinase/Akt apoptotic pathway. [Research Support, Non-U.S. Gov't]. *Oncogene, 23*(47), 7854-7862. doi: 10.1038/sj.onc.1208065

Vasilcanu, R., Vasilcanu, D., Rosengren, L., Natalishvili, N., Sehat, B., Yin, S., . . . Larsson, O. (2008). Picropodophyllin induces downregulation of the insulin-like growth factor 1 receptor: potential mechanistic involvement of Mdm2 and beta-arrestin1. [Research Support, Non-U.S. Gov't]. *Oncogene, 27*(11), 1629-1638. doi: 10.1038/sj.onc.1210797

Vasko, V., Saji, M., Hardy, E., Kruhlak, M., Larin, A., Savchenko, V., . . . Ringel, M. D. (2004). Akt activation and localisation correlate with tumour invasion and oncogene expression in thyroid cancer. [Research Support, Non-U.S. Gov't

Research Support, U.S. Gov't, P.H.S.]. *J Med Genet, 41*(3), 161-170.

Vern-Gross, T. Z., Lawrence, J. A., Case, L. D., McMullen, K. P., Bourland, J. D., Metheny-Barlow, L. J., . . . Chan, M. D. (2012). Breast cancer subtype affects patterns of failure of brain metastases after treatment with stereotactic radiosurgery. *J Neurooncol, 110*(3), 381-388. doi: 10.1007/s11060-012-0976-3

Weil, R. J., Palmieri, D. C., Bronder, J. L., Stark, A. M., & Steeg, P. S. (2005). Breast cancer metastasis to the central nervous system. [Review]. *Am J Pathol, 167*(4), 913-920. doi: 10.1016/S0002-9440(10)61180-7

Welsh, J., Wietzke, J. A., Zinser, G. M., Smyczek, S., Romu, S., Tribble, E., . . . Narvaez, C. J. (2002). Impact of the Vitamin D3 receptor on growth-regulatory pathways in mammary gland and breast cancer. [Research Support, Non-U.S. Gov't

Research Support, U.S. Gov't, Non-P.H.S.

Research Support, U.S. Gov't, P.H.S.

Review]. *J Steroid Biochem Mol Biol, 83*(1-5), 85-92.

Werner, H., Karnieli, E., Rauscher, F. J., & LeRoith, D. (1996). Wild-type and mutant p53 differentially regulate transcription of the insulin-like growth factor I receptor gene. *Proc Natl Acad Sci U S A, 93*(16), 8318-8323.

Werner, H., Re, G. G., Drummond, I. A., Sukhatme, V. P., Rauscher, F. J., 3rd, Sens, D. A., . . . Roberts, C. T., Jr. (1993). Increased expression of the insulin-like growth factor I receptor gene, IGF1R, in Wilms tumor is correlated with modulation of IGF1R promoter activity by the WT1 Wilms tumor gene product. [Research Support, Non-U.S. Gov't

Research Support, U.S. Gov't, P.H.S.]. *Proc Natl Acad Sci U S A, 90*(12), 5828-5832.

Wijnhoven, B. P., Dinjens, W. N., & Pignatelli, M. (2000). E-cadherin-catenin cell-cell adhesion complex and human cancer. [Research Support, Non-U.S. Gov't

Review]. *Br J Surg, 87*(8), 992-1005. doi: 10.1046/j.1365-2168.2000.01513.x

Wilhelm, I., Molnar, J., Fazakas, C., Hasko, J., & Krizbai, I. A. (2013). Role of the blood-brain barrier in the formation of brain metastases. *Int J Mol Sci, 14*(1), 1383-1411. doi: 10.3390/ijms14011383

Wu, X., Northcott, P. A., Dubuc, A., Dupuy, A. J., Shih, D. J., Witt, H., . . . Taylor, M. D. (2012). Clonal selection drives genetic divergence of metastatic medulloblastoma. [Research Support, N.I.H., Extramural

Research Support, Non-U.S. Gov't]. *Nature, 482*(7386), 529-533. doi: 10.1038/nature10825

Xi, Y., Nakajima, G., Hamil, T., Fodstad, O., Riker, A., & Ju, J. (2006). Association of insulin-like growth factor binding protein-3 expression with melanoma progression. [Research Support, Non-U.S. Gov't]. *Mol Cancer Ther, 5*(12), 3078-3084. doi: 10.1158/1535-7163.MCT-06-0424

Xia, W., Chen, J. S., Zhou, X., Sun, P. R., Lee, D. F., Liao, Y., . . . Hung, M. C. (2004). Phosphorylation/cytoplasmic localization of p21Cip1/WAF1 is associated with HER2/neu overexpression and provides a novel combination predictor for poor prognosis in breast cancer patients. [Research Support,

U.S. Gov't, P.H.S.]. *Clin Cancer Res, 10*(11), 3815-3824. doi: 10.1158/1078-0432.CCR-03-0527

Yang, H., Lee, H. W., Kim, Y., Lee, Y., Choi, Y. S., Kim, K. H., . . . Nam, D. H. (2013). Radiosensitization of brain metastasis by targeting c-MET. *Lab Invest*. doi: 10.1038/labinvest.2012.180

Yin, S., Girnita, A., Stromberg, T., Khan, Z., Andersson, S., Zheng, H., . . . Girnita, L. (2010). Targeting the insulin-like growth factor-1 receptor by picropodophyllin as a treatment option for glioblastoma. [Research Support, Non-U.S. Gov't]. *Neuro Oncol, 12*(1), 19-27. doi: 10.1093/neuonc/nop008

Yoneda, T., Williams, P. J., Hiraga, T., Niewolna, M., & Nishimura, R. (2001). A bone-seeking clone exhibits different biological properties from the MDA-MB-231 parental human breast cancer cells and a brain-seeking clone in vivo and in vitro. [Research Support, U.S. Gov't, P.H.S.]. *J Bone Miner Res, 16*(8), 1486-1495. doi: 10.1359/jbmr.2001.16.8.1486

Yoshimine, T., Ushio, Y., Hayakawa, T., Hasegawa, H., Arita, N., Yamada, K., . . . Mogami, H. (1985). Immunohistochemical study of metastatic brain tumors with astroprotein (GFAP), a glia-specific protein. Tissue architecture and the origin of blood vessels. *J Neurosurg, 62*(3), 414-418. doi: 10.3171/jns.1985.62.3.0414

Yu, H., & Rohan, T. (2000). Role of the insulin-like growth factor family in cancer development and progression. [Research Support, U.S. Gov't, P.H.S.

Review]. *J Natl Cancer Inst, 92*(18), 1472-1489.

Yuen, J. S., Cockman, M. E., Sullivan, M., Protheroe, A., Turner, G. D., Roberts, I. S., . . . Macaulay, V. M. (2007). The VHL tumor suppressor inhibits expression of the IGF1R and its loss induces IGF1R upregulation in human clear cell renal carcinoma. [Research Support, Non-U.S. Gov't]. *Oncogene, 26*(45), 6499-6508. doi: 10.1038/sj.onc.1210474

Zha, J., & Lackner, M. R. (2010). Targeting the insulin-like growth factor receptor-1R pathway for cancer therapy. *Clin Cancer Res, 16*(9), 2512-2517. doi: 10.1158/1078-0432.CCR-09-2232

VITA

Sandra Maria Saldaña Sanchez was born in Monterrey, Nuevo Leon, Mexico on August 9th, 1984. She is the daughter of Orlando Saldaña and Maria J. Saldaña, and the older sister of Orlando Saldaña. She moved to Houston, Texas, along with her parents and younger brother when she was 12 years old. She received a Bachelor of Arts in biological sciences, with a minor in microbiology, from the College of Arts and Sciences at Cornell University in 2006. At Cornell, Sandra was an undergraduate research scholar under the Cornell Nanobiotechnology Center. In the Fall of 2006, she enrolled in the PhD program at the UT Health Science Center at Houston Graduate School of Biomedical Sciences and joined the Department of Molecular and Cellular Oncology at the University of Texas MD Anderson Cancer Center. She will complete her Doctorate of Philosophy in Cancer Biology in May of 2013.